A. N. AL-ALOOSI

ATILIM UNIVERSITY 2019

FLOODS CAUSED BY THE FAILURE OF THE HIMREEN DAM IN THE NORTHEASTERN PART OF BAGHDAD, IRAQ USING HEC-RAS PROGRAM

THE GRADUATE SCHOOL OF NATURAL AND APPLIED SCIENCES
OF
ATILIM UNIVERSITY

AHMED NATIQ AHMED AL-ALOOSI

A MASTER OF SCIENCE THESIS
IN
THE DEPARTMENT OF CIVIL ENGINEERING

SEPTEMBER 2019

FLOODS CAUSED BY THE FAILURE OF THE HIMREEN DAM IN THE NORTHEASTERN PART OF BAGHDAD, IRAQ USING HEC-RAS PROGRAM

A THESIS SUBMITTED TO
THE GRADUATE SCHOOL OF NATURAL AND APPLIED SCIENCES
OF
ATILIM UNIVERSITY

BY

AHMED NATIQ AHMED AL-ALOOSI

IN PARTIAL FULFILLMENT OF THE REQUIREMENTS

FOR

THE DEGREE OF MASTER OF SCIENCE

IN

THE DEPARTMENT OF CIVIL ENGINEERING

SEPTEMBER 2019

Approval of the Graduate School of Natural and Applied Sciences, Atilim University.

Prof. Dr. Ali KARA
Director

I certify that this thesis satisfies all the requirements as a thesis for the degree of **Master of Science in Civil Engineering, Atilim University.**

Prof. Dr. Elif AYDIN
Acting
Head of Department

This is to certify that we have read the thesis. "FLOODS CAUSED BY THE FAILURE OF THE HIMREEN DAM IN THE NORTHEASTERN PART OF BAGHDAD, IRAQ USING HEC-RAS PROGRAM", submitted by "AHMED NATIQ AHMED Al-ALOOSI" and that in our opinion it is fully adequate, in scope and quality, as a thesis for the degree of Master of Science.

---	---
Assoc. Prof. Dr. Maha Rashid AL-ZAIDY	Assoc. Prof. Dr. Yakup DARAMA
Co-Supervisor	Supervisor

Examining Committee Members

Assistant Prof. Dr. Aslı Numanoğlu GENÇ ----------
Civil Eng. Dept. TED University

Assoc. Prof. Dr. Yakup DARAMA ----------
Civil Eng. Dept. Atılım University

Assistant Prof. Dr. Meriç YILMAZ ----------
Civil Eng. Dept. Atılım University

Date: 19/09/2019

I hereby declare that all information in this document has been obtained and presented in accordance with academic rules and ethical conduct. I also declare that, as required by these rules and conduct, I have fully cited and referenced all material and results that are not original to this work.

Name, Last Name : AHMED NATIQ AHMED AL-ALOOSI

Signature :

ABSTRACT

FLOOD CAUSED BY THE FAILURE OF THE HIMREEN DAM IN THE NORTHEASTERN PART OF BAGDAD, IRAQ

USING HEC-RAS PROGRAM

AL-Aloosi, Ahmed Natiq
M.S., Civil Engineering Department
Supervisor: Assoc. Prof. Dr.Yakup Darama
Co-Supervisor: Assoc. Prof. Dr. Maha Rashid Al-Zaidi

September 2019, 99 Pages

Catastrophic flooding due to dam failures is a major concern for Nations because of the destructive damage to the surrounding environment and loss of lives. When dam failure occurs, a huge amount of water impounded in the dams reservoir discharges to a downstream valley causing damage to the properties, houses, agricultural areas and loss of lives of cattle and people living downstream of the failed dam.

In this study, a hypothetical overtopping failure of the Himreen Dam in the Diayla River northeastern part of Baghdad is investigated by using HEC–RAS numerical model. In the study, the numerical model is calibrated to determine the value of average Manning's roughness coefficient n=0.028 of the Diayla River bed. This value of Manning's roughness coefficient is determined based on the comparison of flood levels calculated by the modelling study and previous observed flood levels during flooding events that occurred in the area. Sensivity analysis is performed by using three different n values 0.028, 0.030 and 0.035 of the Diayla riverbed in order to determine the effect of Manning's roughness on the magnitude, depth velocity and arrival time of flood. Maximum flood discharge resulting from the failure of the Himreen Dam, flood elevations and water depths in the inundated areas, time of flood peak arrival to Baquba City (whose population is 400000 people) are calculated in

each scenario. The failure of the dam will cause extensive damage to properties and lives of people downstream of the dam because of the severe flooding. The most damage will be in Baquba city because of the high population. A comparison of flood parameters showed that for n=0.035 (scenario 3) the maximum wave height of 35.77 m occurred downstream of the dam in Baquba City 12.61 m and in Nomania 5.64 m. In contrast to the water level and size of the inundation areas, the magnitude of the discharge and time of arrival of the flood wave in scenario 1 for n=0.028 are more critical. The results show that maximum discharge at Baquba City located downstream of the dam is 77201.8 m^3/sec and this value decreased to 131905.89 m^3/sec in Nomania, , and the arrival time of the flood wave to Baquba city is 17.15 hours and to Nomania is 105.45 hours. The results showed that the damage to the properties and the loss of lives will be maximum between the region near the dam and Baghdad city especially in Baquba (centre of Diayla state), because of its population. In comparison among the three scenarios, the worst scenario is 3, because of the highest wave and causing more damage and being more affected.

Key words: Dam failure, Himreen Dam, Diayla River, Flooding, HEC-RAS Model

ÖZ

BAĞDAT'IN KUZEYDOĞUSUNDAKİ HİMREEN BARAJININ YIKILMASI SONUCU OLUŞACAK TAŞKININ HEC-RAS PROGRAMI KULLANILARAK BELİRLENMESİ

Al-Aloosi, Ahmed Natiq
M.S., İnşaat Mühendisliği Bölümü
Danışman: Doç. Dr.Yakup Darama
Yardımcı Danışman: Doç. Dr. Maha Rashid Al-Zaidi

Eylül 2019, 99 Sayfa

Baraj yıkılmasıyla oluşan katastrofik taşkın sonucu meydana gelen baraj çevresinde ve mansabında meydana gelen yıkıcı tahribat ve can kaybı ülkelerin önemli endişe kaynağı olmuştur. Baraj yıkıldığı zaman barajın rezervuarında birikmiş olan büyük miktardaki su kütlesi su mansaba doğru akarak bu bölgelerde bulunan yerleşim alanlarındaki evlere, tarım alanlarına büyük hasarlar verir ve bu alanlardaki yaşayan insanların ve hayvanların can kaybına neden olur.

Bu çalışmada, Bağdat'ın Kuzeydoğusunda Diayla Nehri üzerinde bulunan Himreen Barajının hipotetik olarak yıkılma analizi HEC-RAS sayısal yazılım modeli ile araştırılmıştır Bu çalışmada sayısal model kaibre edilerek Diayla Nehri tabanının ortalama pürüzlülüğü n=0.028 olarak belirlenmiştir. Model kalibrasyon aşamasında Manning's pürüzlülüğünün bu değeri model simulasyonundan elde edilen su derinlikleriyle geçmişte bölgede gözlemlenmiş taşkın seviyeleri karşılatırılarak belirlenmiştir. Üç farklı Manning's pürüzlülük katsayısı değerleri kullanılarak, nehir tabanı pürüzlülüğünün taşkın debisine, taşkın derinliğine, taşkın hızına ve taşkının yerleşim alanlarına ulaşma zamanına etkisini belirmemek için üç farklı senaryo analiziyle duyarlılık analizi yapılmıştır. Diayla nehir tabanı için seçilen bu üç farklı Manning's pürüzlülük değerleri 0.028, 0.030 and 0.035 tir. Himreen Barajının hipotetik olarak yıkılması sonucunda barajın mansabındaki 400,000 nufuslu Bakuba şehrine ulaşacak taşkın debisi, su seviyeleri, su basma alanları, ve taşkın debisinin

(dalgasının) Bakuba şehrine ulaşma ve uyarı süreleri her üç senaryo için hesaplanmıştır. Analizler sonucunda barajın yıkılması sonucu savaklanan taşkının mansapta bulunan Bakuba şehrine büyük zararlar verebileceği, can kaybına neden olabileceği belirlenmiştir. Üç farklı senaryo sonucu elde edilen verilerin karşılaştırılmasıyla 3. senaryoda (n=0.035) maksimum taşkın dalgası yüksekliği Bakuba şehrinde 35.77 m ve daha mansaptaki Numunia'da is 5.46 m olarak hesaplanmıştır. Bu duruma karşın taşkın dalgasının ulaşma zamanı Senaryo 1 de daha kritik olmuştur. Bu senaryoda Bakuba şehrine ulaşan takın debisi 77201.8 m^3/sec, dalganın ulaşma süresi ise 11 saat ve bu debi Numuniada 31905.89 m^3/sec düşmüş ve ulaşma süresi ise 105.45 saat olarak hesaplanmıştır Bu sonuçlardan da görülebileceği gibi en fazla tahribatın ve can ve mal kaybının barajla Bağdatın arasında bulunan Diayla bölgesinin şehri olan Baquba şehrinde olabileceği gösterilmiştir..

Anahtar Kelimeler: Baraj Yılılması, Himreen Barajı, Diayla Nehri, Taşkın, HEC-RAS Modeli

To my parents …

To my lovely wife ….

To my children …

ACKNOWLEDGMENTS

First, I would like to express my special thanks to my supervisor Assoc. Prof. Dr. Yakup Darama for his continuous support, help, guidance and insight throughout my thesis study. During this period, he showed great enthusiasm and patience.

I would like to thank my Co-Supervisor Assoc. Prof. Dr. Maha Rashid Al-zaidy for her guidance and helping me getting hydrological, hydraulic and topographic data of the Diayla River and data for the Himreen dam from the Ministry of Water resources of Iraq. Without her help, this work would not have been realized.

I would also like to express my gratitude to managers of the Ministry of Water Resources of Iraq for proving all data related to the study area.

Furthermore, I thank the members of the examination committee Assist. Prof. Dr. Meriç Yılmaz and Assist. Prof. Dr. Aslı Numanoğlu Genç for their valuable time, comments and suggestions.

Finally yet importantly, I would like to give a huge thank you to my parents and family for all the support they gave me. They have given me great encouragement throughout my thesis studies. Their belief in me is definitely, what has made this thesis possible.

TABLE OF CONTENTS

LIST OF TABLES

LIST OF FIGURES

LIST OF ABBREVIATIONS

L	Length of Dam.
Q	Discharge.
T	Time.
V	Velocity.
S	Channel Slope.
W.S	Water Surface.
Min.Chnl.El	Minimum channel elevation.
Sta	Station.
HEC-RAS	Hydraulic Engineer Centre –River Analysis System.
C.R	Critical.
n	Manning's Coefficient for roughness .
E.G	Edge.
E	Elevation (above sea level) meter.
Hr.min	Hour. Minute.
Fr	Froude number.
ICOLD	International Committee of Large Dams

CHAPTER 1

INTRODUCTION

1.1 Importance of Study

Dams are constructed to serve a variety of purposes such as, supply drinking, irrigation water, generation of hydroelectric power, flood protection and agriculture. In contrast to these benefits, flooding events caused by dam failure results in considerable property damage and loss of human life in the towns located downstream of the dam. Some of the most popular dam failures in the past are the Buffalo Creek Coal–Waste dam near Saunders and the Teton Dam in Idaho, and most recently the Kelly Barnes lake dam near Toccoa, and the Laurel Run R-Servitors dam near Johnston. At the Laurel dam, heavy rainstorm caused heavy flooding in many areas near Johnston. Flooding in the valley caused heavy damages to property and more than 40 lives lost [1], [2]. The failure of the dam resulted in the sudden release of about 550,000 m^3 of water whose effects on the flow rates and stages along the valley downstream of the reservoir were significant [1]. 300 million m^3 of water discharged during the failure of the Teton Dam in Idaho in 1976 in USA. The casualties during this event were 11 people dead, 200 homeless, 560000 acres of flooded agricultural area and 13000 cattle lost, which constituted 2 billion dollars damage [3]. After these events, a number of studies were made [4]. For the safety of existing dams and to determine the extent of damage several numerical models such as dam break were used to learn if the dam failed for some reason [5].

Therefore, evaluation of the safety of exiting dams is necessary to determine the extent of damage, which may occur if dams fail. When dams fail, a large amount of water impounded behind the dam flows downstream and generally exceeds the capacity of the river channel and produces floods. This event is approximately described by using numerical models solving one-dimensional or two-dimensional flow problems in the natural channel. If adequate field data are available, solutions obtained from the numerical models are adequate and satisfactory. Therefore, a simulation of a mathematical model to a hypothetical dam-break and flood routing for the Al-Adhaim dam was formulated considering its unsteady flow using a four point –implicit

numerical method and specified time intervals [1]. Previous studies used the Saint-Venant equations, which employs continuity and momentum equations to find the flow parameters of the advancing flood wave [1].

In the numerical dam break analysis, description of breach of dam is an important parameter for the numerical model. Either in the models, the user describes this parameter or several breach equations are included in the numerical model for estimating the geometric and temporal characteristics of breach width to simulate failure phase of the dam. Data on time of breaching and estimating the peak outflows from different types of failures have been collected and prepared for this purpose. Other information assumed according to reliable results, which have already been discussed, verified, and recommended by many researchers [1]. The breach formation is gradual with respect to time and its width as measured along the crest of the dam usually encompasses only a portion of the dams crest length. In many instances, the bottom of the breach progressively erodes downward until it reaches the bottom of the dam. The size of the breach constituted by its depth and its width as well as the rate of breach formation, determines the magnitude and shape of the resulting breach outflow hydrograph [4], [6]. In the US, there are approximately 5000 dams, and 40 % of these dams classified as potentially dangerous to life and property in the event of failure. The majority of these dams are earth embankments, which were subjected to failure from either overtopping or piping, which erodes a trench breach through the dam [4], [6].

Most of the recorded failures took place for the following reasons:

The first reason for failure is foundation problems, which were found to be the major reason among many causes of earth dam failures. According to US Commission of Large Dams data in 79% of 4918 operating dams, a leakage in foundation and embankments has been the most frequent causes of failure. Most foundation incidents have resulted due to geological condition not being properly interpreted and treated during construction, whereas seepage through embankment has resulted from poor construction practice. To reduce the seepage under the dam and piping erosion of materials, a multiple row grout curtain is constructed. Proper construction and maintenance save the dams and make the percentage of failure less [4], [7]. The second reason causing failure is overtopping and inadequate spillway capacity, which is

caused by a disturbed flood discharge, such as spillway blockage. Overtopping could also be responsible for landslides in the reservoir area causing high wave in the reservoir [3]. The third reason for failure of dams is earthquakes, however it may be noted that no large dam (higher than 15 m) has been destroyed until now by earthquake and even incidents are few in number. This may be due to the thorough investigation preceding the selection of site location [4], [3].

Several investigations have been carried out in recent years concerning the development and application of various numerical methods for the analysis of one-dimensional dam break flow and a few studies for two-dimensional flow. However, limited experimental data for simulating dam break in the laboratories is available using straight flume. Experimental reported data on dam break in a straight-rectangular channel are shown in similar tests conducted in a straight flume between 1960-1961 at the Waterways Experimental Station, WES, in U.S [8], [9], and [10].

In many countries, the determination of the wave parameters that would follow the collapse of every large dam is legislated by law in order to determine inundated areas, flood hazard and flood risk maps that protect in habitants and structures in the valley downstream. In the last 10 years, several mathematical models have been developed to simulate this flow. Since it is impossible to predict the extent and duration of collapse, most of them deal with total and instantaneous collapse as the most dangerous case [11].

1.2 Scope and Aim of this Study

The aim of this study is to determine the peak discharge, flood elevation, time reach wave, and flood inundation maps of the areas of the northeastern part of Baghdad because of hypothetical failure of the Himreen Dam on the Diayla River.

The other purpose of the study is using the flood inundation areas of the northeastern part of Baghdad because of failure of the Himreen Dam by the water authorities in Iraq in order prepare a flood risk map.

In this study, HEC-RAS numerical model is used to simulate a flooding event caused by hypothetical failure due to overtopping of the Himreen dam of the Diayla River in the northern part of Baghdad. By using HEC-RAS, software developed by the

hydrological centre of US army corps of engineers, this analysis has been done to shows the extent of flooding areas downstream of the Himreen Dam and to determine inundation maps of the Diayla River from the failure of the dam. This would help to prepare an emergency plan for a hypothetical dam failure, which is unlikely to occur. The results shows the worst case of failure for the Himreen dam, which causes a peak discharge release of 77201.8 m^3/sec at the dam site. This will produce a water level of 98.73 m above sea level, and wave height of 35.77 m downstream of the dam, flood waves shall reach Baghdad city after 34.45 hrs with a peak discharge of 60475.07 m^3/sec, corresponding to wave height of 12.95 m. The devastation by flood and the disaster caused from the failure of the dam always cause large loss of human life and cause extensive property damage.

The thesis is divided into 5 chapters. The subject matter of each chapter with the exception of the introduction are as follows:

The literature review discussed in Chapter 2. First, the previous studies in dam failures and damage which occurred in different parts of the world are highlighted, then numerical modelling of failed dams or hypothetical failures of existing dams are discussed briefly. Finally, the literature on the numerical modeling conducted in flooding by dam failures in Iraq is presented briefly.

Study area is discussed in detail, methodology; hydraulic modelling and application of the hydraulic modelling to the study area are also presented in methodology Chapter 3.

The results of the numerical models for three different scenarios are presented and discussed in Chapter 4.

Chapter 5 provides conclusions and recommendations of the thesis. It highlights the main findings of the study with suggested future studies

CHAPTER 2

LITRATURE REVIEW

2.1 Studies on Dams Failure:

Several hypothetical studies were conducted for existing dams for the development of flood risk management plans for those dams if they failed. In Iraq hypothetical failure of Al-Adhaim Dam was studied using a numerical model and it was determined that the failure is caused by peak flow about Q=100000 m^3/sec. The height of the flood wave was 31m for Baghdad city [1]. Another hypothetical dam break analysis was conducted for the Gona Dam in Syria by using 1-D HEC-RAS numerical model, 82 million m^3 floodwater produced 3 m water depth downstream of the dam and inundated large settlement areas and caused property damage [12],[13] .

Hypothetical Failure of the Sennacherib Dam Failure using NWS DAMBRK model was studied and it was determined the max flow of the flood wave is 439560 m^3/sec, and elevation is 274.65 m [3].

Comparative Analysis is the simplest way to analyze dam failure. It depends on comparing dams which have already failed, and finding out the similarities between them in height, slope, water storage, and then specified failure parameters. Parametric models such as HEC-RAS numerical programs were used to calculate time of failure and peak flow [14].

Generally, empirical methods were used to calculate outflow hydrograph from the failed dam. These methods use the breech parameters and volume of water impounded in the reservoir of the dam. Moreover, there are some complex 2-Dimensional modelling studies for determination of flooded areas resulting from dam failures. These models uses either Saint Venant equation or Shallow water equation together with the continuity and momentum equations in an unsteady case. Some of these models were named Dam break simulation using a two-dimensional finite volume method. Numerical simulation of dam break floods with material point method (MPM) [8]. Boss Dam break software to find travel time and velocity of the flood wave in a valley downstream of the failed dam [10]. Artificial Neural Network method was also

used for 2-Dimensional space to describe how a flood wave moves downstream of the valley of the failed dam [11]. Recently a new model named Numerical Simulation-Based Decision Support System for Water Infrastructure Security (DDS-WISE), developed by the National Center for Computational Hydro Science and Engineering (NCCHE) at the Mississippi University, is also used. This model uses unsteady 2-Dimensional shallow water equations together with Satellite imagery; digital elevation maps integrated ARC-GIS (CCHE2D-Dam Break model) so that inundated areas, flood maps can be determined from the output of the model [15].

Analyzing the flood wave of Han River dam break in China using HEC-RAS model and ARC-GIS, the peak flow discharge reaching Nangyang city is 47000 m^3/sec with high velocity [16]. The 2-D unsteady flood wave propagation in channel transition was solved by using finite difference numerical scheme with initial and boundary conditions to simulate dam break problem by Mac-Cormik [17].Overtopping dam failure using Numerical Modelling, the 1-D model using Mac-Cormack finite to solve the 1-D equations .The model was applied to Buffalo Greek Dam. The comparison between Mac-Cormack 1971 and Momentum for unsteady varied flow gives satisfactory results [18].

Two numerical models (SMPDBK and DAMBRK) were developed in the National Weather Service (NWS). The laboratory data were obtained from these two models by using three scenarios .The two models built in 14 months at Hydraulic Laboratory. The results shows that the numerical failure simulations NWS, SMPDBK and DAMBRK, gave a reasonable accuracy. However, there are differences between the numerical and physical model in peak water surface, especially of the SMPDBK, because of high sensitivity of the numerical model to bottom friction [19].

2.2 Social Impacts and Damage caused by dam Floods:

Flooding events resulting from a dam's failure cause many serious social impacts and economic losses. The majority of dam failures are due to catastrophic floods flowing over the dam body and leading to dam failure. These events affected more than 220 million people with an economic loss of about 20 million dollars per day [4], [6]. Many studies show that the floods are the most important disaster that causes damage in terms of deaths and economics [20], [14]. Floods caused by dam failure cause more damage than other natural disasters because of the large quantity of the impounded

water in the reservoir of the dam released in a very short time as in the case of the Yeon–Cheon dam in China [21].

2.3 The Reasons of Dam Failure:

There are many dams in the world, which represent hazards in more than 150,000. The information reported by the International Commission on Large Dams (ICOLD) shows 191 dams failure have been reported from 1900 until 1965 [4], [6].

There are many phenomena which threaten dam safety such as floods, earthquakes storms. In addition, there are many reasons like seepage sliding. The continuous monitoring of a dam to make sure of any flows, which may be a reason for failure. That matter will be the responsibility of the dam management and their experience and knowledge. Of course, there are many differences between one dam and another, but the problems are the same [12], [21].

Analysis of performance in various types of dams shows their stability. Each kind of failure depends on the dam type, e.g. A gravity dam collapses because one section or more has been overstressed. A buttress dam may fail because of the successive collapse of one or more buttresses; arch dams may also fail if the concrete body cracks due to high hydrostatic pressure [21]. The Japanese made a survey of impairment dams between 1950 and 1965. The total number of dams was 1046. The conclusion of this survey is:| "Impairment caused by heavy runoff affected 38% of the total" [12].

Another study on 300 dam failures studied by Biswas and Chatterjee in1971 was "Dam Disaster an Assessment, they conclude about 35% were a direct result of floods in excess of the spillway capacity [22].

In 1979, in India, New Delhi, the 13th report of ICOLD presented 52 dam failures in Spain during 200 years, classifying the list of dam failures caused by overtopping. It may lead to complete failure in a dam, it is different from the others, it may save a little water from total collapse [23].

The problems of dam failure can be specified below:

There are many reasons in foundation such as differential condition settlement, sliding, in control seepage, high piezometric pressure cracks, and original soil of a dam, like the Mosul Dam in northern Baghdad, which contains gypsum in the original soil. The

increase of water movement on the limits design may be a serious problem; water tends to carry away constituents of the fill material that could be vital to the integrity of the dam. Embankments may be subjected to erosion if they are not protected from waves upstream due to increasing depth and intensity of rain. Riprap are important to protect the embankment upstream from waves. The instability of an embankment due to deleterious materials which are used. Soluble minerals like gypsum maybe carried away, leaving channels or cavities, leading to settlement because of loss of volume. Improved methods for analyzing the stability of dams subjected to seismic loading provide reliable indications that many old dams are vulnerable [21], [22] and [4].

Concrete dams may be attributed to chemical and physical factors. In chemical actions caused by organic acids, salts, sulphates, these chemical reactions led to deterioration in a few years. Physical reactions, such as temperature (freezing) wetting and drying, led to thermal expansions, therefore water pressure in joints caused sliding or overturning failure,as in the case of the Bouuzey dam in France in 1895 [12].

Another important part of a dam, sometimes medium sized, has many reasons for failure and has led to complete failure; poor design, lack of maintenance, in the capability of emptying a reservoir. Deliberate efforts were especially made to destroy dams or sabotage them to keep the public safe from enemies. It was subjected sometimes to military strategists to see the advantages of attacking enemies. In past wars, commanders destroyed dams to flood enemy forces and to cut routes across them. The Burguillo dam near Avila and the Ordinate dam near Bilbao were both attacked and damaged in 1937 during the Spanish war. The Soviet Union used the same strategy in the German attack in 1941 on the Dnjeprstroj Dam [12].

The overtopping water of the dam releases a huge discharge of water. It is the most common cause of dam failure. Several failures refer to spillways, such as the Oros Dam in Brazil in 1960, the Sempor Dam in Indonesia in 1967, and the Oroville Dam in 2016, which almost failed [24]. One of the important criteria is slope embankments and calculating their capability to store water. The consequences of landslides produces large waves cause overtopping of a dam, such as the Vaiont reservoir in Italy in 1963 [24] .The Ohio River Dam can be a good example. After its compellation in 1911, it failed in 1912 [22].

Earthquakes also causes failure of large reservoirs by producing earthquake waves, which overflow from the crest of the dam and can cause failure. As examples a Richter Magnitude, greater than six occurred in the Kariba Dam in Zambia, the Koyna Dam in India, the Kremasta Dam in Greece and the Hsinfengkiang Dam in China causing failure [6]. Therefore, the most common reasons for dam failure are floods or heavy rains, earthquake, weak design, and bad maintenance [25].

One of the important criteria for dam safety is good design, taking in to consideration catastrophic rains and floods, which have increased recently because of the climate changes and increase in the return periods [23], [26]. The amount water, which is released, should not be more than 10% of the peak volume of the flood and the spillways should be designed for probable maximum flood concept. The reference point assessing whether the damage is great cannot be the first site below the dam, a millor road bridge [23].

Providing data from monitoring and evaluation steps can be helpful, determining the weakness of all parts for dam safety. By using these results, adjustments can be made in the policies and processes [27], [24]. Therefore, a dam safety objective, which meaning that all reasonable measures which are taken to prevent a dam from failure [21].

CHAPTER 3

METHODOLOGY

In this chapter, a study area where the Himreen Dam is located is explained in the first part. The characteristics of the dam and the climate of the area also given in this part. The second part is related to hydraulic modelling and application of hydraulic model HEC-RAS for the hypothetical failure of the Himreen Dam [14], [13].

3.1 Study Area:

In this part, the Himreen Dam is chosen as a case for this study. The Himreen dam is located on the Diayla river, 120 km from northeast of Baghdad in the Diayla State of Iraq, Fig. 3.1. The dam is on the Diayla River. In this study, data from the Ministry of Water Resources is used. These data include discharges, cross-sections and other information about the dam. (Fig 3.2. Table 3.1 and Fig 3.3). The study area begins from the Himreen Dam to the south of Baghdad until Nomania, which covers villages like the Abou-Saida, Al-Sewera, Barwana, Baquba. The distance between the Himreen dam and Nomania is 300 km. (Fig 3.4). The aim of the Himreen dam is to control floods, to provide irrigation water, and to produce hydroelectric power. The nearest city is Baquba, which is in the centre of the Diayla State, whose population is 400,000 people. In the study area the population of more than 1,000,000 people affected by dam failure is shown, [28], [29] and [30].

The overtopping case is chosen because of the occurrence of heavy precipitations as shown in Fig 3.5. This figure shows that the amount of the average precipitation. In 2018-2019 period, it is about 450 mm, which is three times higher than that value of long term average precipitation, which is 150 mm.

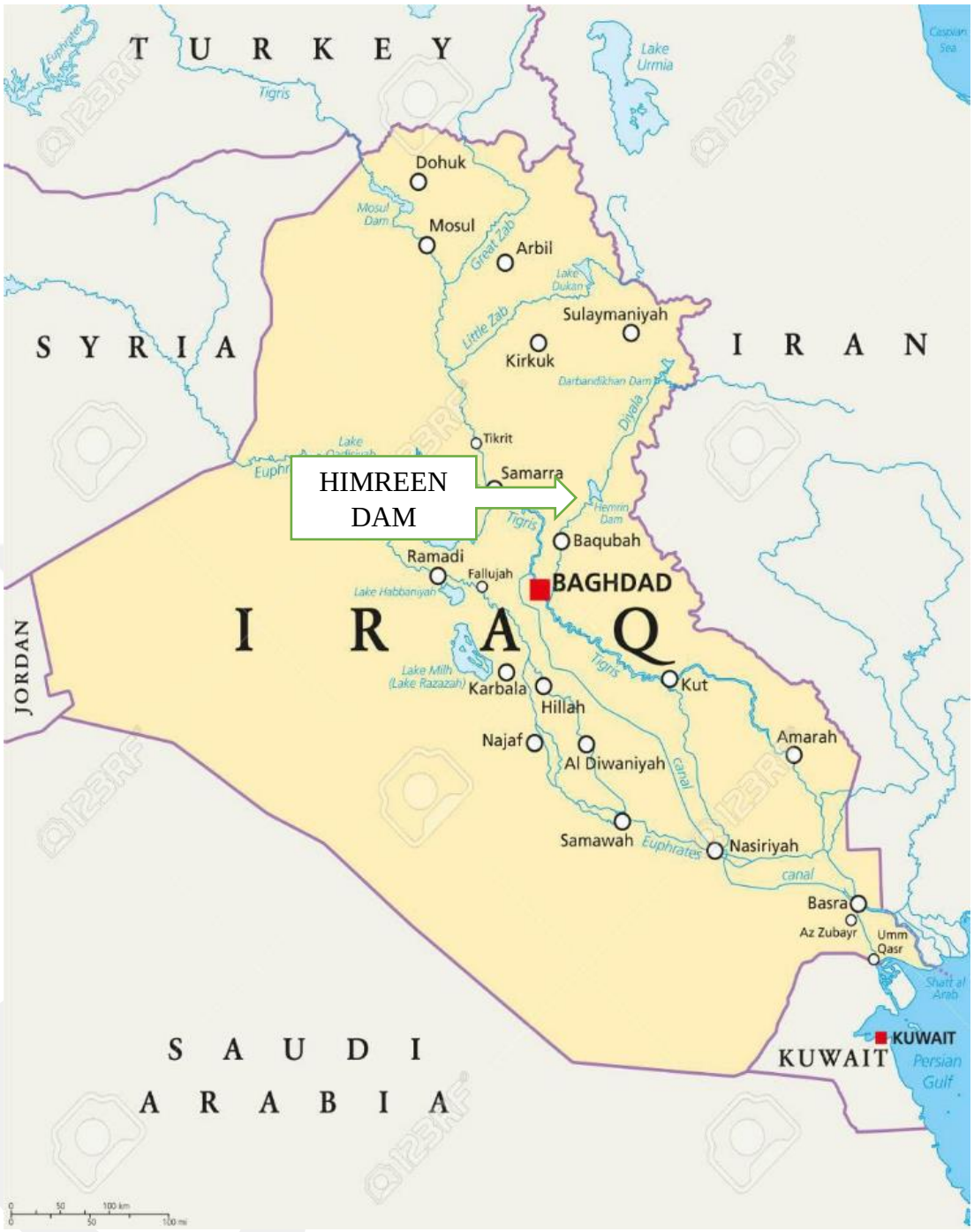

Figure 3.1 Study Area on Iraq Map

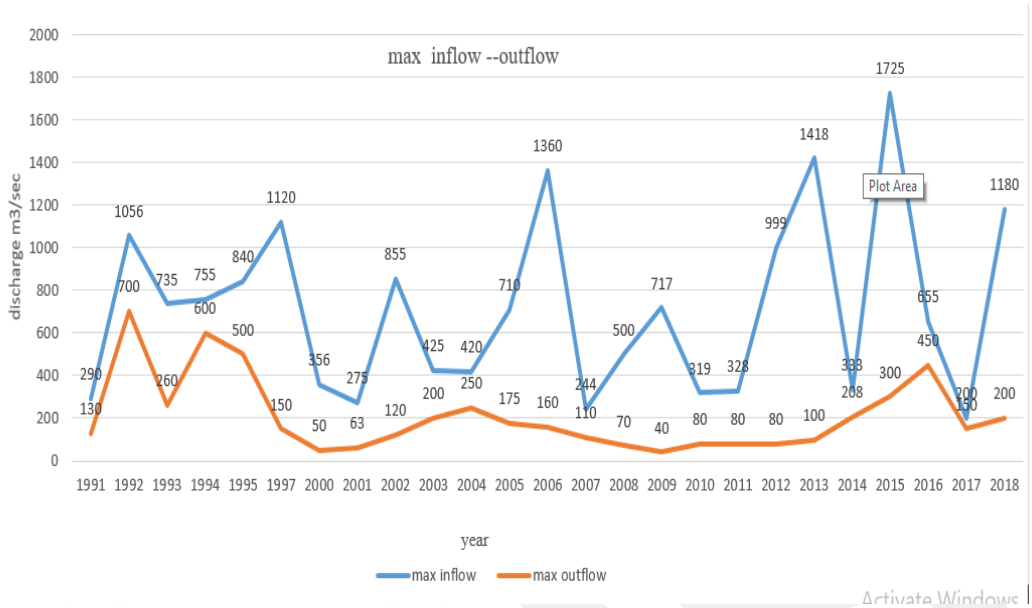

Figure 3.2 The Outflow and Inflow in Himreen Dam

Table 3.1 Himreen Dam Data

No	Item	Value
1	Height of dam	40 m
2	Length of Dam	3360 m.
3	Max Floods Elevation	107.5 m (above sea level)
4	Area of Reservoir Lake	450 k m^2
5	Max Water Storage	3,560,000,000 m^3
6	Ordinary Storage	2,060,000,000 m^3
7	Live Load Water Storage	2,040,000,000 m^3
8	Spillway Capacity	6800 m^3/sec
10	Type of dam	High zone earth embankment
11	Generating power	Two units (50) MW
12	Dam crest elevation	109.5 m (above sea level)

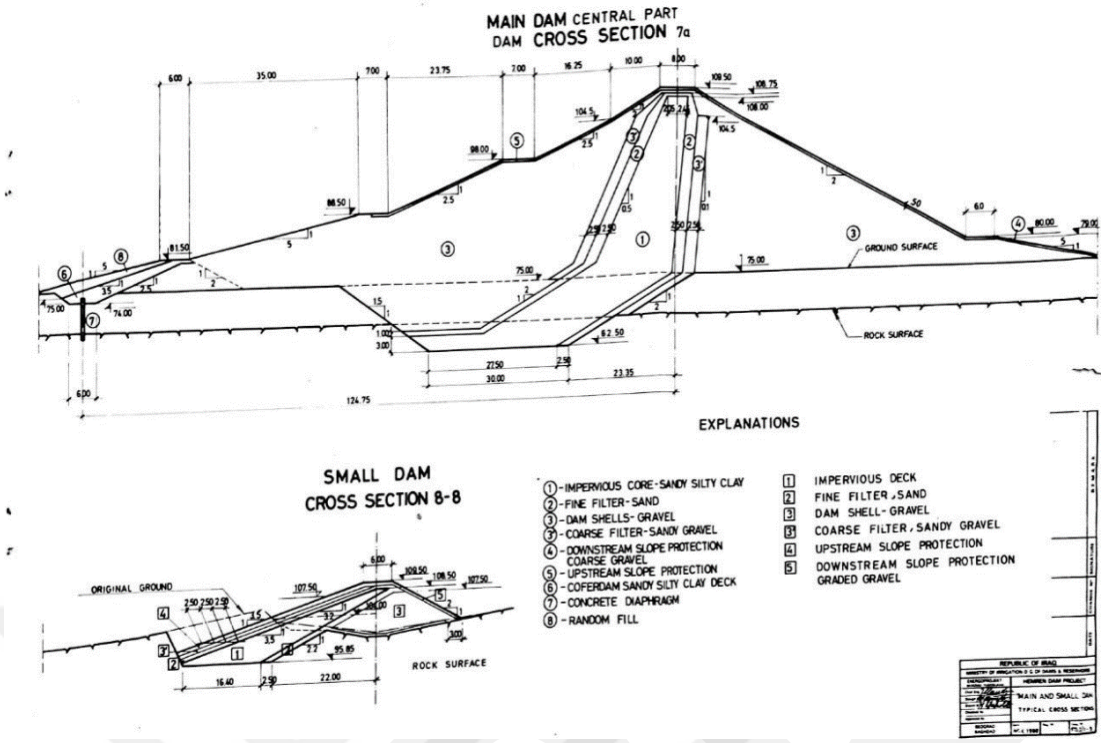

Figure 3.3 Cross-Section on the Himreen Dam

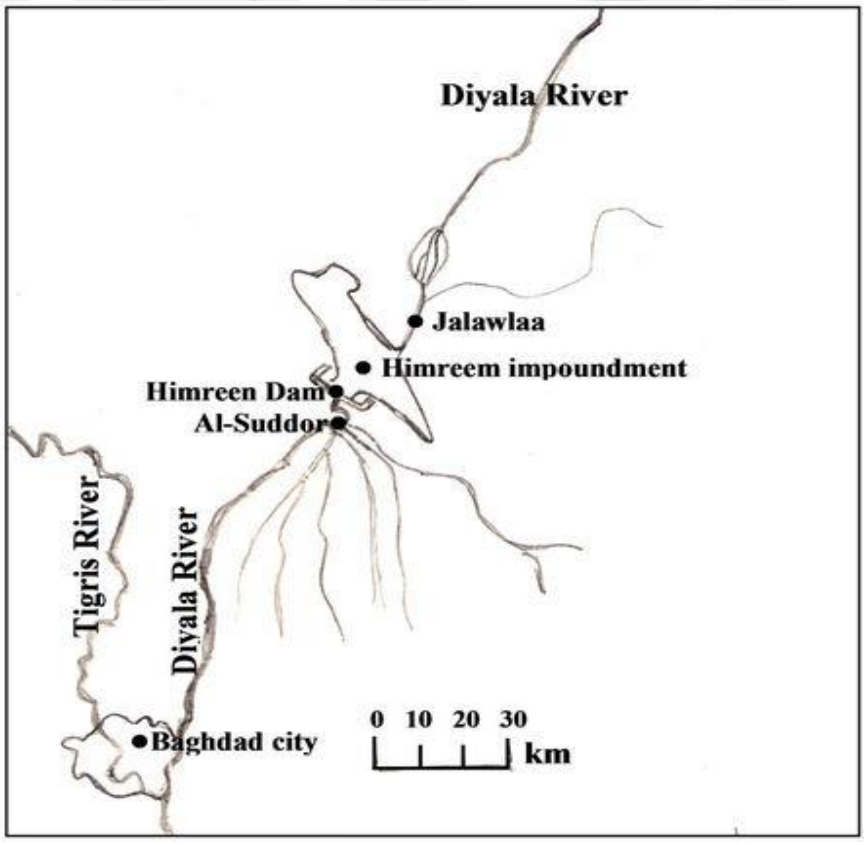

Figure 3.4 The location of Himreen Dam with Respect to Baghdad city

3.2 Hydraulic Model:

HEC-RAS software program is used to simulate overtopping failure in the modelling studies. As shown in Fig. 3.4, the Himreen dam is a clay core earth filled dam. Failure of the majority of these kinds of dams occurs by either overtopping or piping [4]. Overtopping failure is chosen for the failure of the Himreen dam because of unexpected rainfall as seen in Fig 3.5 that might produce a high flood which causes overtopping failure. Fig 3.6. Fig 3.7 show the stages of overtopping dam failure. These figures show conceptual failure of earth dams by overtopping. In this case, water starts flowing on the dam body and starts eroding the dam body (stage A).Then scouring starts at the toe of the dam (stage B). After this stage, the downstream face of the dam body starts to fail by increased discharge, (stage C). Finally, the whole body fails and water impounded behind the dam body discharges to the downstream channel (stages D and E) [31].

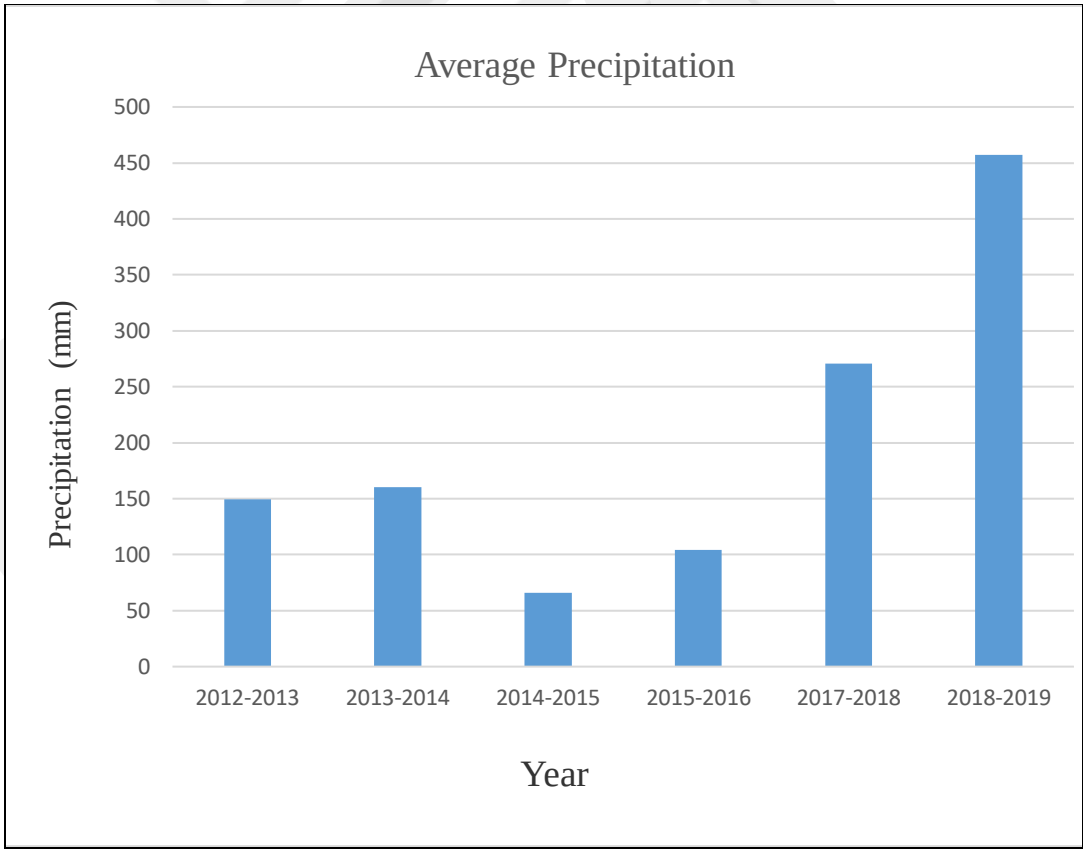

Figure 3.5 The Average Rainfall (precipitations) in mm in Diayla State

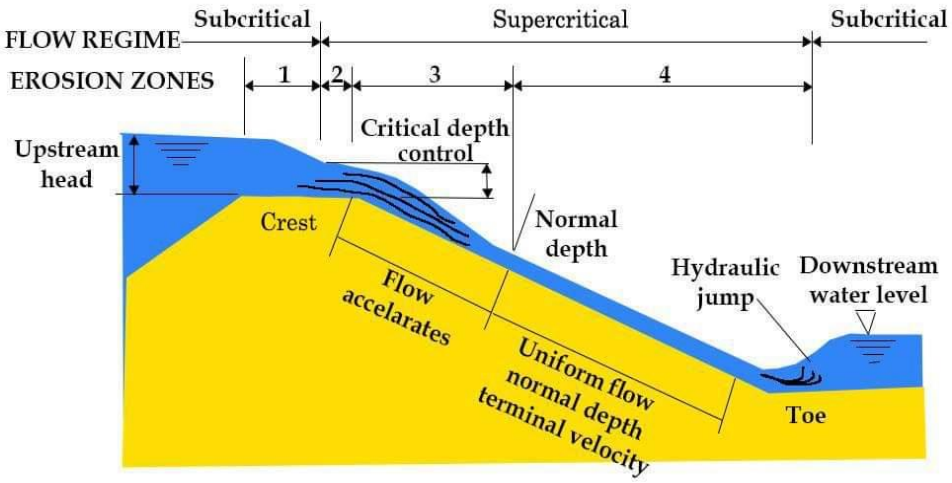

Figure 3.6 Hydraulic Flow Regime

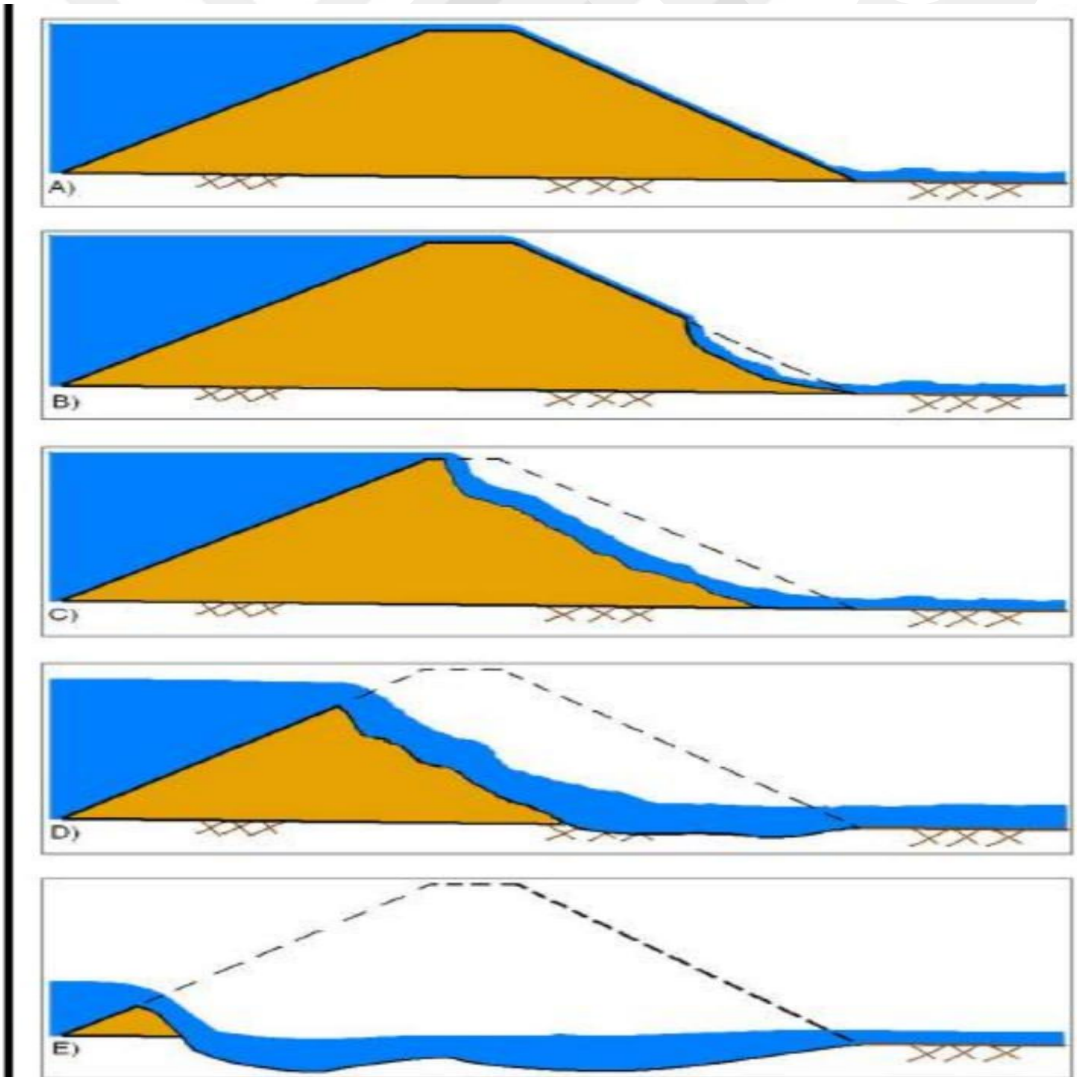

Figure 3.7 Conceptual Model for Earth Dam's Failure Stages

3.3 Application of HEC-RAS:

Numerical model HEC-RAS was applied to Himreen Dam failure on the Diayla River for three different scenarios using unsteady flow analysis. The numerical model was calibrated to determine the average roughness of n representing the Diayla River bed.

The numerical model is calibrated to determine the value of Manning's roughness coefficient n=0.028 of the Diayla riverbed. This value of Manning's roughness coefficient is determined based on a comparison of flood levels calculated by the modelling study and previous observed flood levels during flooding events that occurred in the area (see Fig A.1 to A.14 in the Appendix). Sensivity analysis is performed by using three different n values 0.028, 0.030 and 0.035 of the Diayla riverbed in order to determine the effect of roughness on the magnitude, depth velocity and arrival time of flood. Fig 3.8 shows the chart flow of the study. Three scenarios are considered in the analysis and after comparing them, the most critical case is chosen as the critical case.

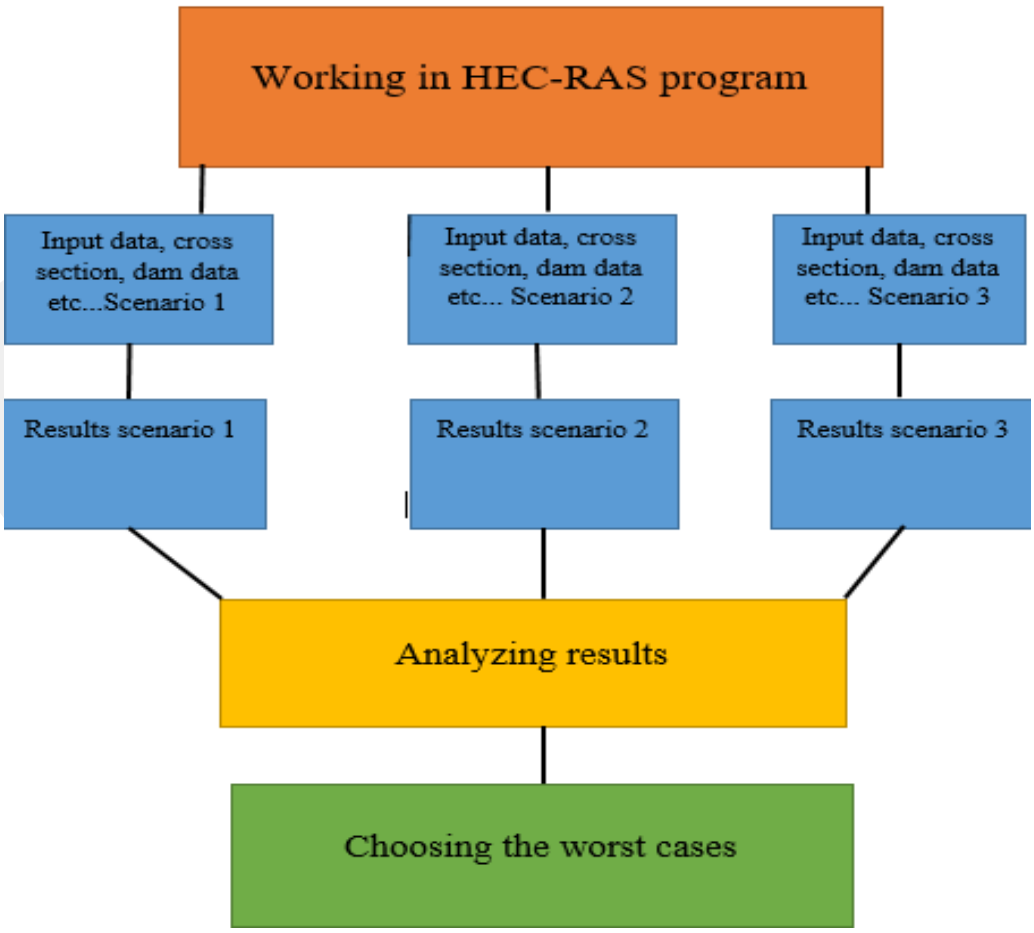

Figure 3.8 Flow Chart for The Study

The input data to the program consist of dam cross-section data, the reach between the dam and the Nomania, which is divided in to 41 cross-sections. The reach and cross-section window is given in Fig 3.9.

The data for these cross-sections were obtained from the Ministry of Water Resources of Iraq. Some of these cross-sections are given in Fig 3.10 to 3.15. Since the area is flat, the cross-sections are extended horizontally about 50 km to cover the inundation area as accurately as possible.

Considering 3 different values of n roughness coefficient simulations were performed. These values of roughness, for scenario 1, n=0.028, for scenario 2 n=0.03, and for scenario 3, n=0.035, were determined based on observation. The aim of using these scenarios is to calibrate and find the most critical case. [15], [32]. Fig 3.16 shows unsteady flow analysis for the Diayla River in HEC-RAS window [14], [15].

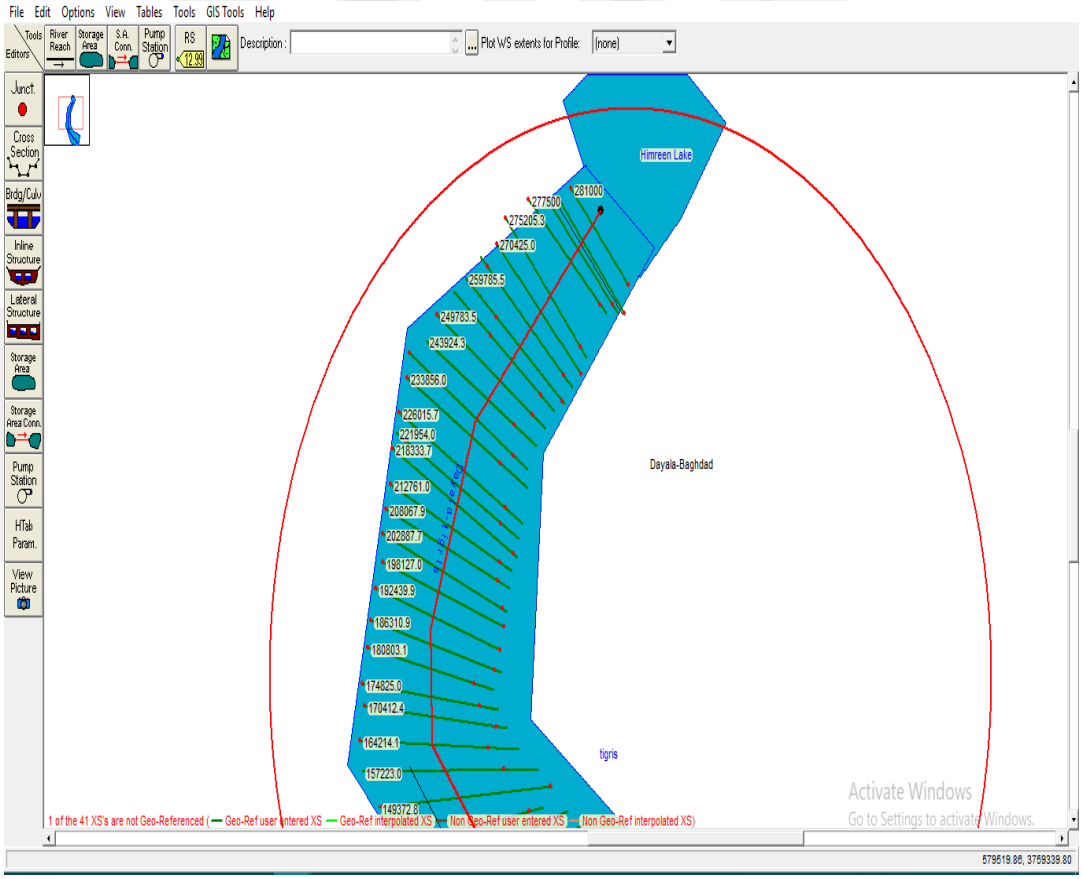

Figure 3.9 Cross-Section Location of the Diayla River Downstream of the Himreen Dam

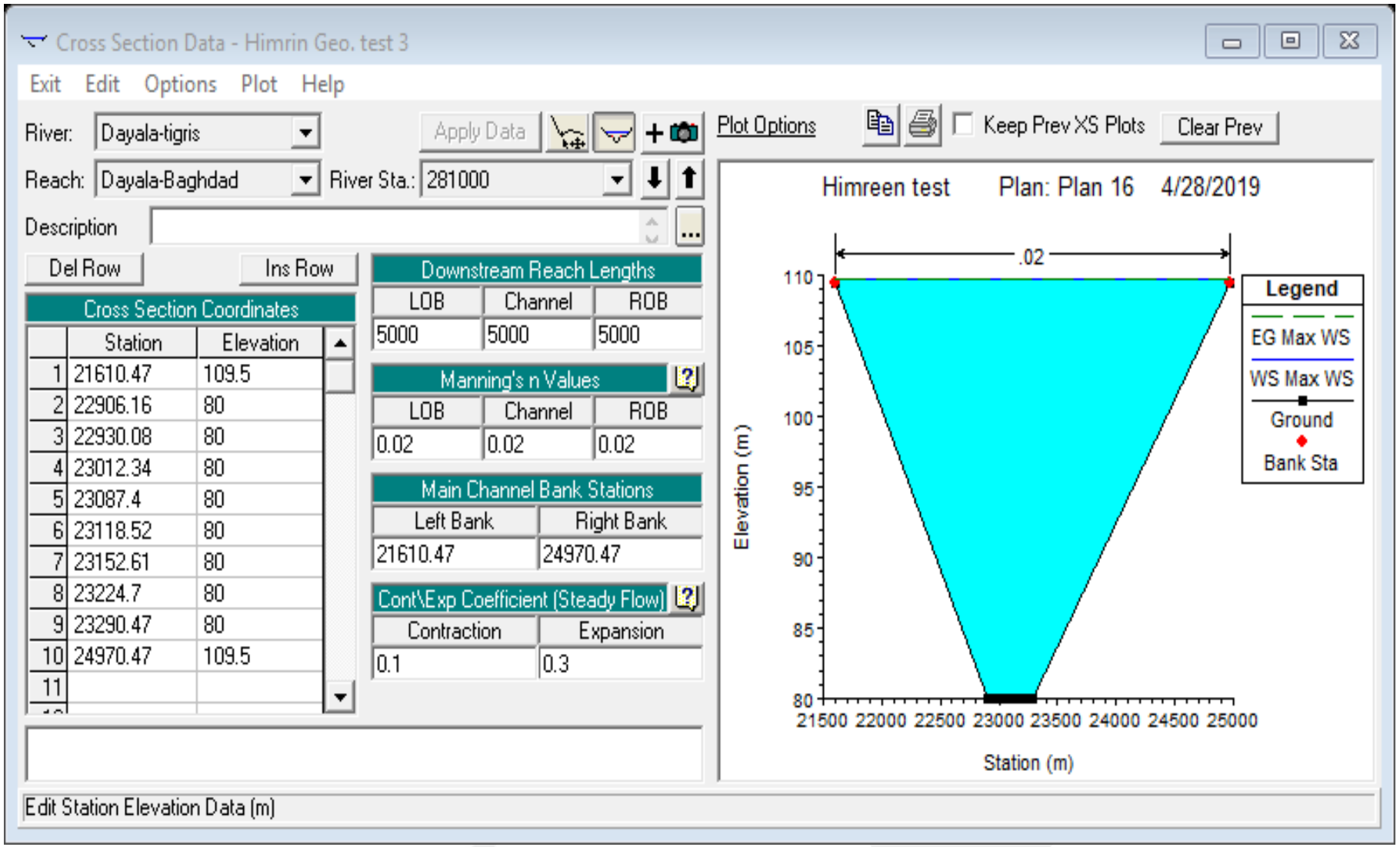

Figure 3.10 Cross-Section Number 281000 Upstream of Himreen Dam

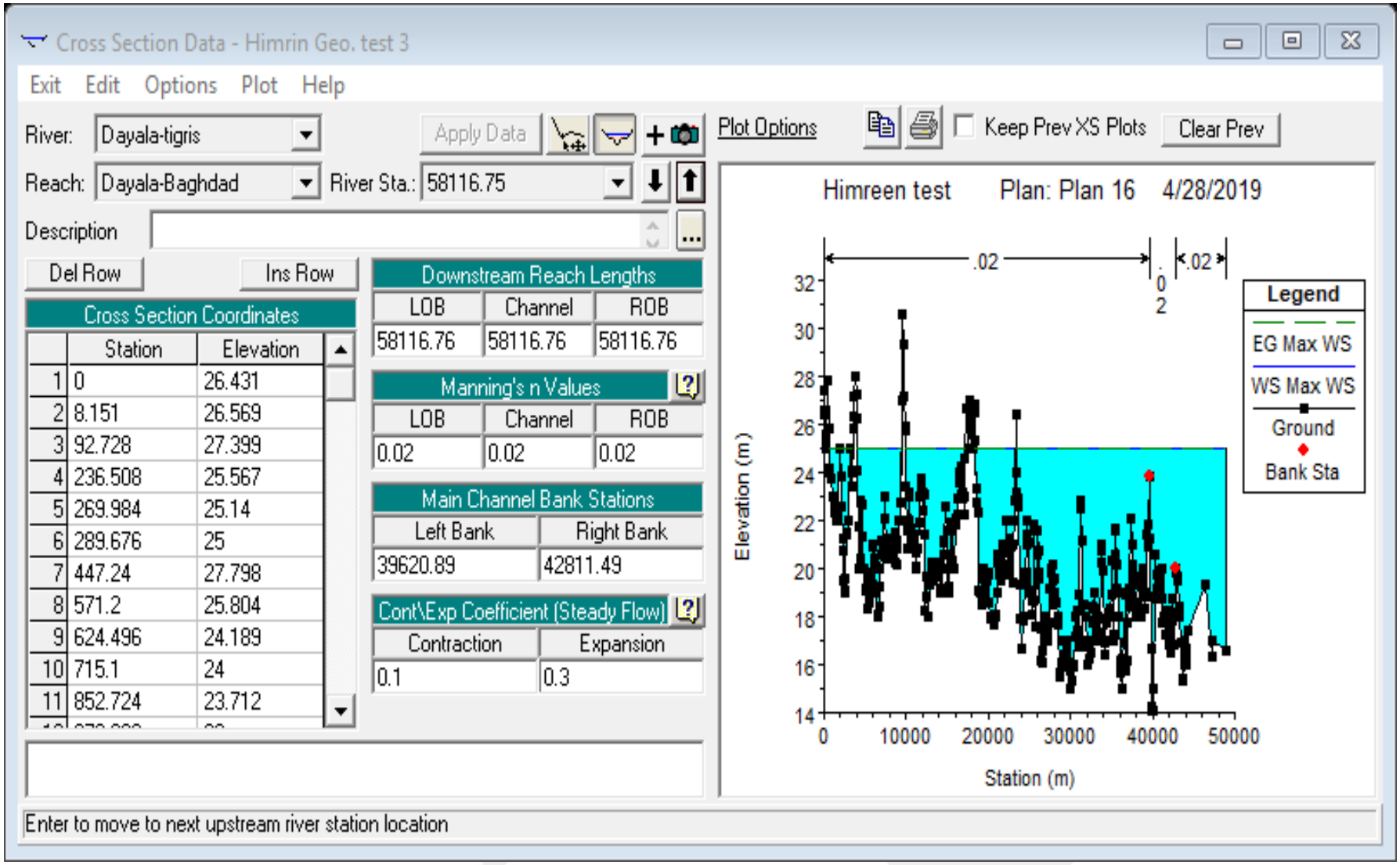

Figure 3.11 Cross-Section Data

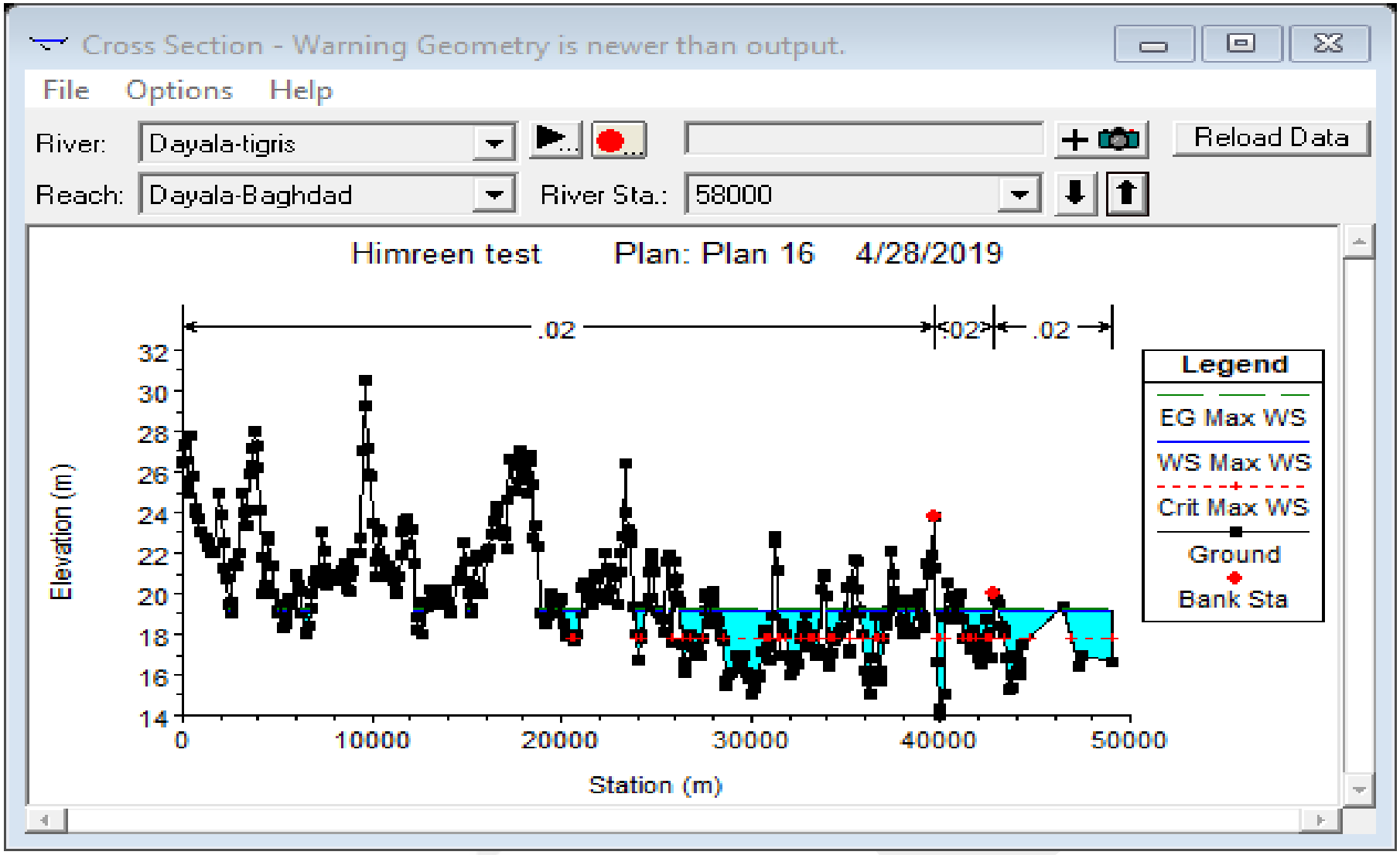

Figure 3.12 Cross-Section Number 58000

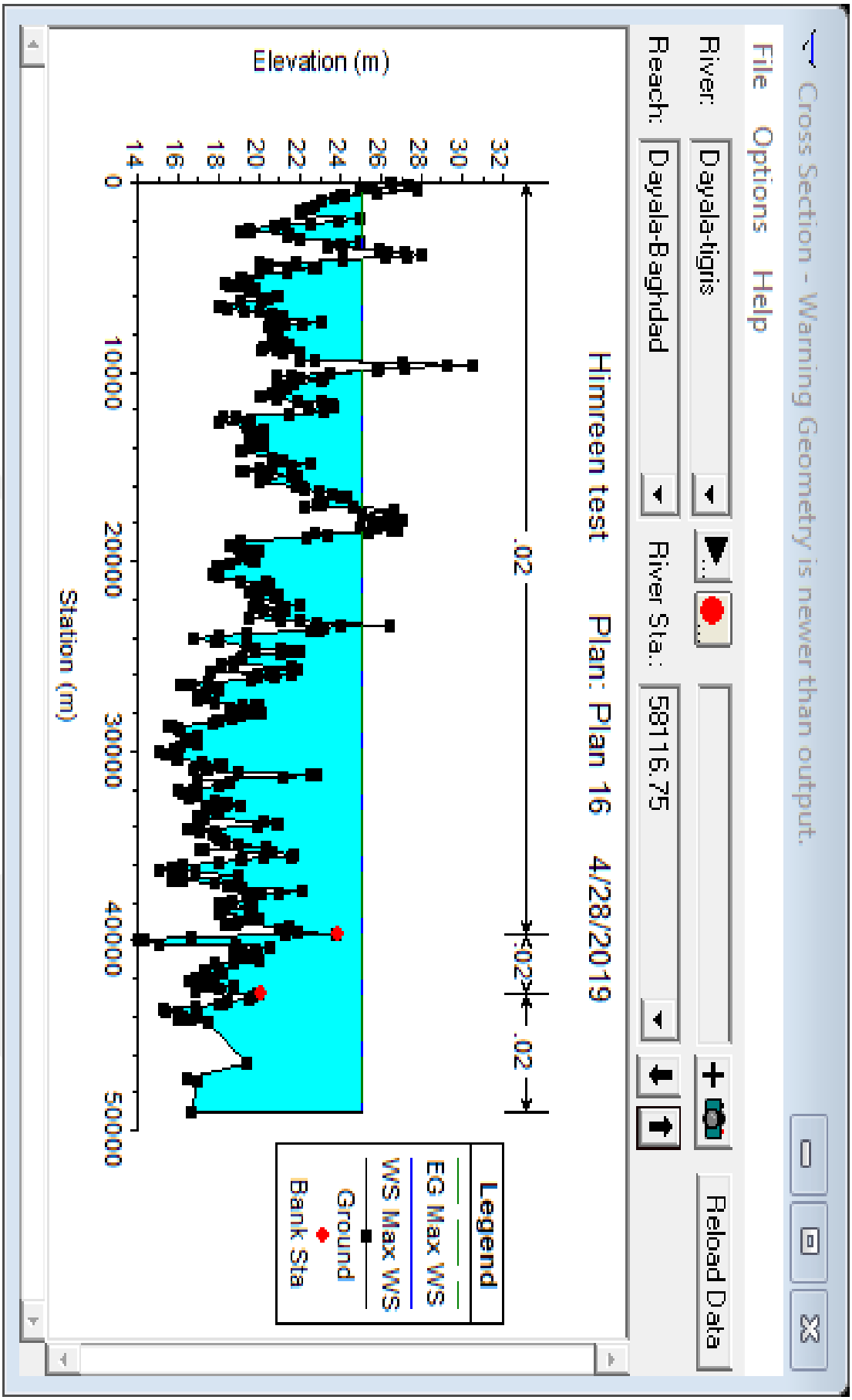

Figure 3.13 Cross-Section Number 58116.75

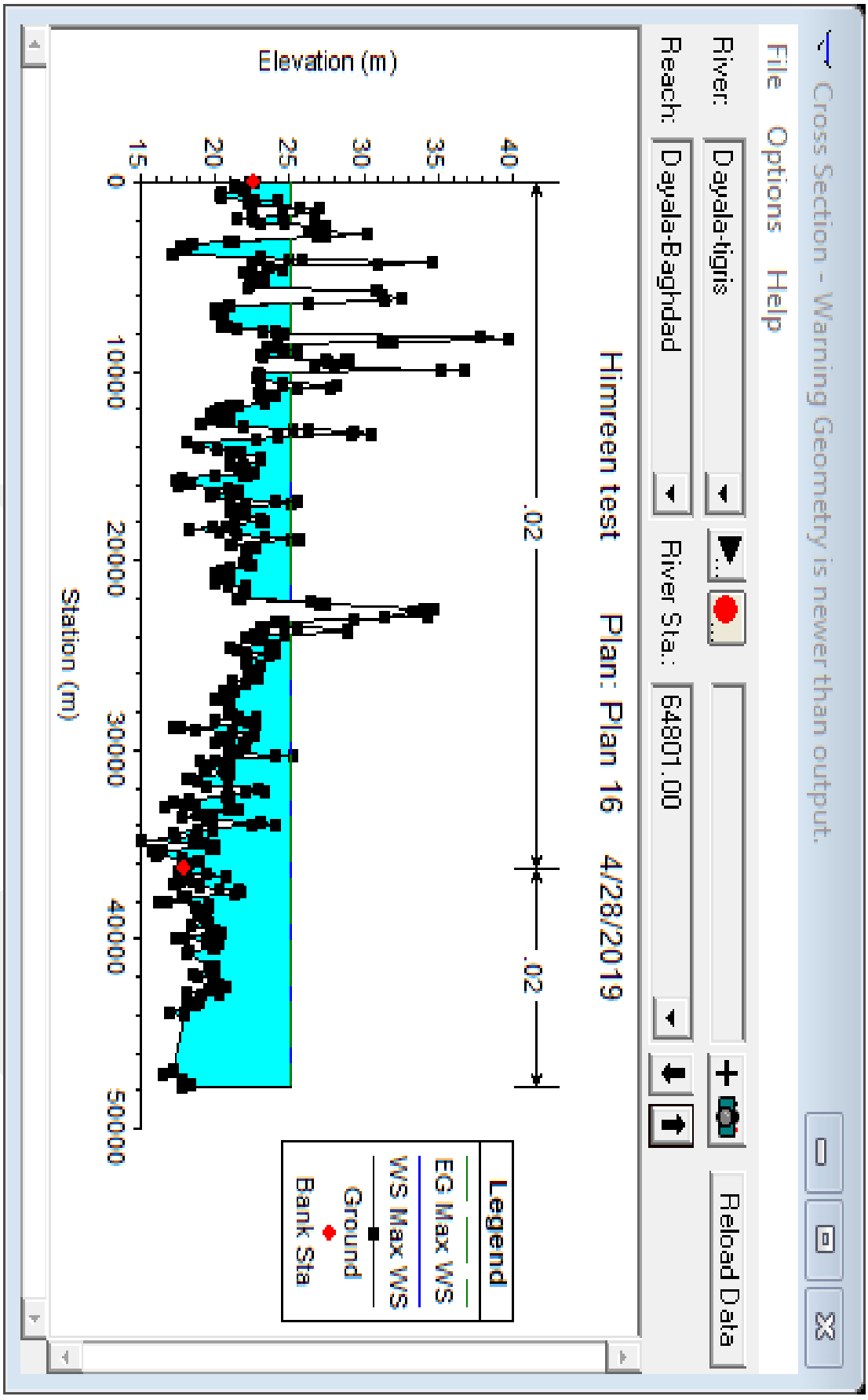

Figure 3.14 Cross-Section Number 64801.00

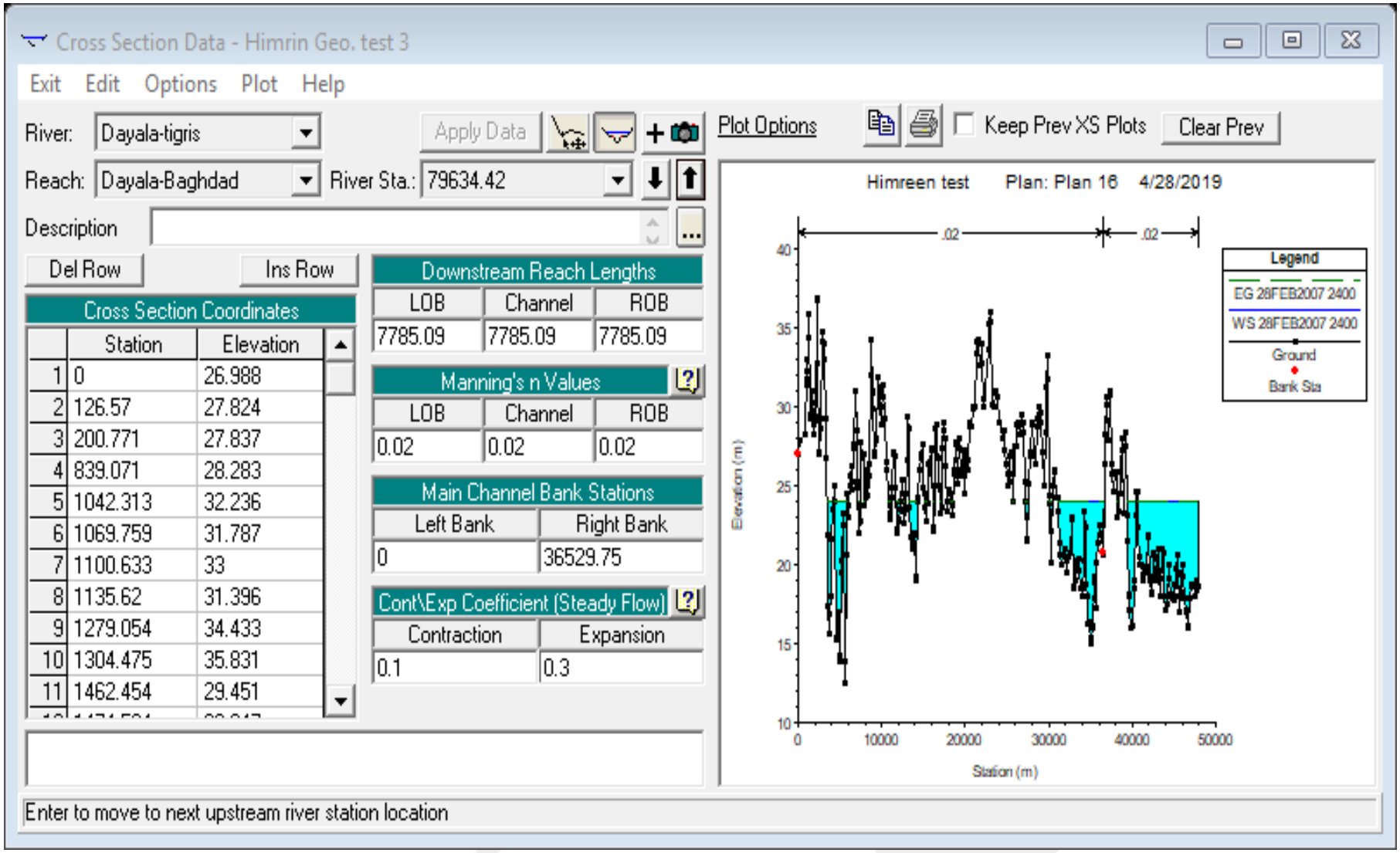

Figure 3.15 Cross-Section Number 79634.42

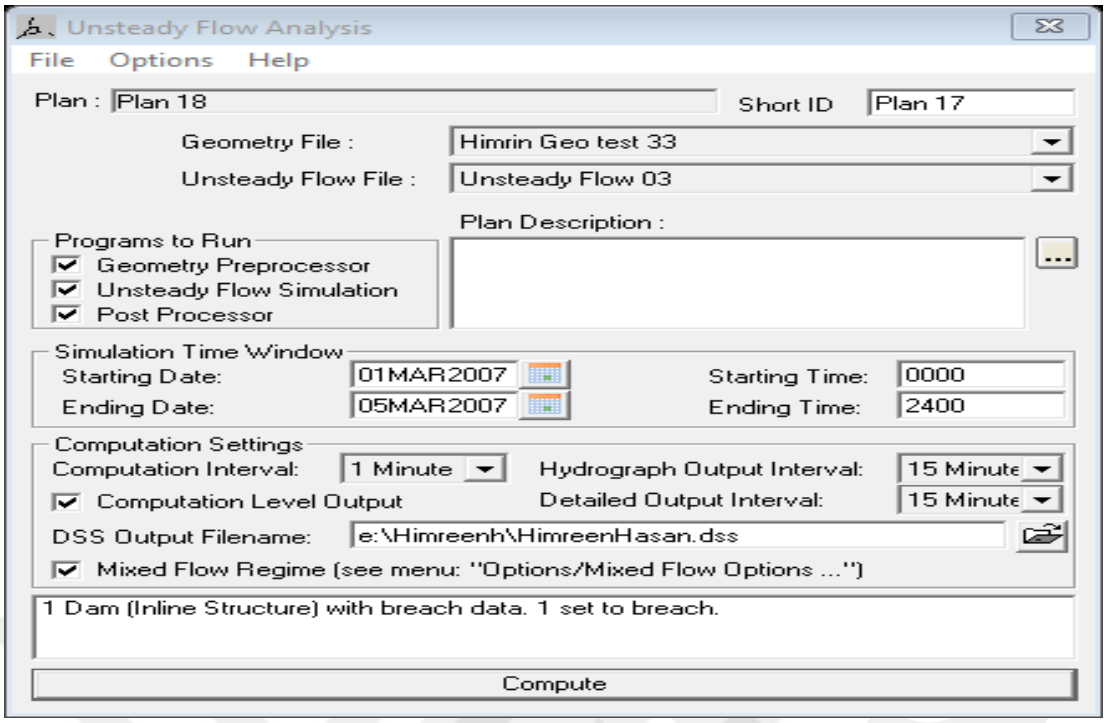

Figure 3.16 Unsteady Flow Analysis

3.3.1 Application of HEC-RAS for Scenario 1 :

In this scenario simulations were performed, using a value of Manning's roughness coefficient, which is equal to 0.028 for the whole cross-section. This value was chosen based on field observation and corresponding value in the tables given in Open Channels Hydraulics by Ven Te Chow [32]. In this scenario, unsteady flow analysis was performed and the results of the unsteady analysis of the simulation results are given in Fig 3.17, 3.18, 3.19, 3.20, and 3.21.

These cross-sections show the water surface, ground elevations, and horizontal propagation of water in the flood plain of the channel data provided from the Ministry of Water Resources [28].

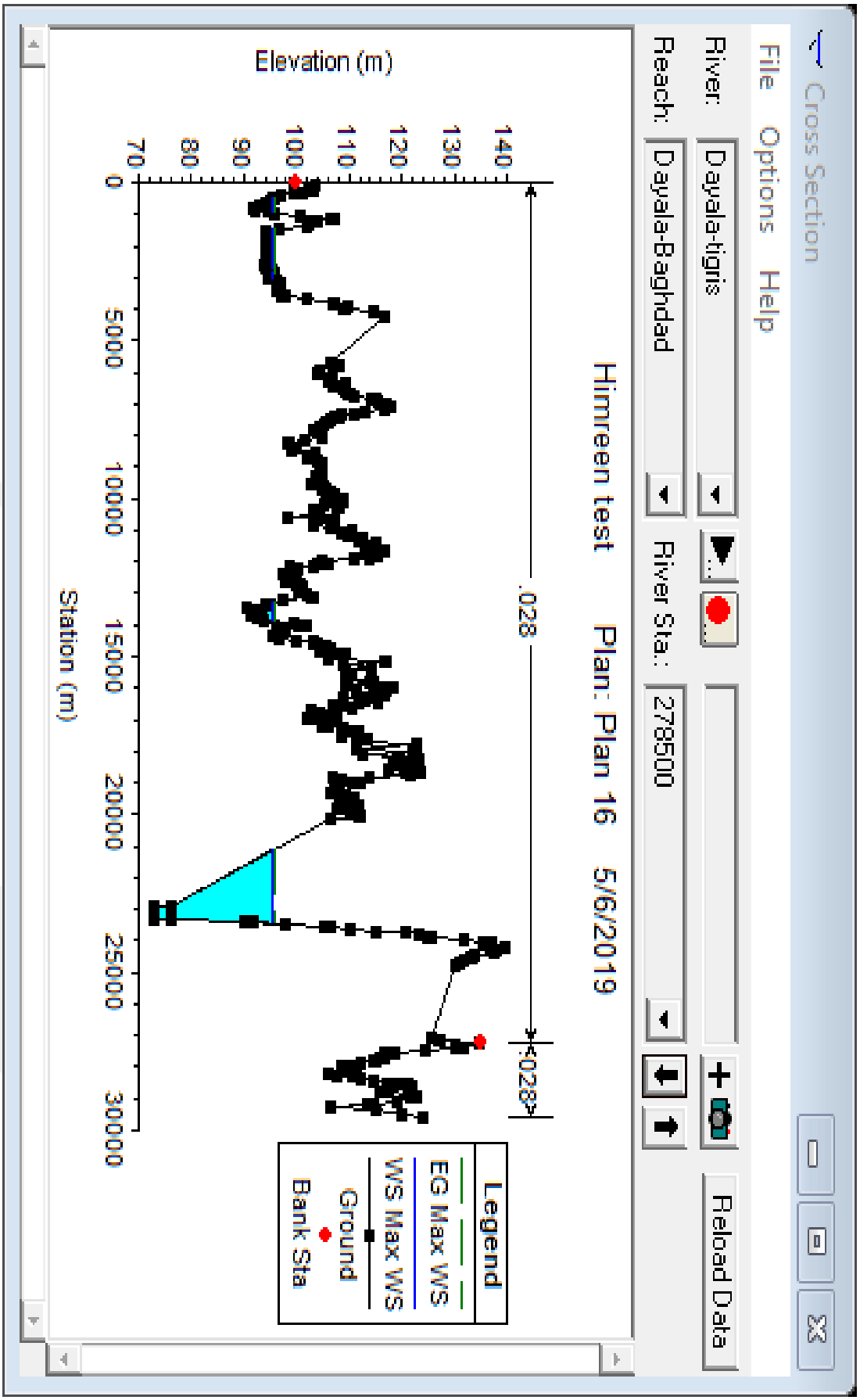

Figure 3.17 Cross-Section Number 278500 of Scenario 1

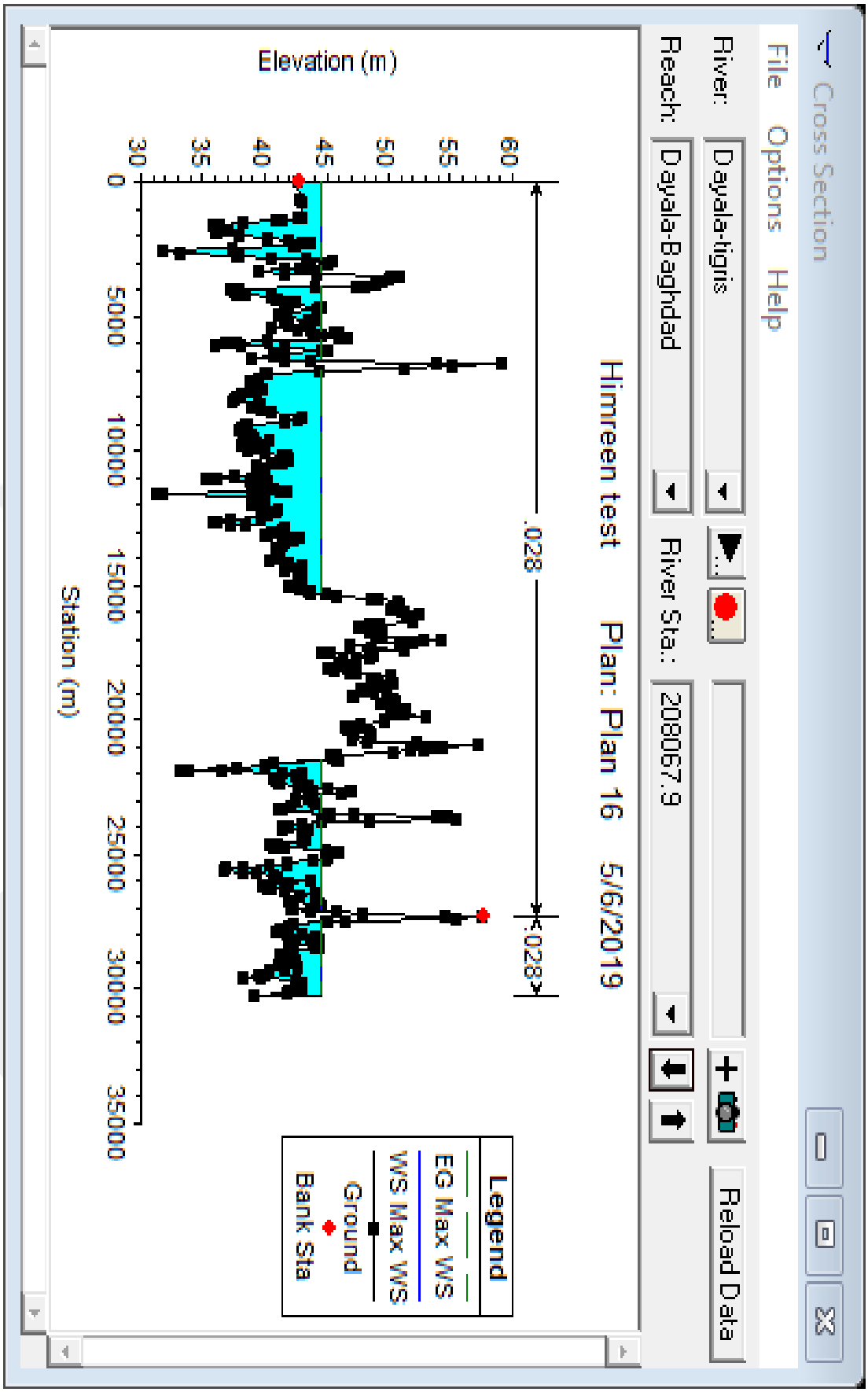

Figure 3.18 Cross-Section Number 208067.9 of Scenario 1

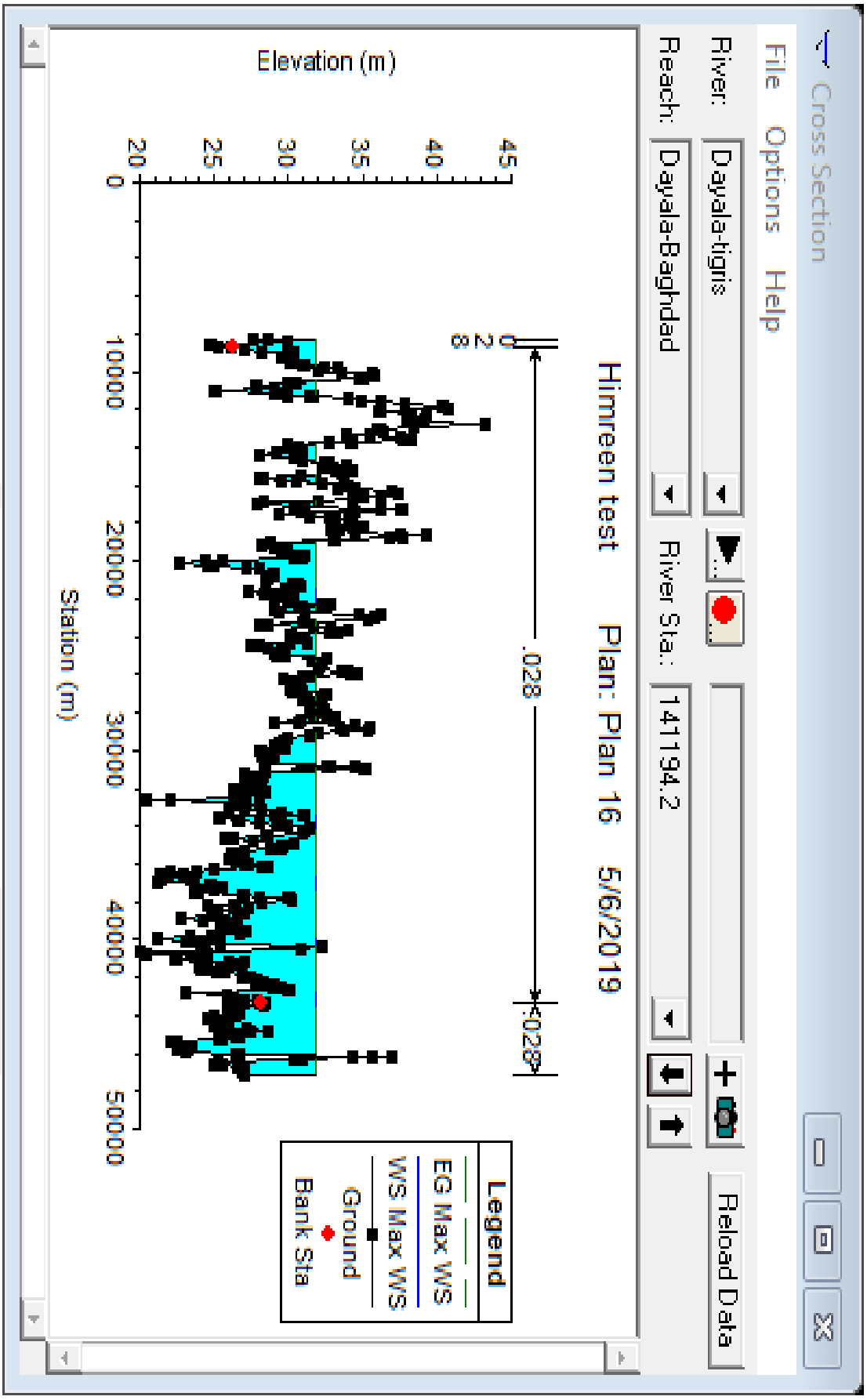

Figure 3.19 Cross-Section Number 141194.2 of Scenario 1

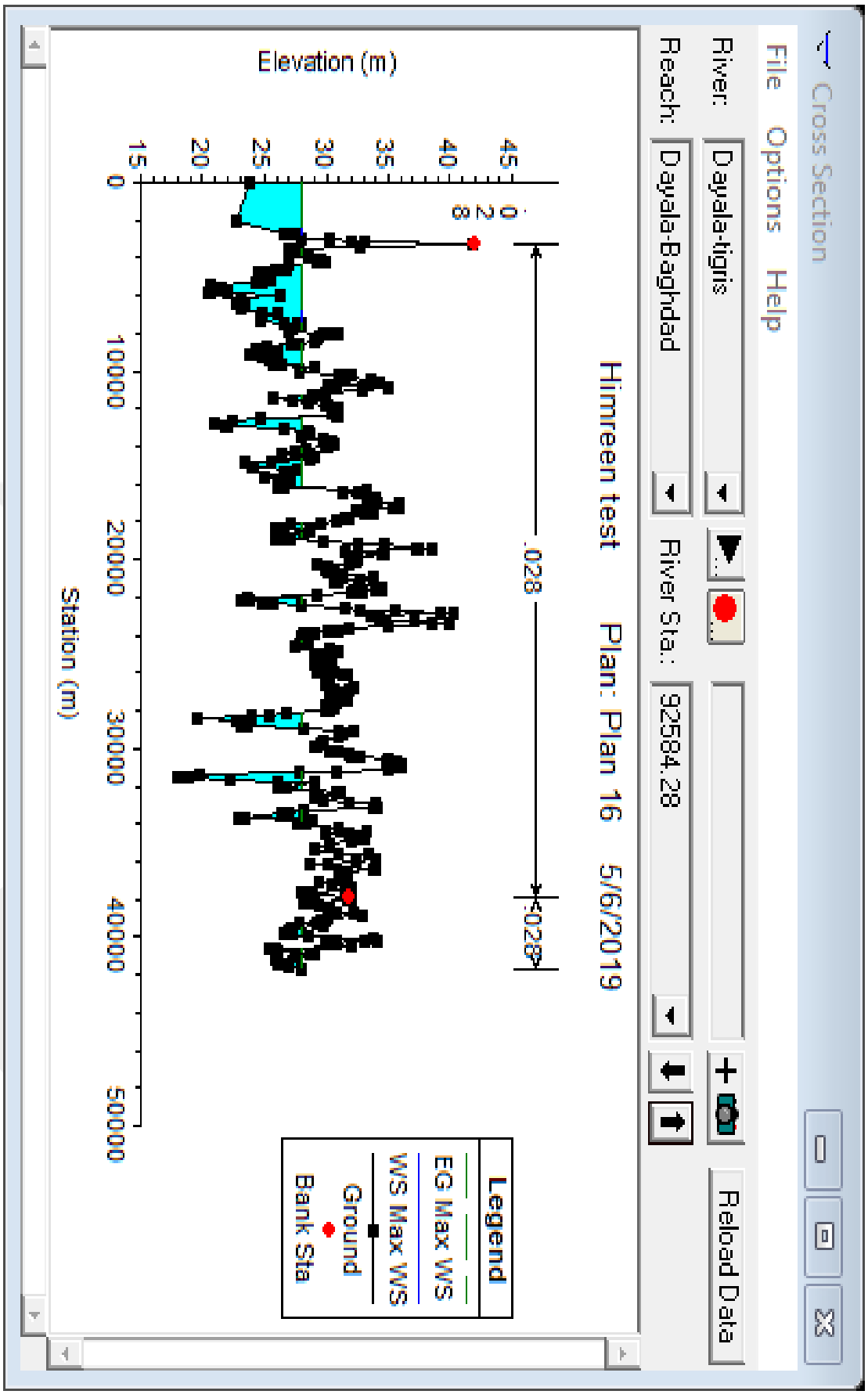

Figure 3.20 Cross-Section Number 92584.28 of Scenario 1

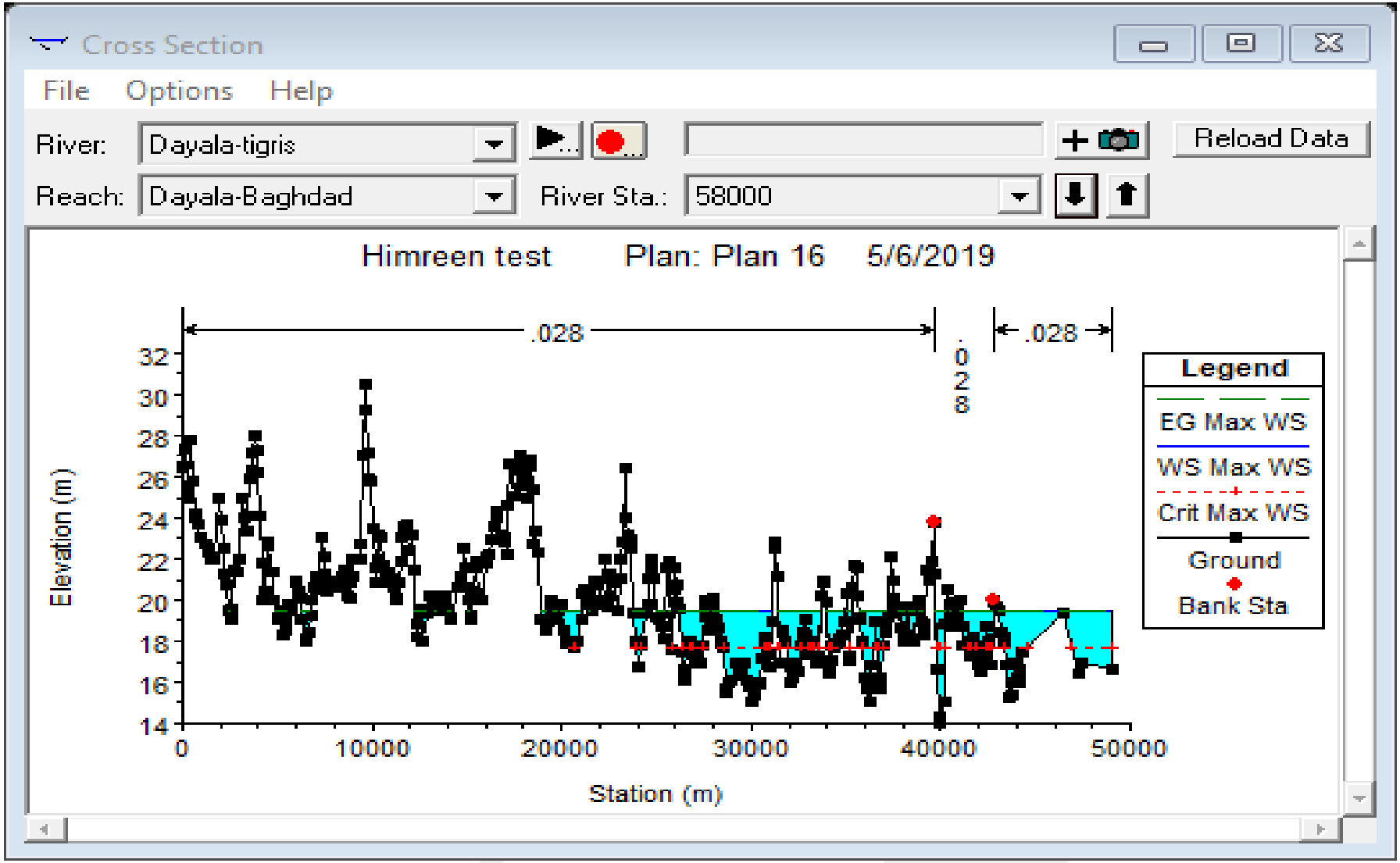

Figure 3.21 Cross-Section Number 58000 of Scenario 1

3.3.1.1 Water Surface Profile:

Water surface profile from the dam axis to the end of the cross-sections (a long distance 300 km) is shown in Fig 3.22. In this figure, the x-axis shows the distance between the Himreen dam and the Nomania city and the y-axis shows the water surface elevations. The water surface elevation is at the maximum downstream of the dam failure, and decreases in the downstream direction.

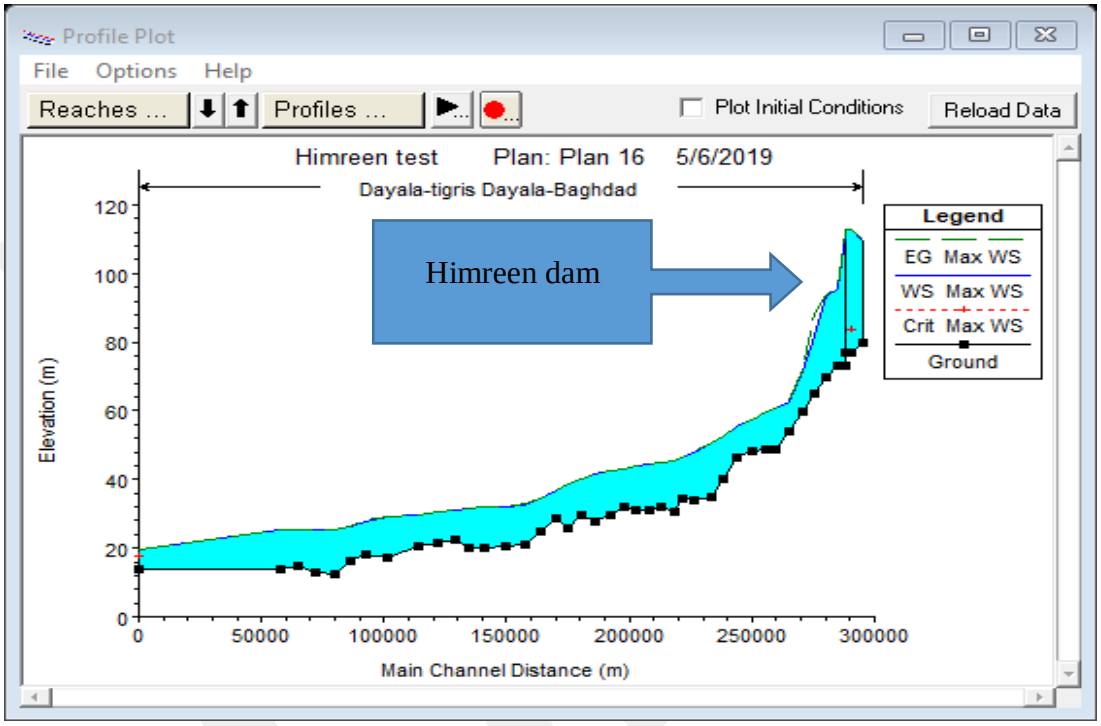

Figure 3.22 Longitudinal Water Surface Profile of Scenario 1

3.3.1.2 Velocity Profile and Water Propagation Area:

This part shows (1) velocity of the left and right banks and the centre of the cross-sections along the longitudinal profile ;(2) maximum water surface elevations of the left and right banks and at the centre of the cross-sections along the longitudinal profile (3) water propagation inundation areas (m^2) along the longitudinal profile of the reach. Fig 3.23 shows velocity values for left and right banks and the centre of the channel of the Diayla River. The velocity is maximum at the point of dam failure because it has high energy; this velocity decreases at the longitudinal profile of the Diayla River. Fig 3.24 shows the variation of the discharge along the longitudinal profile. Outflow from the Himreen Dam failure will be at the maximum in the dam failure and it decreased along the longitudinal profile of the Diayla River.

Fig 3.25 shows the flooded area of the Diayla River. The flooded area is minimum in the dam failure location and it increases and decreases in the flow area, because, as flooded discharge moves downstream, it spreads over the area thus flooded areas increase towards the downstream.

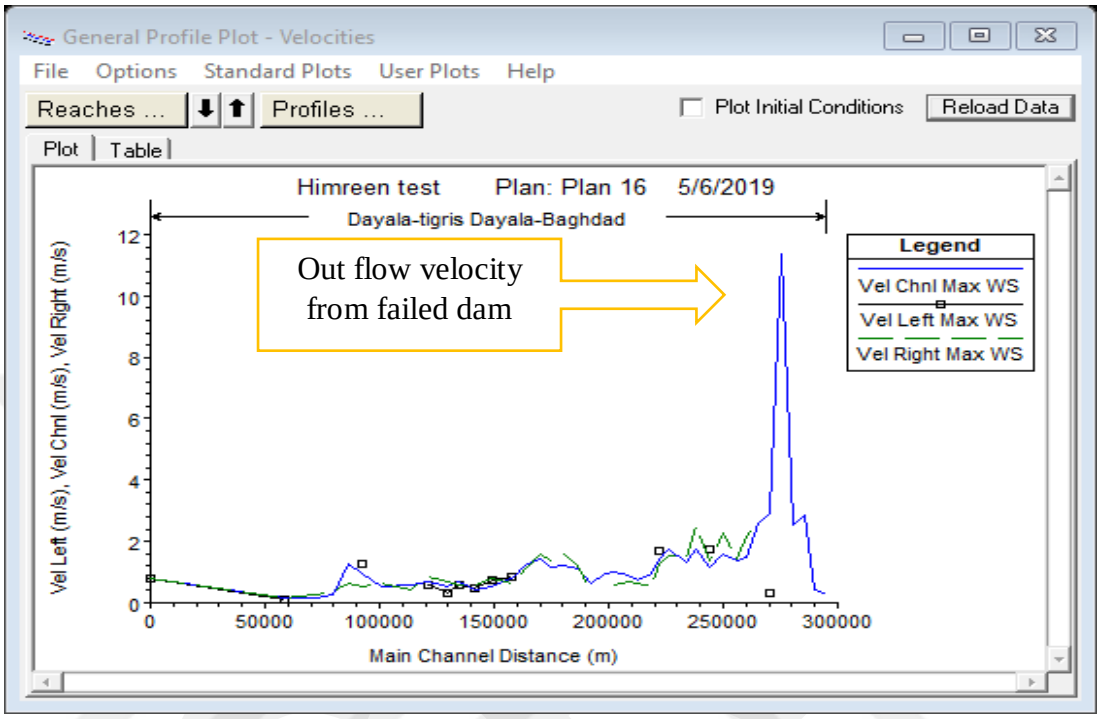

Figure 3.23 Velocity (m/s) Values at the left, right Banks and in the Center Channel along the Diayla River of Scenario 1

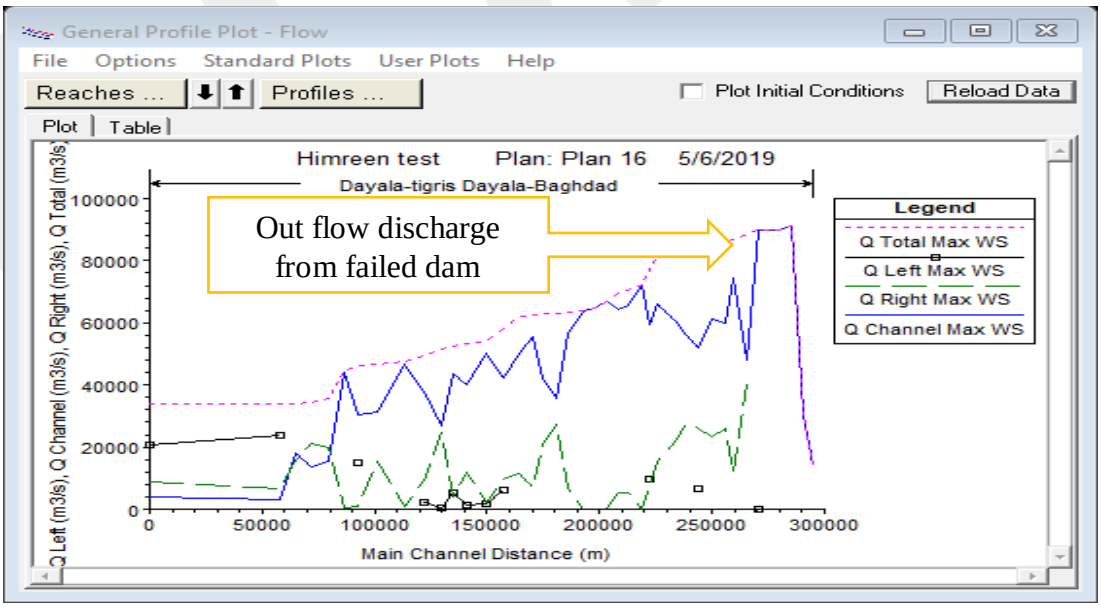

Figure 3.24 Variation of Flood Discharge along the Longitudinal Profile of the Diayla River of Scenario 1

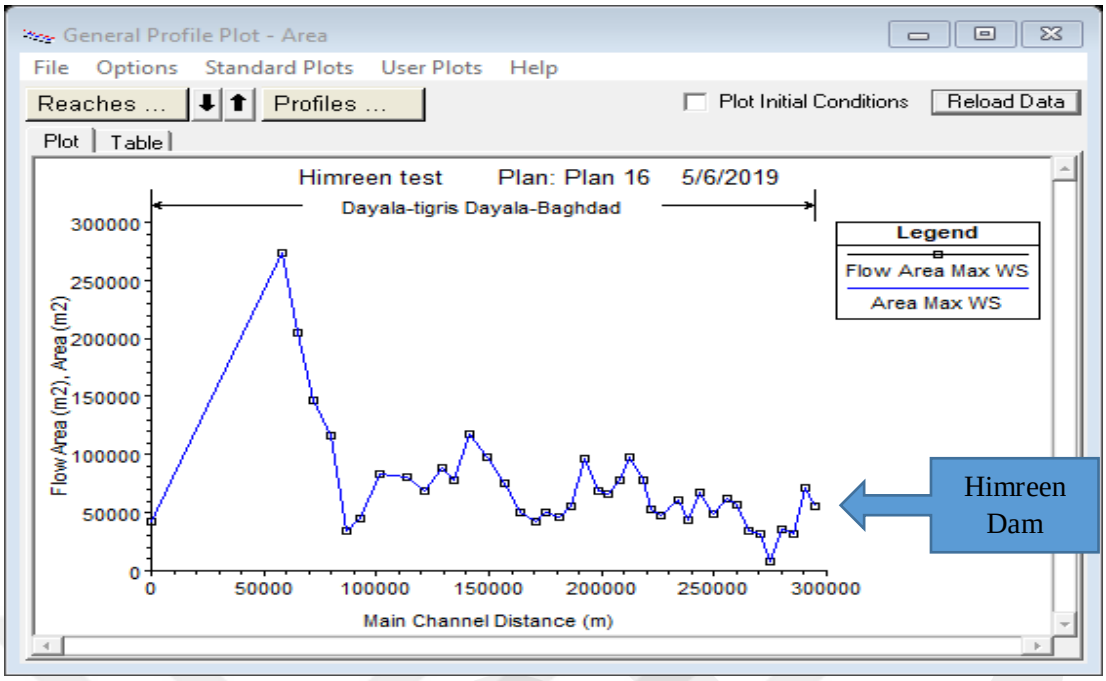

Figure 3.25 Flow Areas for Diayla River of Scenario 1

Fig 3.26 shows the stages and flow hydrograph during the failure stage. Fig 3.27 shows the detailed output tables for a cross-section. Fig 3.28 shows unsteady flow analysis. Fig 3.29 shows input data on Himreen overtopping case. As the dam starts to fail, outflow occurs and in a 24 hour period, the dam fails completely. From the start of the failure period to complete failure of the dam, it takes 4 days for the flood wave to reach Nomania.

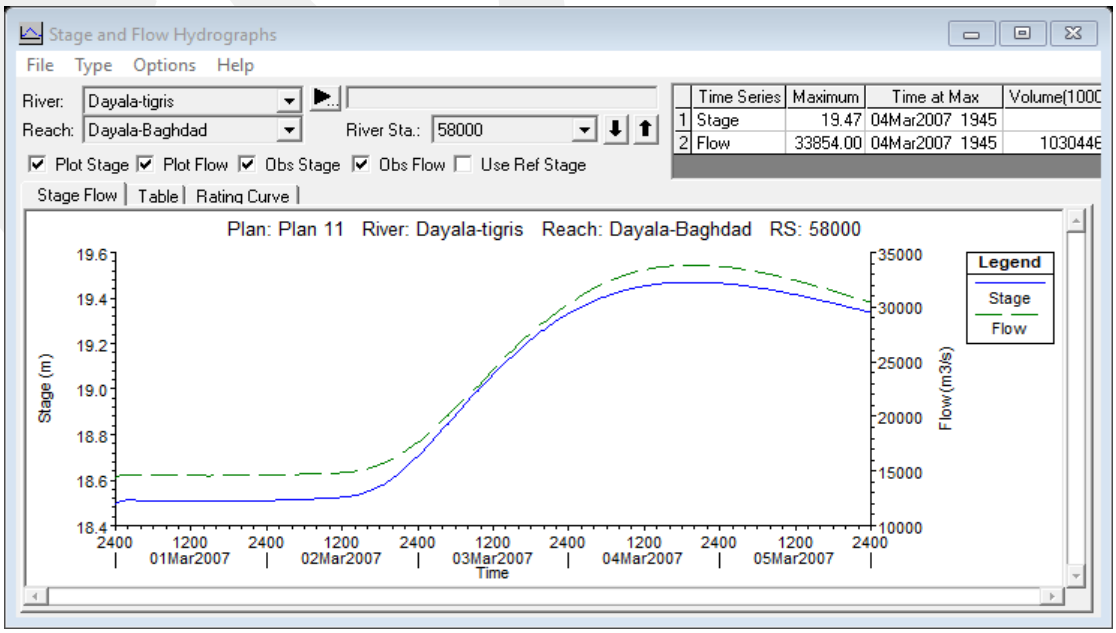

Figure 3.26 Stage and Flow Hydrograph of Station Number 58000 of Scenario 1

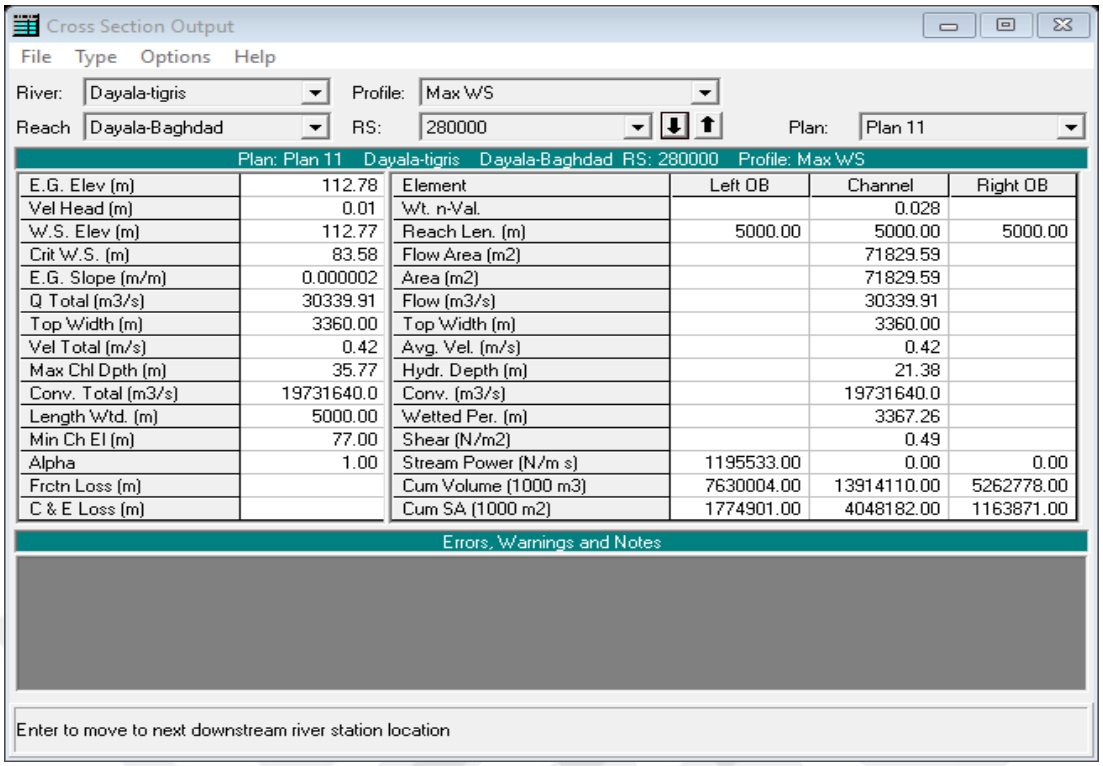

Figure 3.27 Detailed Output Tables of Scenario 1

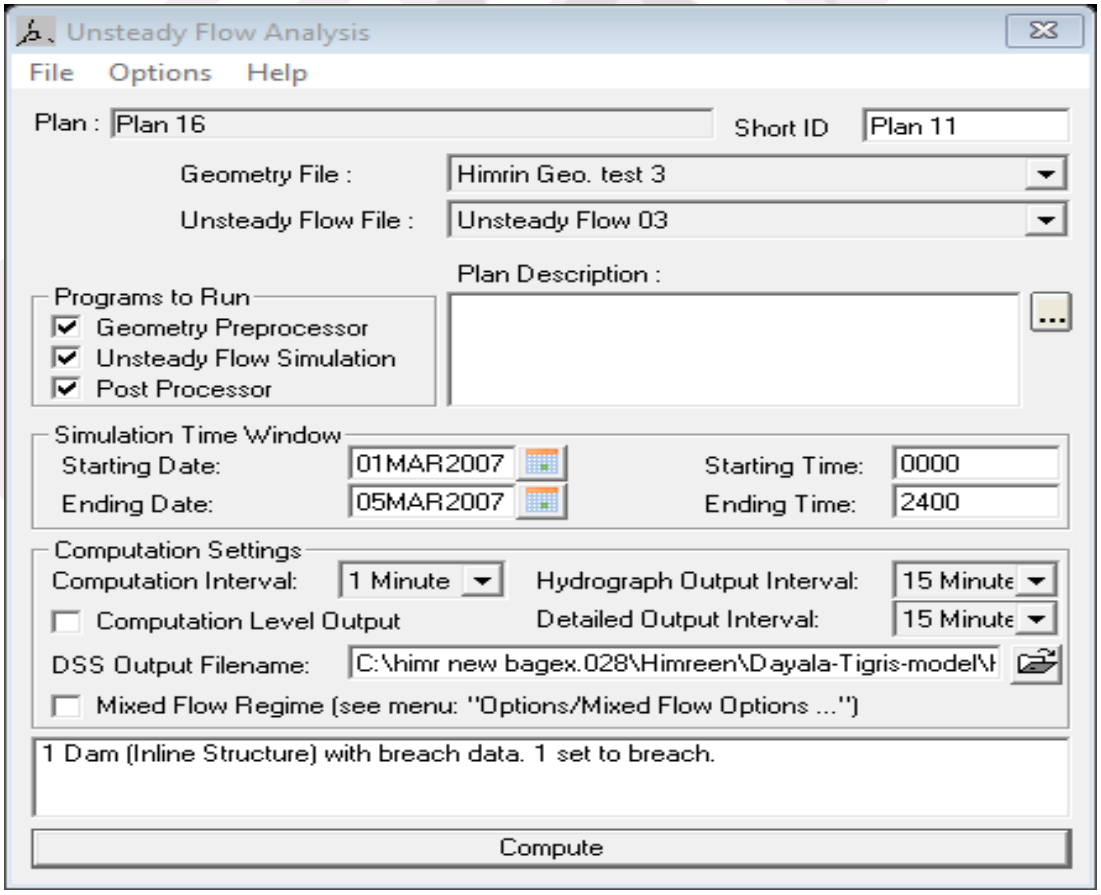

Figure 3.28 Unsteady Flow of Scenario 1

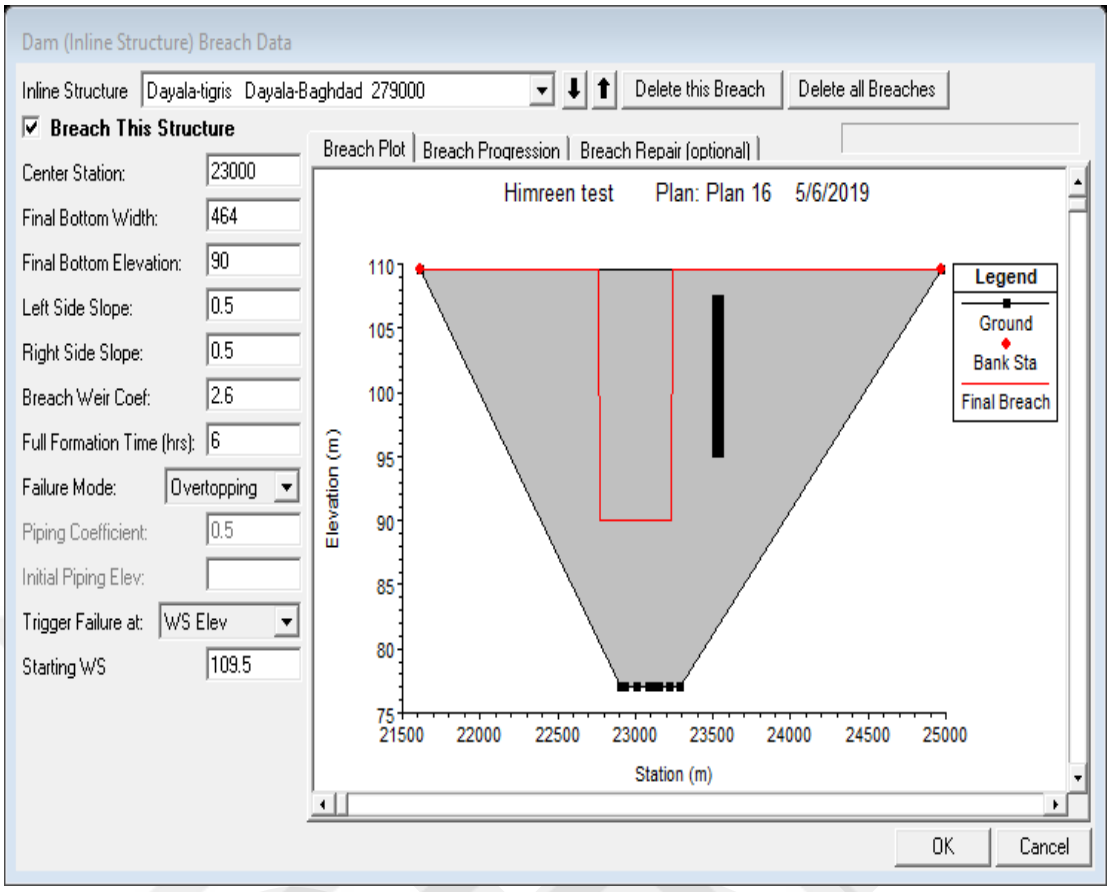

Figure 3.29 Input Himreen Dam Data Overtopping Case of Scenario 1

3.3.2 Application of HEC-RAS for Scenario 2 :

In this scenario simulations were performed, using a value of Manning's roughness coefficient, which is equal to 0.030 for the whole cross-section. To determine how sensitive the simulation results are with respect to different roughness [32]. In this scenario, unsteady flow analysis was performed and the results of the unsteady analysis of the program were given as output data. Simulation results are given in Figures 3.30, 3.31, 3.32, 3.33 and 3.34. Comparing water surface elevation in these with those in scenario 1 showed that water levels increased due to resistance caused by roughness [28]. These cross-sections show the water surface, ground elevations, and horizontal propagation of water in the flood plain of the channel data provided from the Ministry of Water Resources [28].

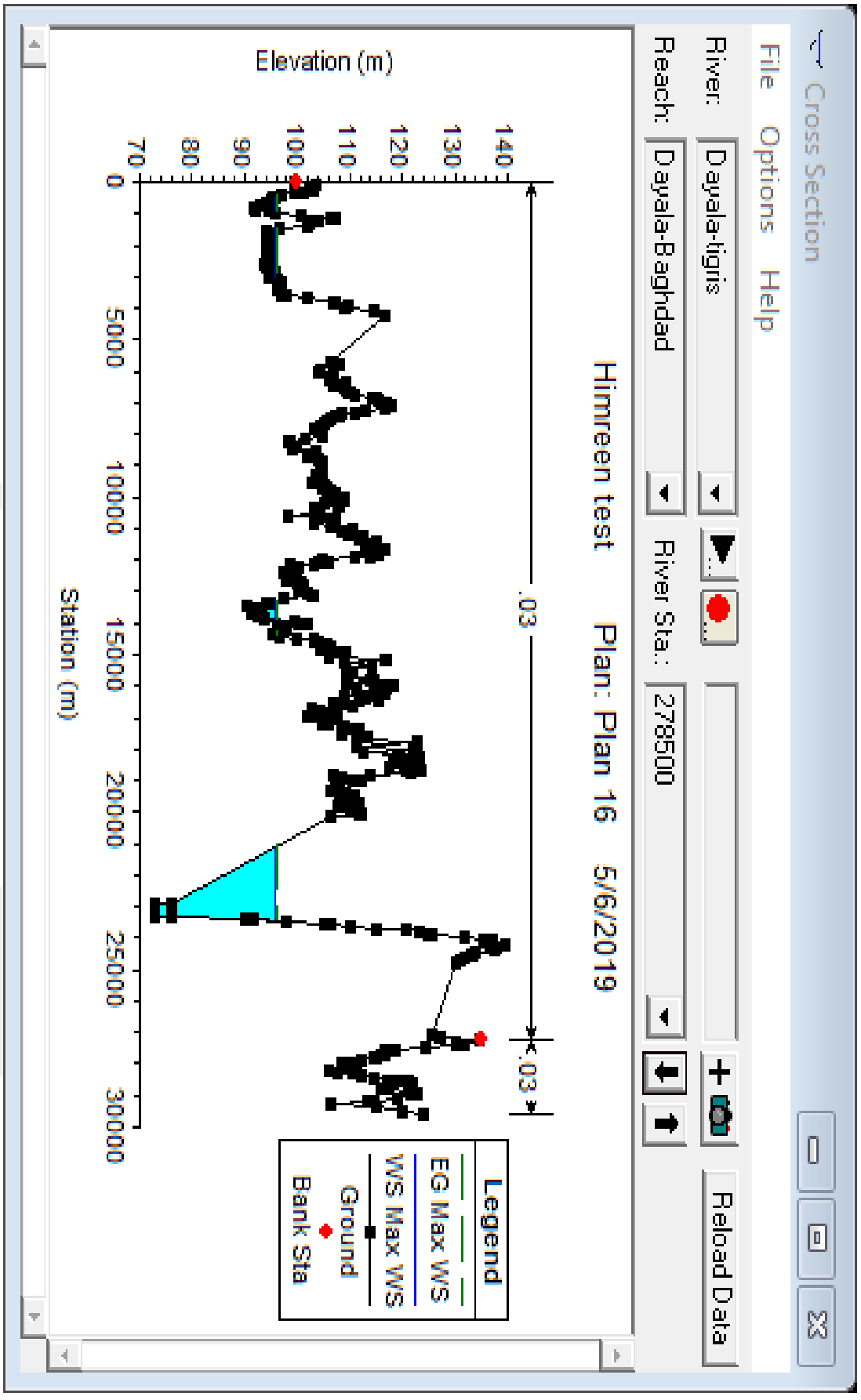

Figure 3.30 Cross-Section Number 278500 of Scenario 2

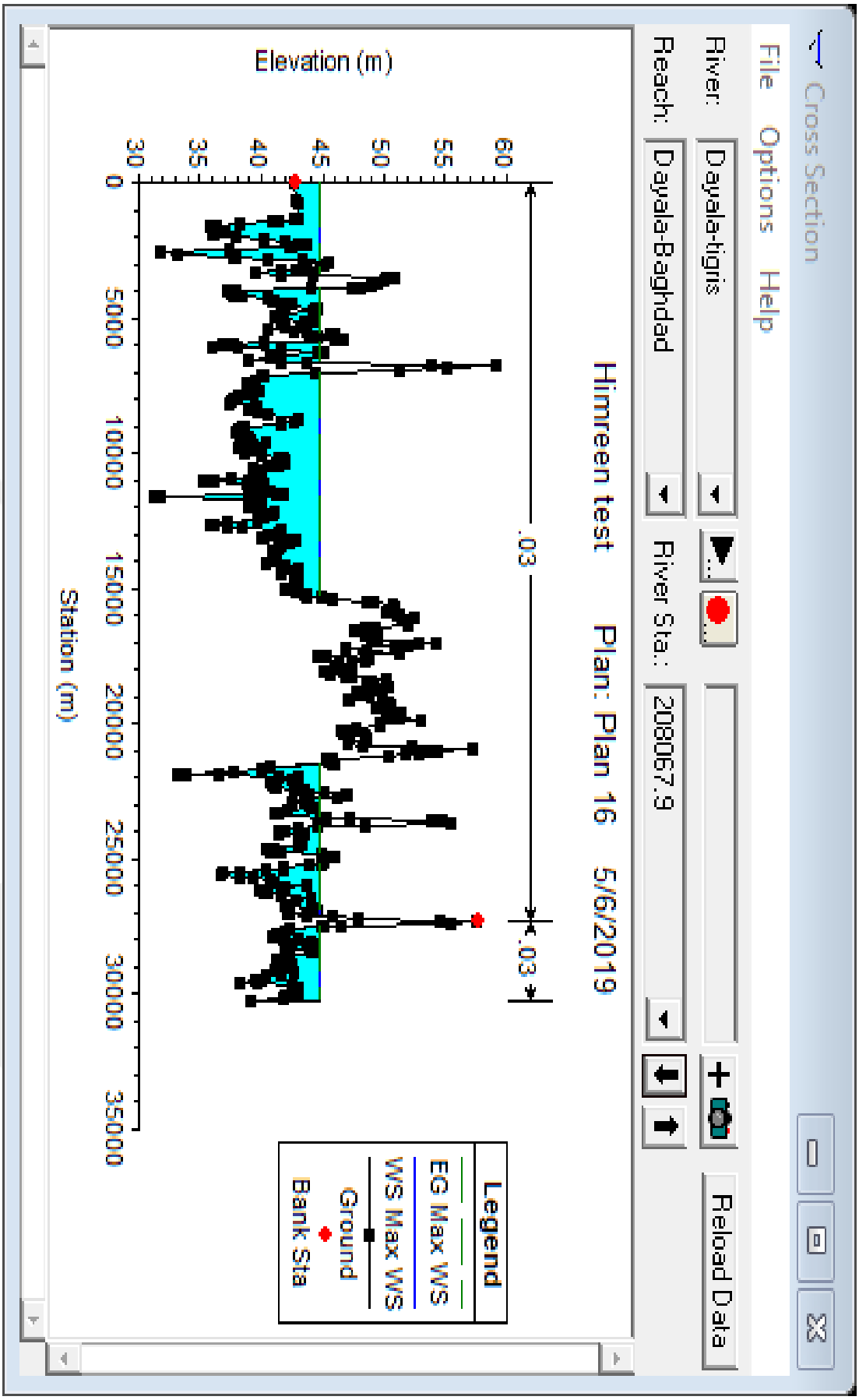

Figure 3.31 Cross-Section Number 208067.9 of Scenario 2

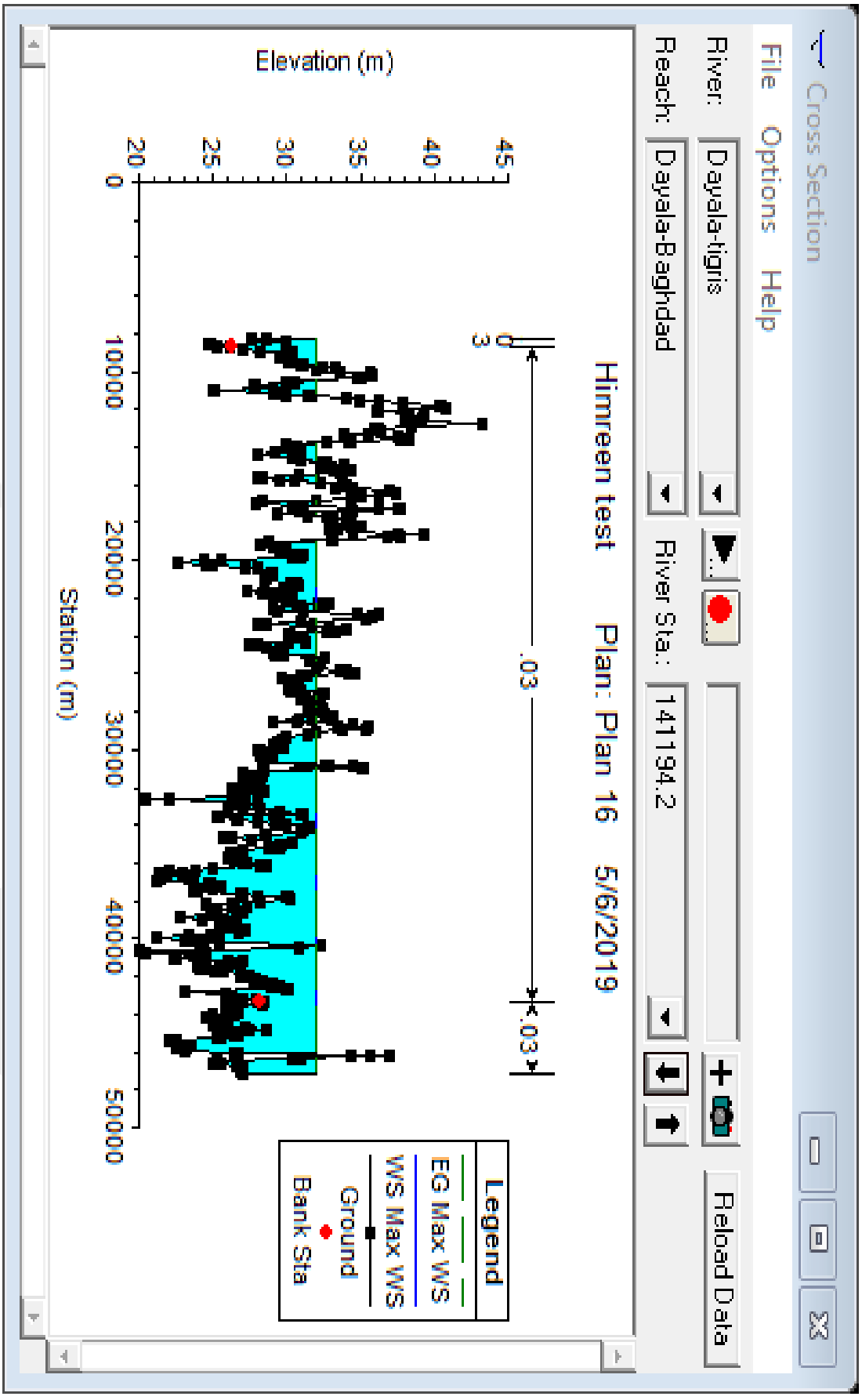

Figure 3.32 Cross-Section Number 141194.2 of Scenario 2

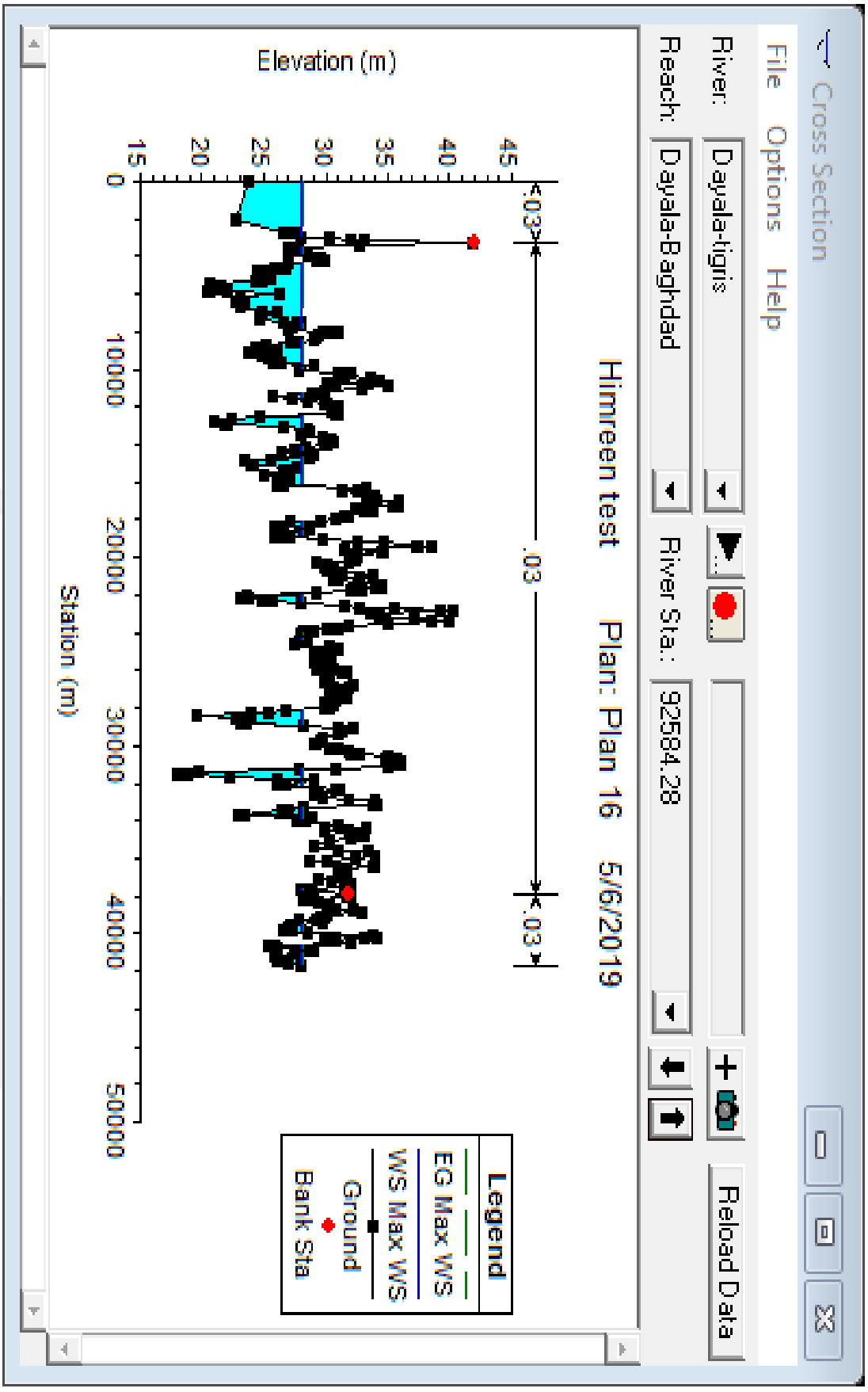

Figure 3.33 Cross-Section Number 92584.28 of Scenario 2

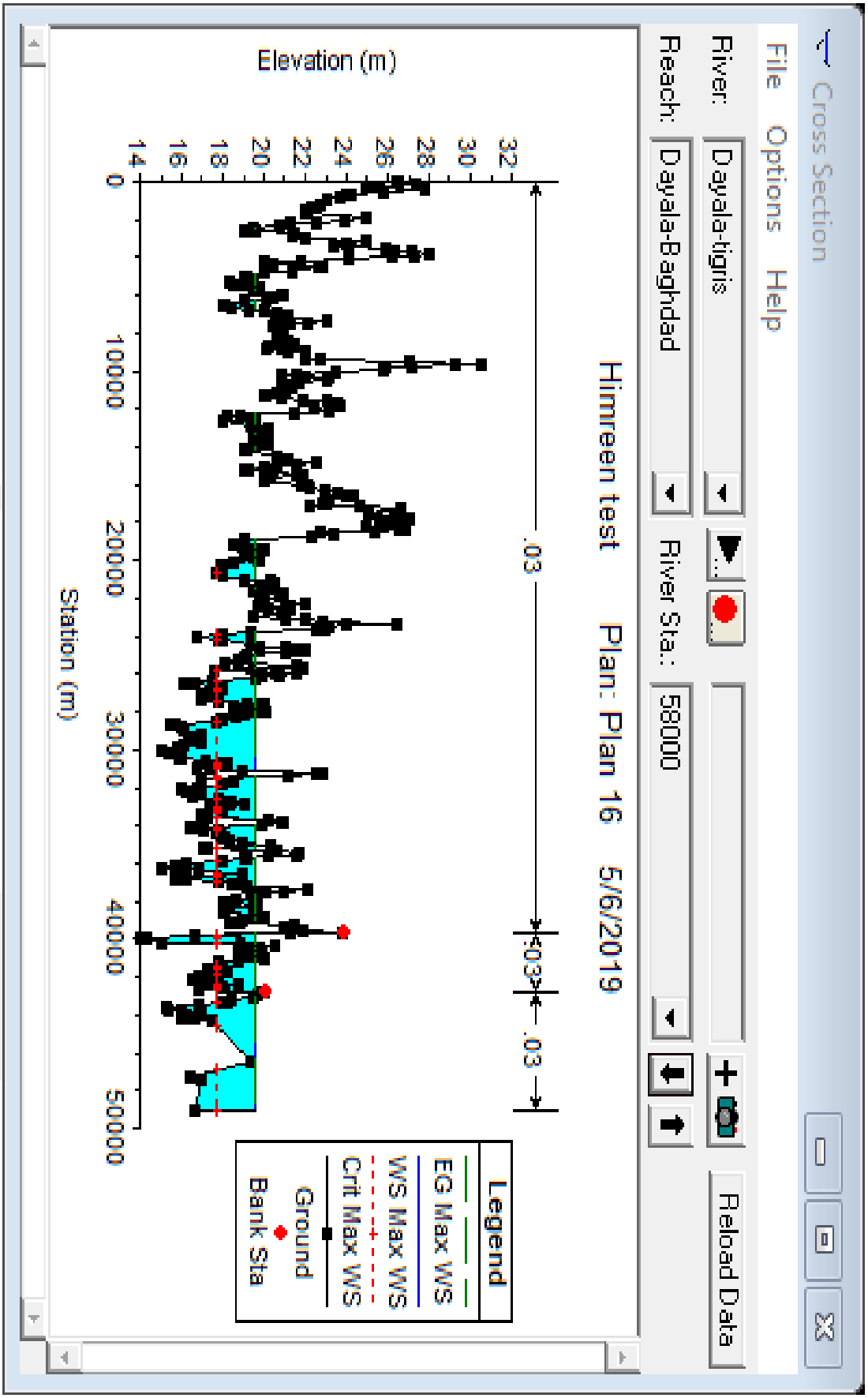

Figure 3.34 Cross-Section Number 58000 of Scenario 2

3.3.2.1 Water Surface Profile:

Water surface profile from the dam axis to the end of the cross-sections (a long distance 300 km) as shown in Fig 3.35. In this figure, the x-axis shows the distance and the y-axis shows the water surface elevation. The water surface elevation is at the maximum downstream of the dam failure, and decreasesd at the end of the downstream direction.

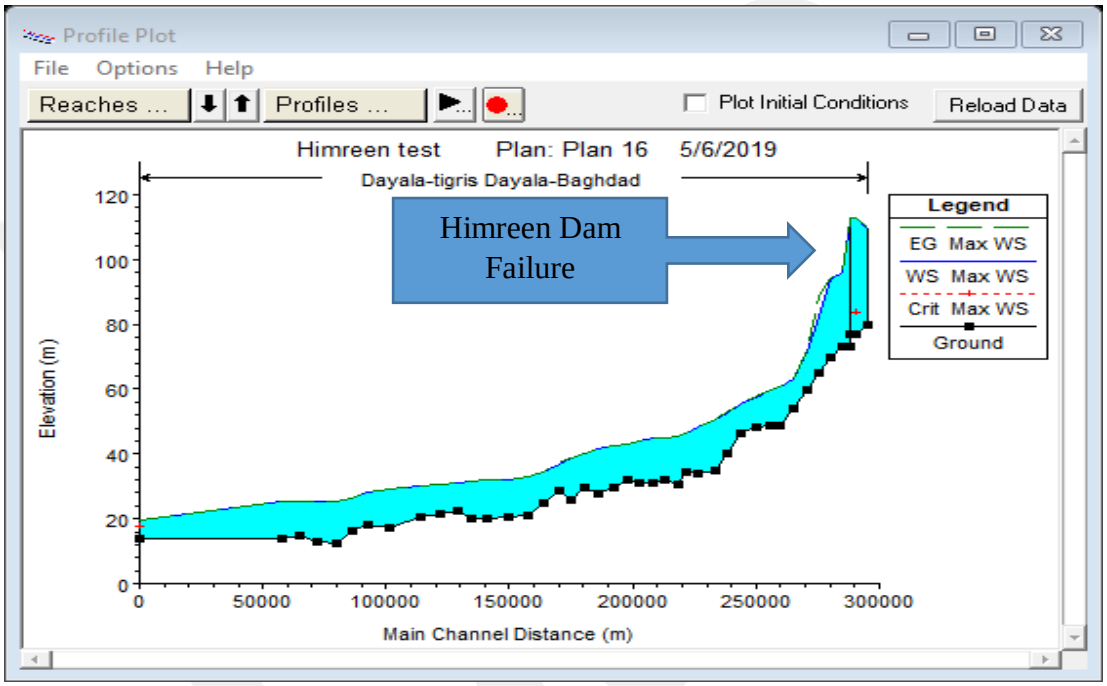

Figure 3.35 Longitudinal Water Surface Profile of Scenario 2

3.3.2.2 Velocity Profile and Water Propagation Area:

This part shows (1) velocity of the left and right banks and the centre of the cross-sections along the longitudinal profile; (2) maximum water surface elevations of the left and right banks and the centre of the cross-sections along the longitudinal profile (3) water propagation accumulation areas (m^2) along the longitudinal profile of the reach. Fig 3.36 shows velocity values for left and right banks and centre of the channel of the Diayla River. The velocity is maximum at the point of dam failure because it has high energy; this velocity decreases at the longitudinal profile of the Diayla River. Fig 3.37 shows the variation of the water surface elevations along the longitudinal

profile. Outflow from the Himreen Dam failure will be at the maximum in the dam failure and it decreased along the longitudinal profile on the Diayla River.

Fig 3.38 shows the flow area of the Diayla River. The flow area is minimum in dam failure location and it increases and decreases in other cross-sections because of the increase in the flooded area.

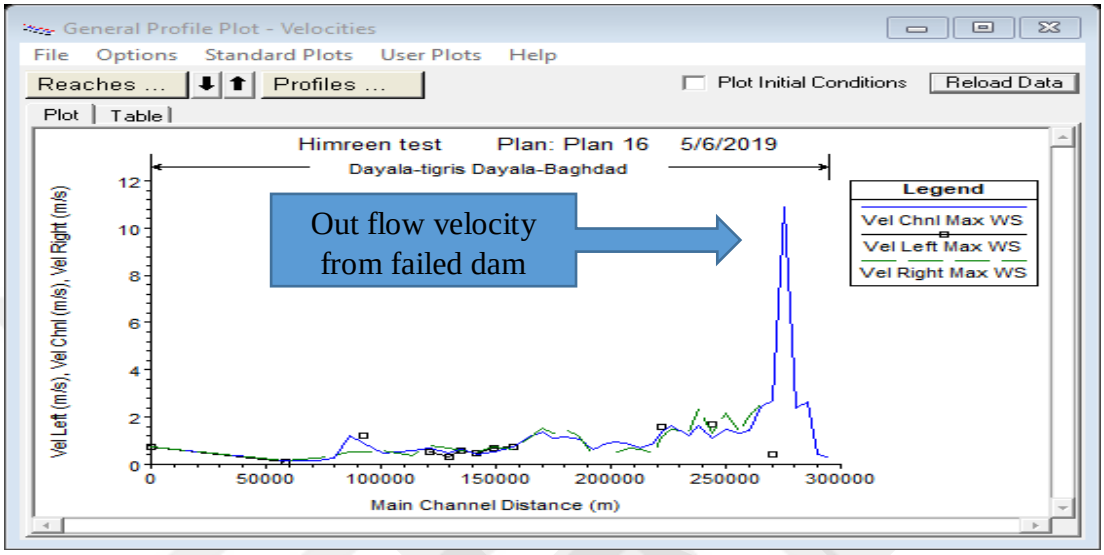

Figure 3.36 Velocity (m/s) Values at the Left, Right Banks and in the Center Channel Along the Diayla River of Scenario 2

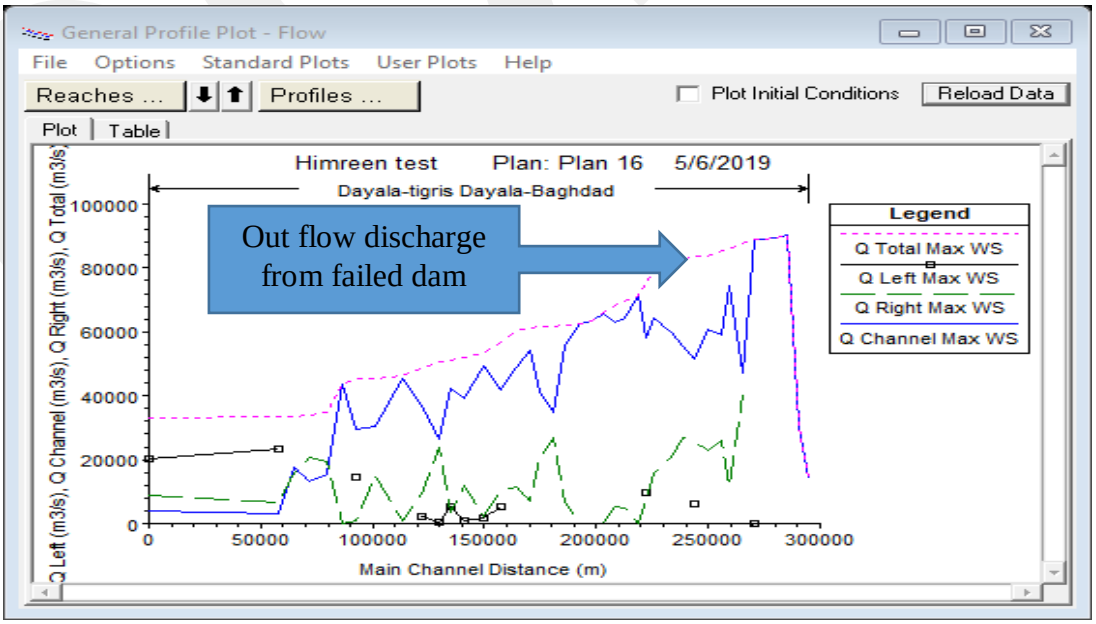

Figure 3.37 Variation of Flood Discharge along the Longitudinal Profile of the Diayla River of Scenario 2

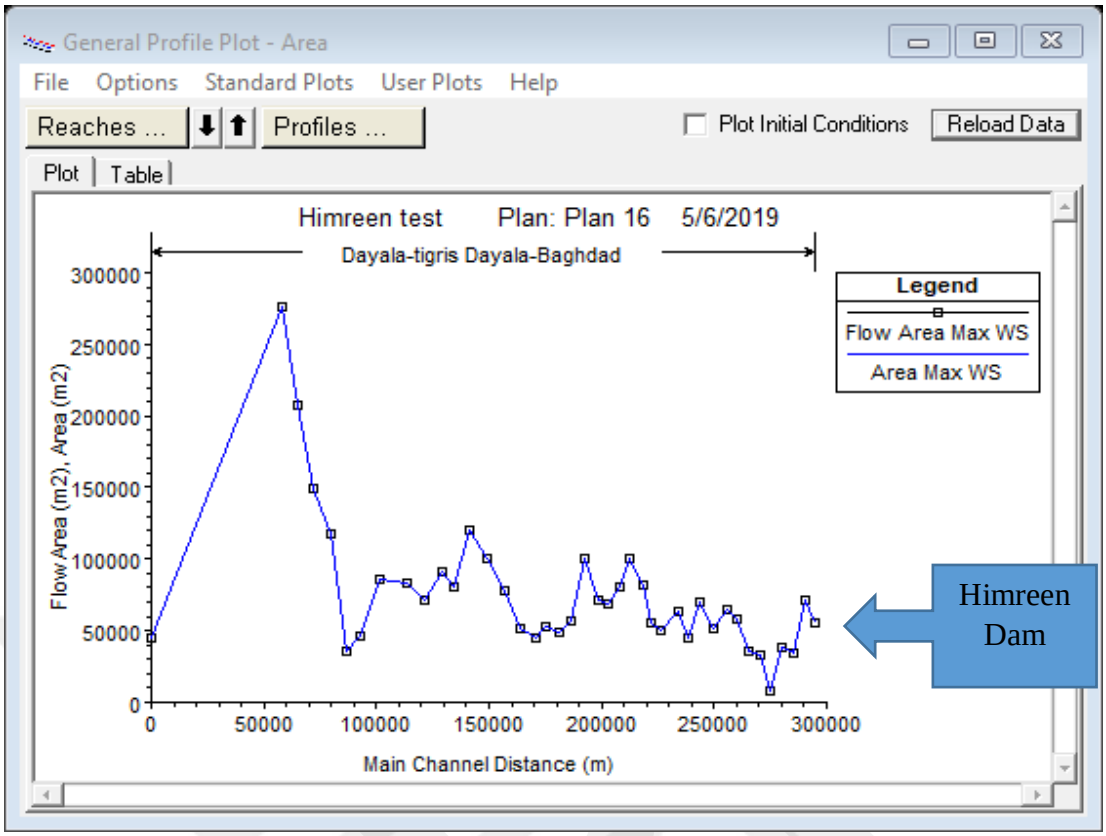

Figure 3.38 Flow Area of Diayla River of Scenario 2

Fig 3.39 shows the stages and flow hydrograph during the failure stage in scenario 2. Fig 3.40 shows the detailed output tables for a cross-section. Fig 3.41 shows unsteady flow analysis of scenario 2. Figure 3.42 shows input data on Himreen overtopping case. The starting time to dam failure is 24 hours which means the maximum time from overtopping to total failure while processing progress for the wave's continuity for 4 days, which means the maximum time needed to reach the water wave to Nomania and also to cover the whole 300 km distance.

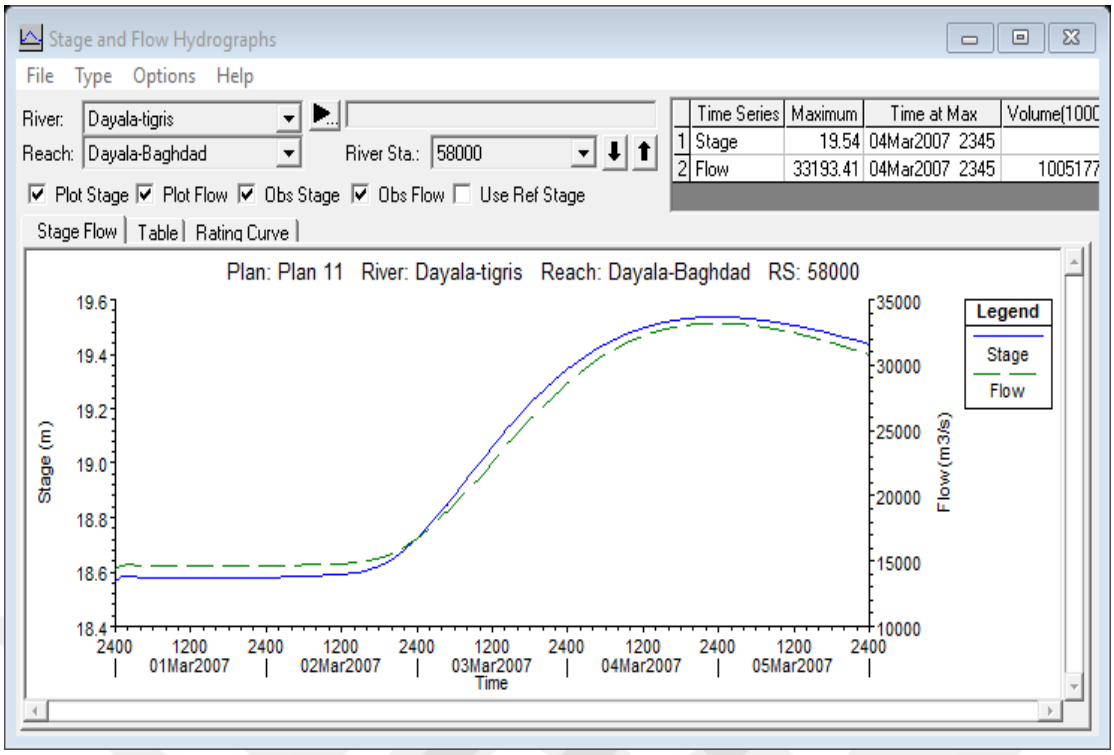

Figure 3.39 Stage and Flow Hydrograph of Station Number 58000 of Scenario 2

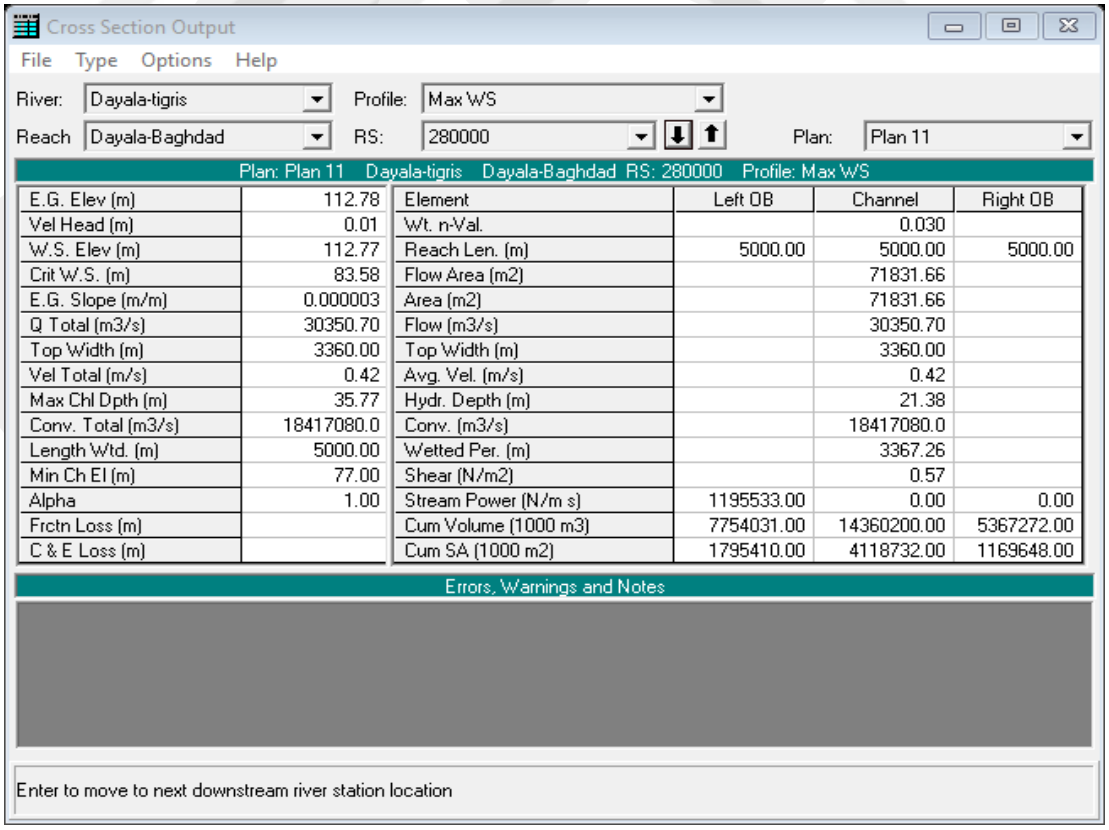

Figure 3.40 Detailed Output Tables of Scenario 2

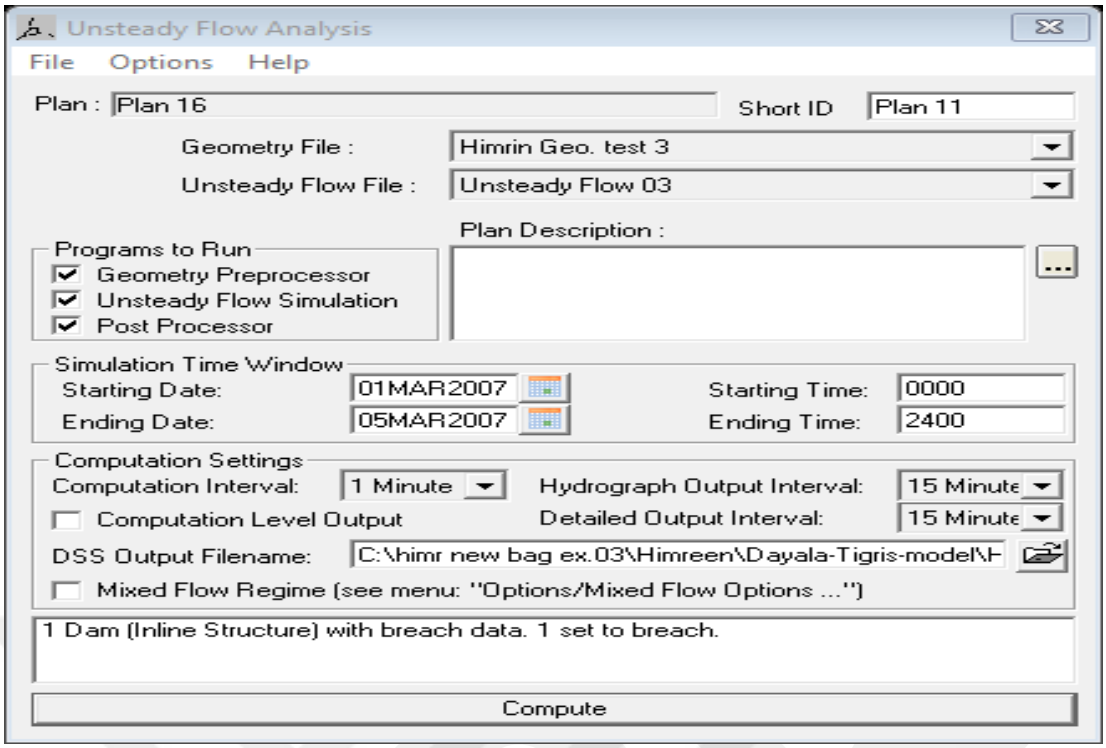

Figure 3.41 Unsteady Flow Analysis of Scenario 2

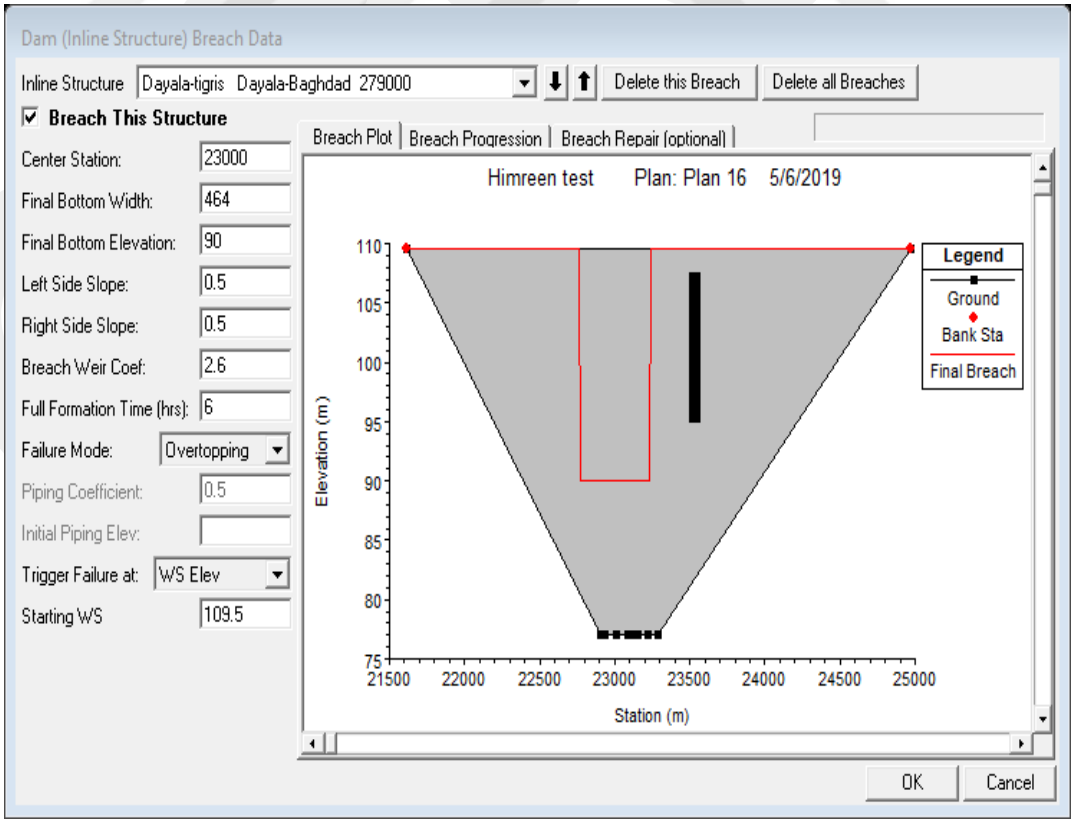

Figure 3.42 Data of Himreen Dam (Overtopping case) of Scenario 2

3.3.3 Application of HEC-RAS for Scenario 3 :

In this scenario simulations were performed, using a value of Manning's roughness coefficient, which is equal to 0.035 for the whole cross-section. This value was chosen for sensivity analysis of the high value of Manning's roughness on the magnitude, depth and arrival time of the flood. In this scenario, unsteady flow analysis was performed and the results of the unsteady analysis of the simulation results are given in Figs 3.43, 3.44, 3.45, 3.46, and 3.47.

These cross-sections show the water surface, ground elevations, and horizontal propagation of water in the flood plain of the channel data provided by the Ministry of Water Resources [28].

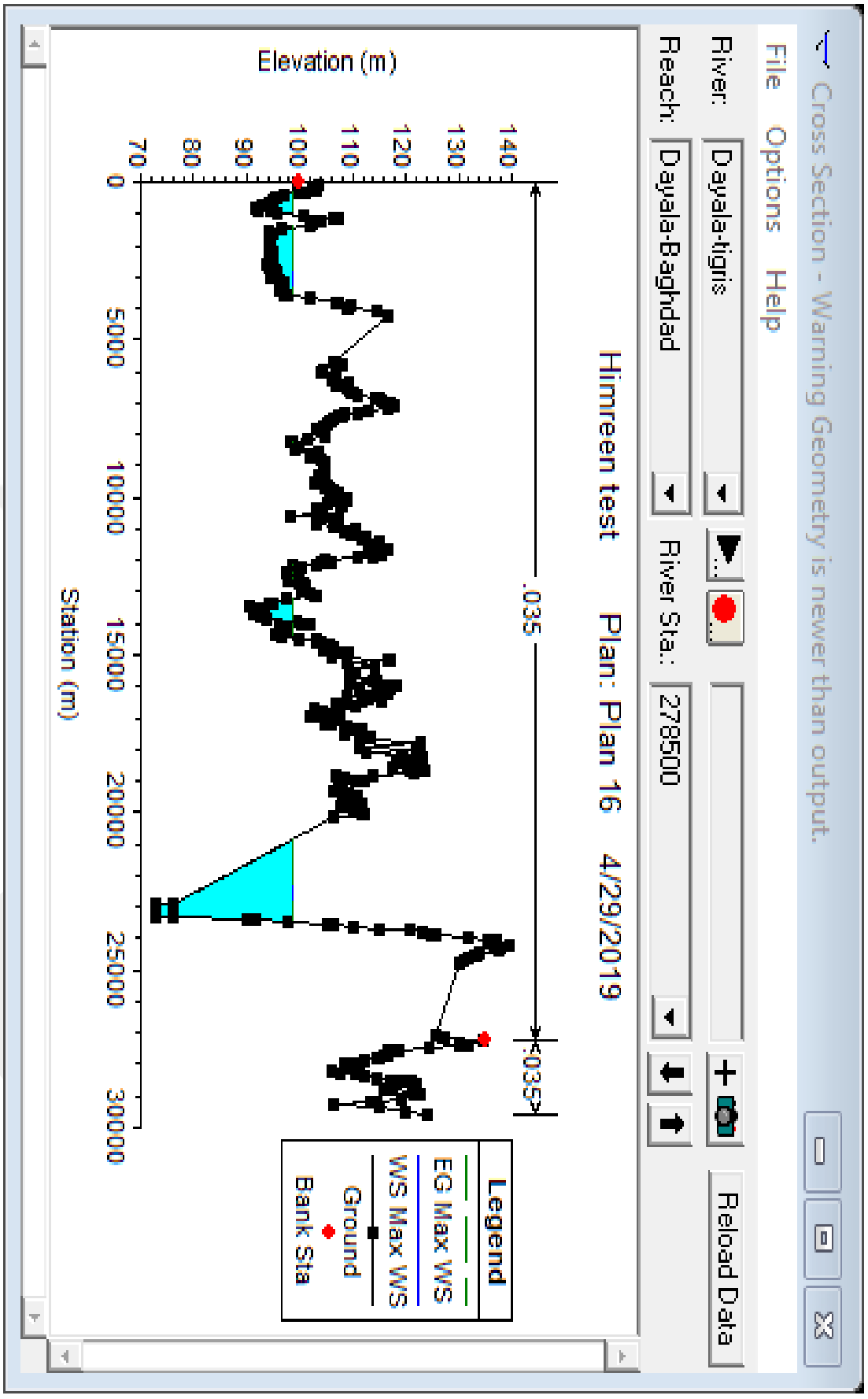

Figure 3.43 Cross-Section Number 278500 of Scenario 3

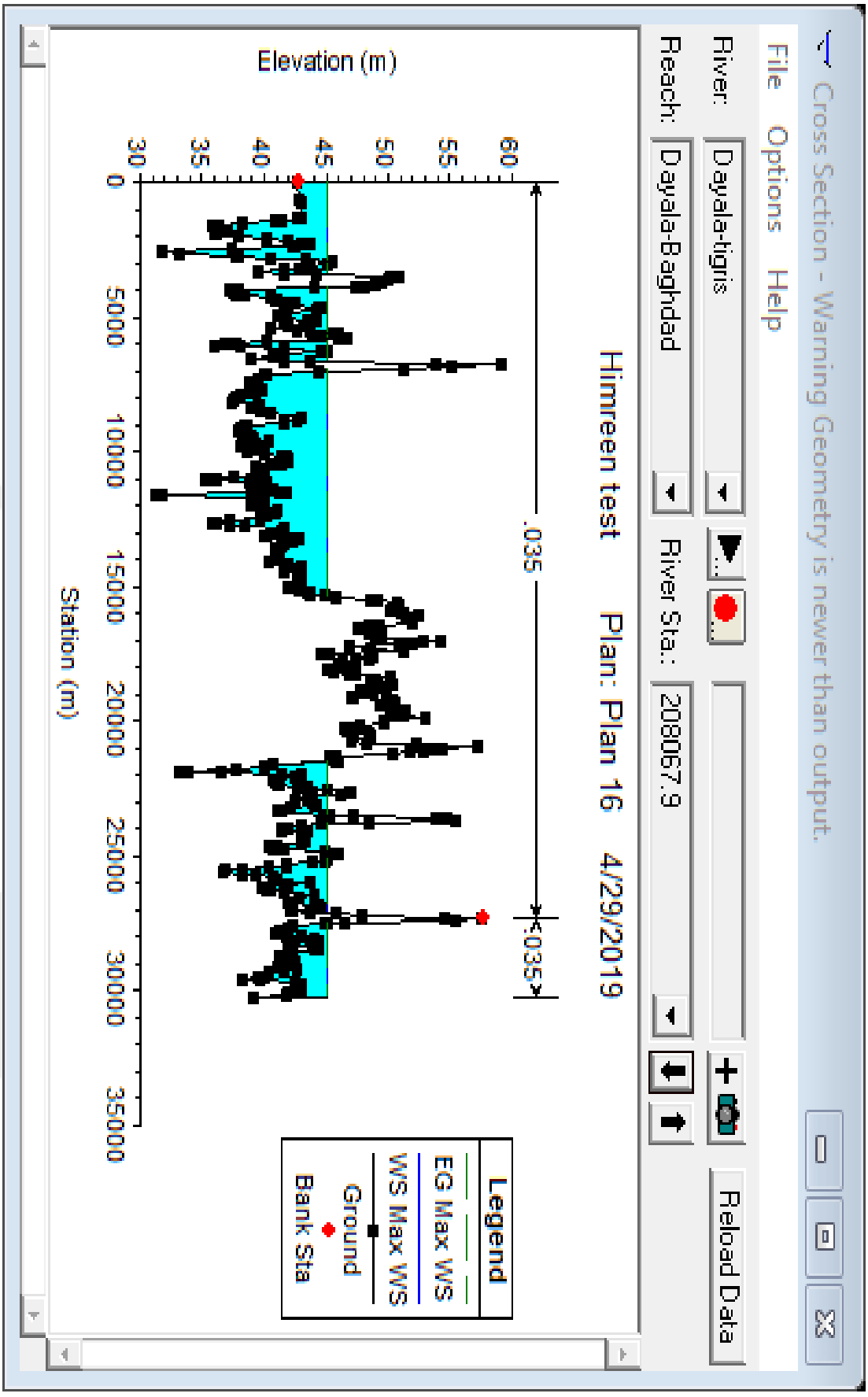

Figure 3.44 Cross-Section Number 208067.9 of Scenario 3

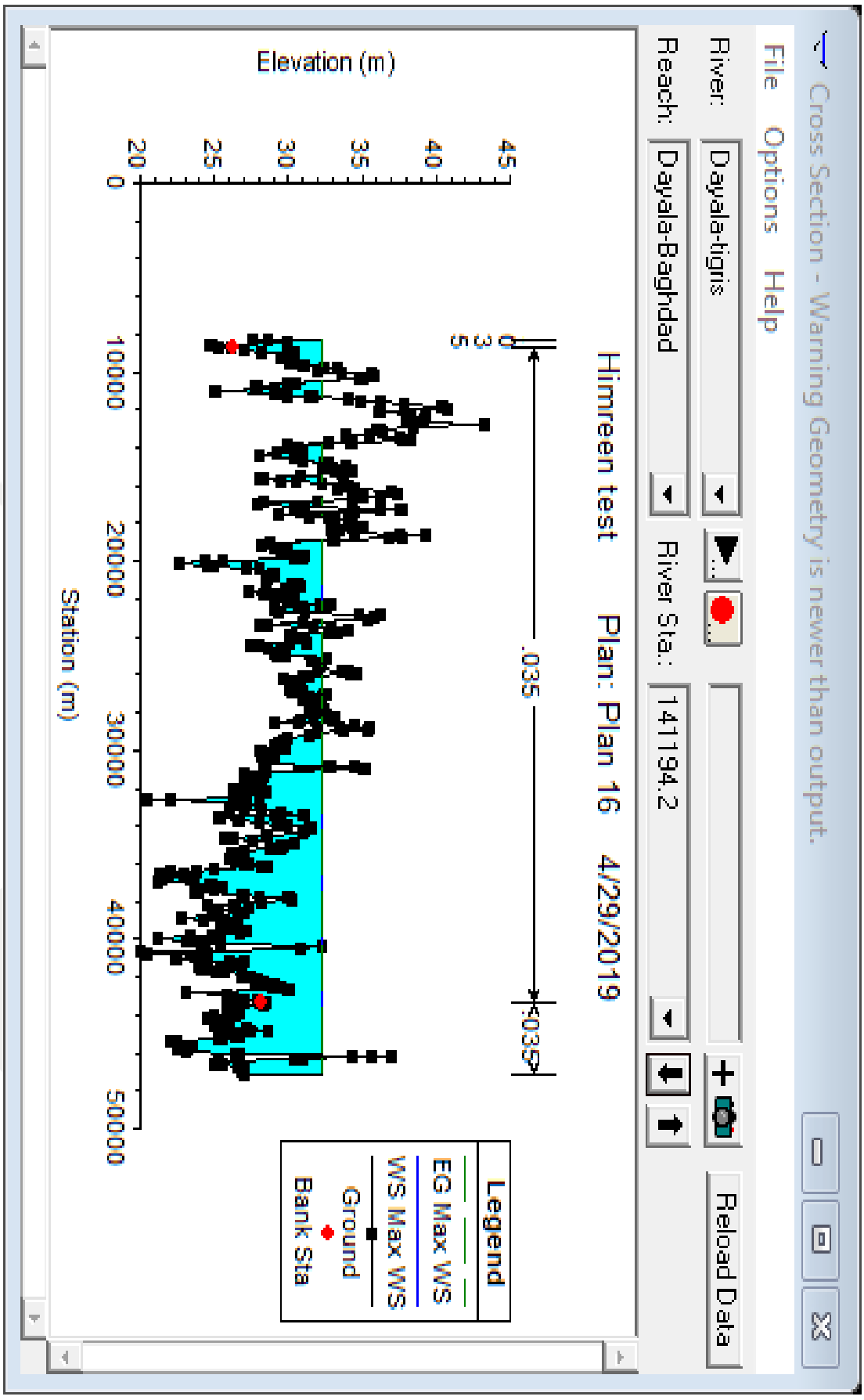

Figure 3.45 Cross-Section Number 141194.2 of Scenario 3

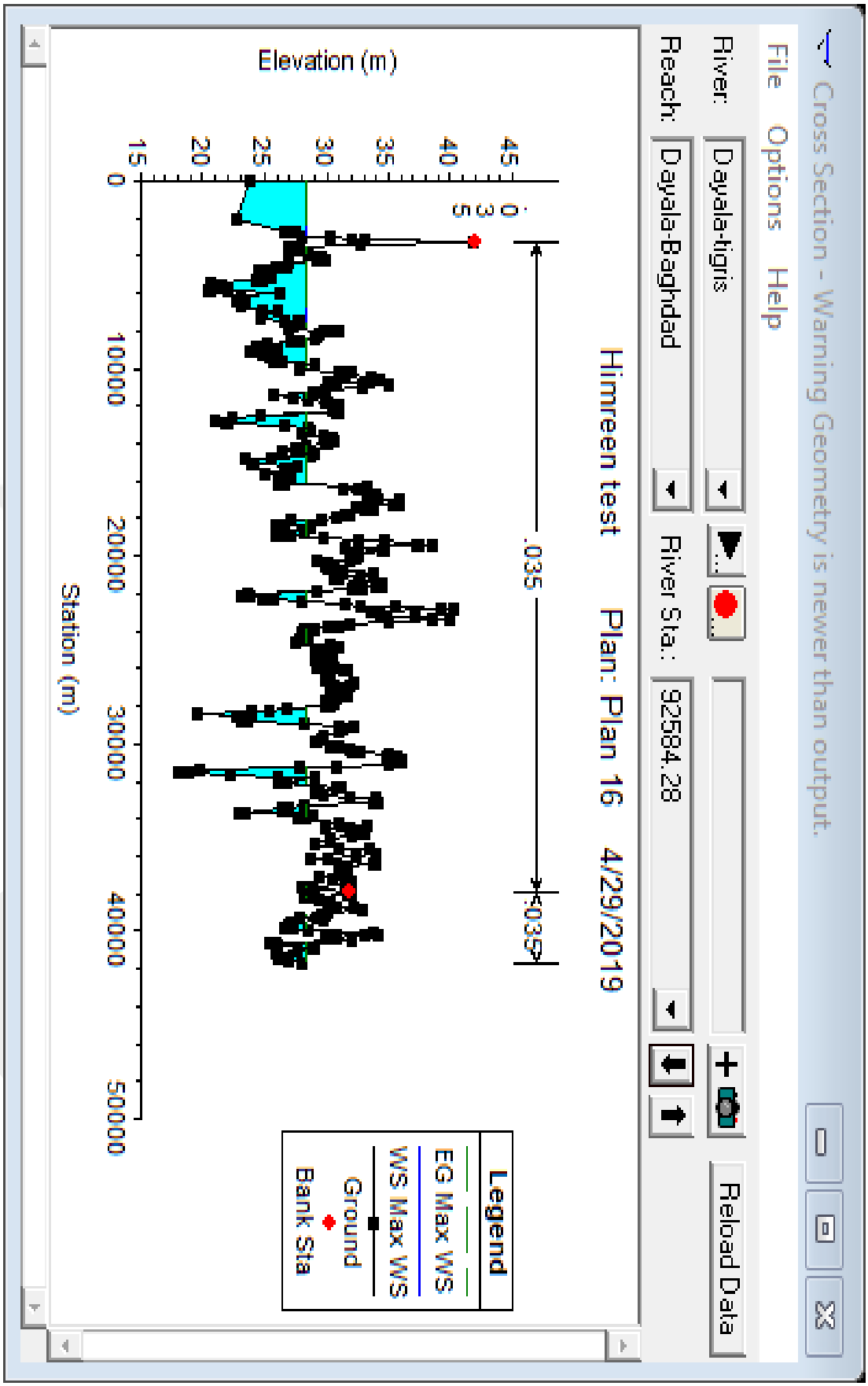

Figure 3.46 Cross-Section Number 92584.28 of Scenario 3

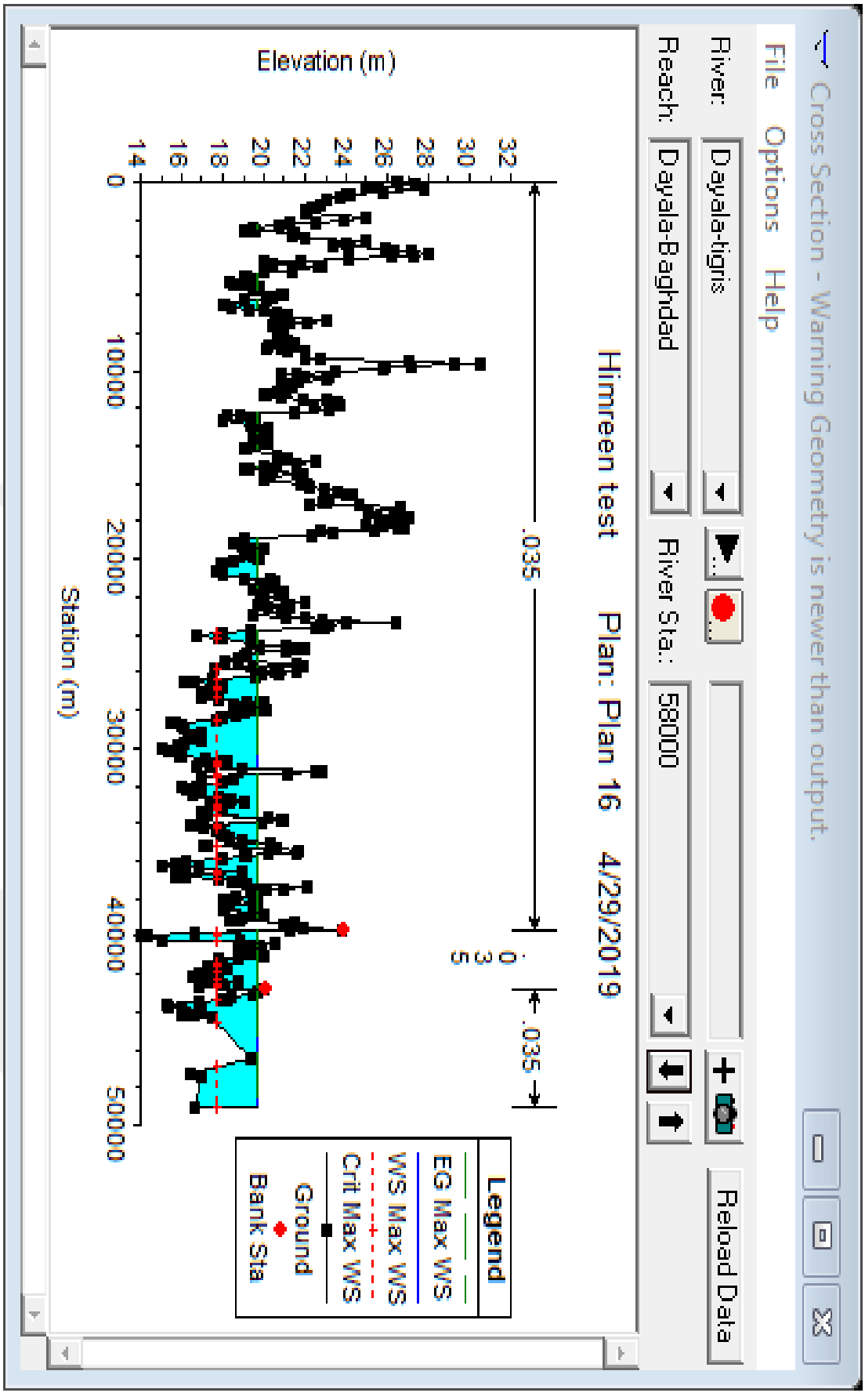

Figure 3.47 Cross-Section Number 58000 of Scenario 3

3.3.3.1 Water Surface Profile:

Water surface profile from the dam axis to the end of the cross-section (a long distance 300 km) is shown in Fig 3.48. In this figure, the x-axis shows the distance between the Himreen dam and the Nomania city and the y-axis shows the water surface elevation. The water surface elevation is at the maximum downstream of the dam failure, and decreases in the downstream direction.

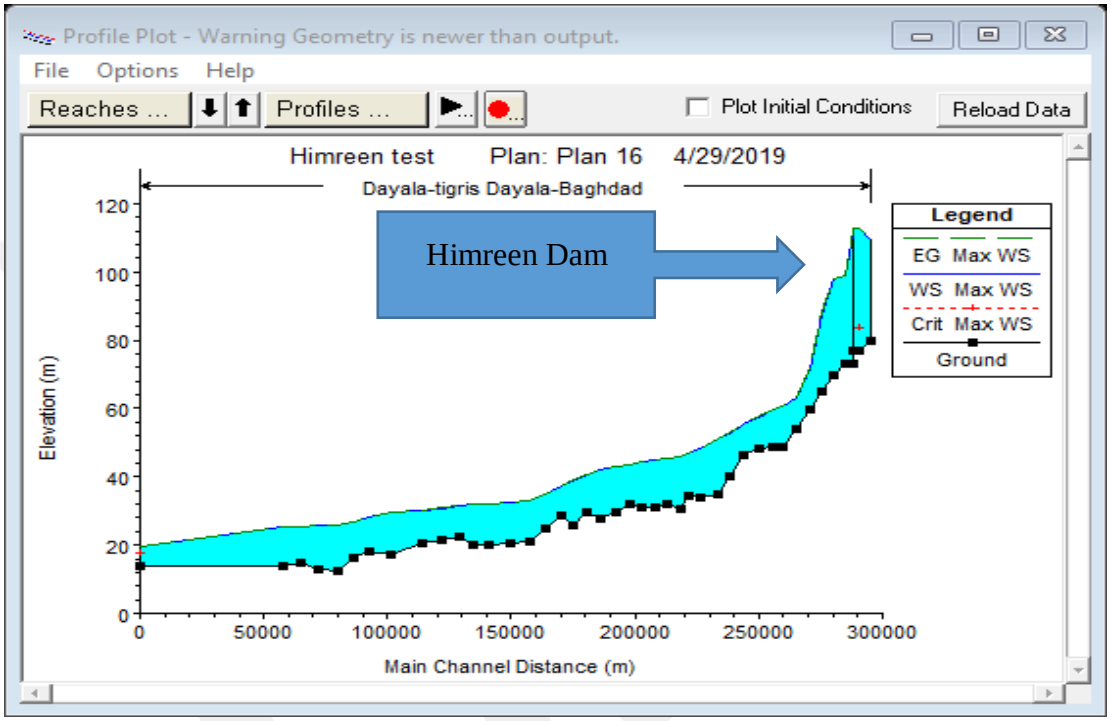

Figure 3.48 Longitudinal Water Surface of Scenario 3

3.3.1.2 Velocity Profile and Water Propagation Area:

This part shows (1) velocity of the left and right banks and the centre of the cross-sections along the longitudinal profile; (2) maximum water surface elevations of the left and right banks and the centre of the cross-sections along the longitudinal profile (3) water propagation inundation areas (m^2) along the longitudinal profile of the reach. Fig 3.49 shows velocity values for the left and right banks and centre of the channel of the Diayla River. The velocity is maximum at the point of dam failure because it has high energy; this velocity decreases at the longitudinal profile of the Diayla River. Fig 3.50 shows the variation of the water surface elevations along the longitudinal profile.

Outflow from the Himreen Dam failure will be at the maximum in the dam failure and it decreases along the longitudinal profile on the Diayla River.

Fig 3.51 shows the flow area of the Diayla River. The flow area is minimum in the dam failure location and it increases in all cross-sections, because of the increase in the flooded area.

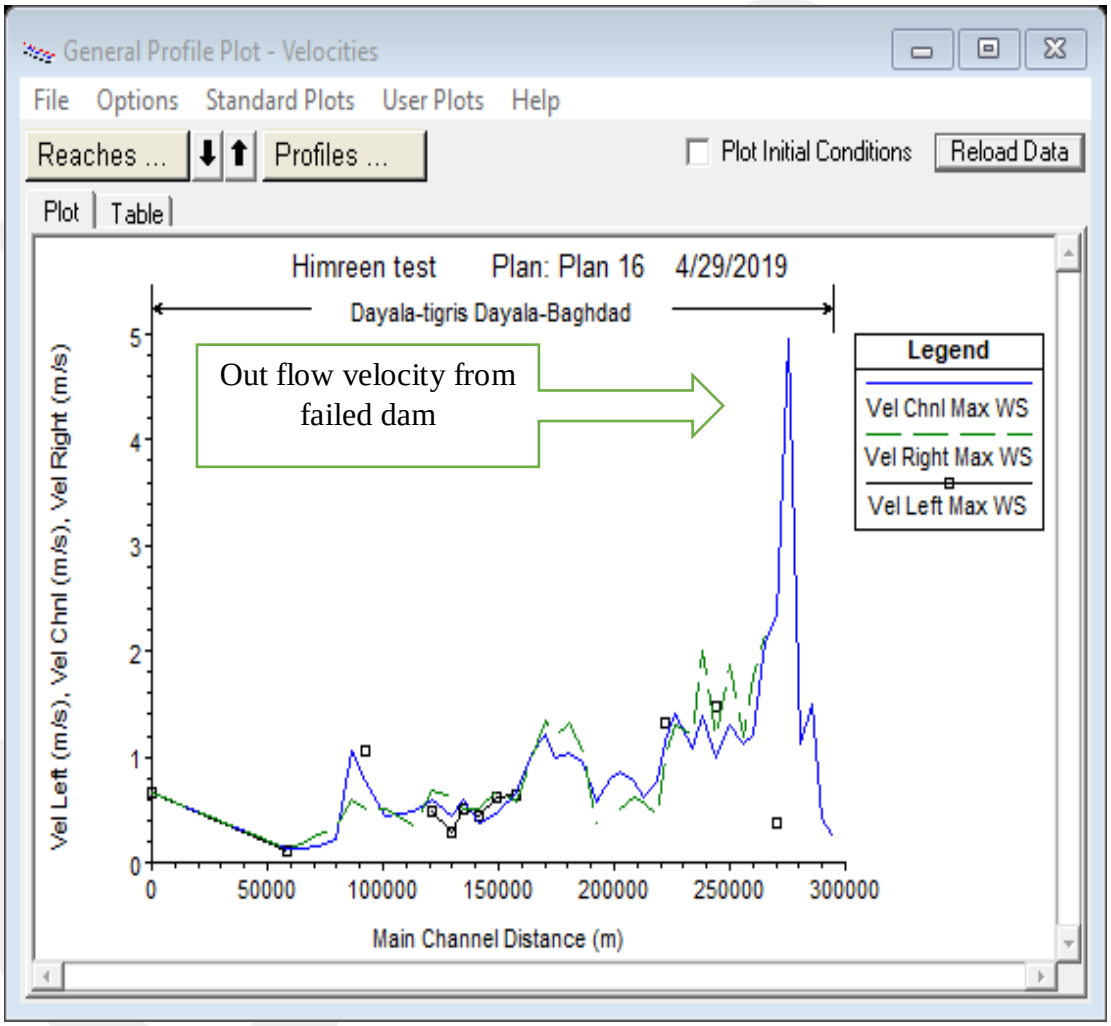

Figure 3.49 Velocity (m/s) Values at the Left, Right Banks and in the Center Channel along the Diayla River of Scenario 3

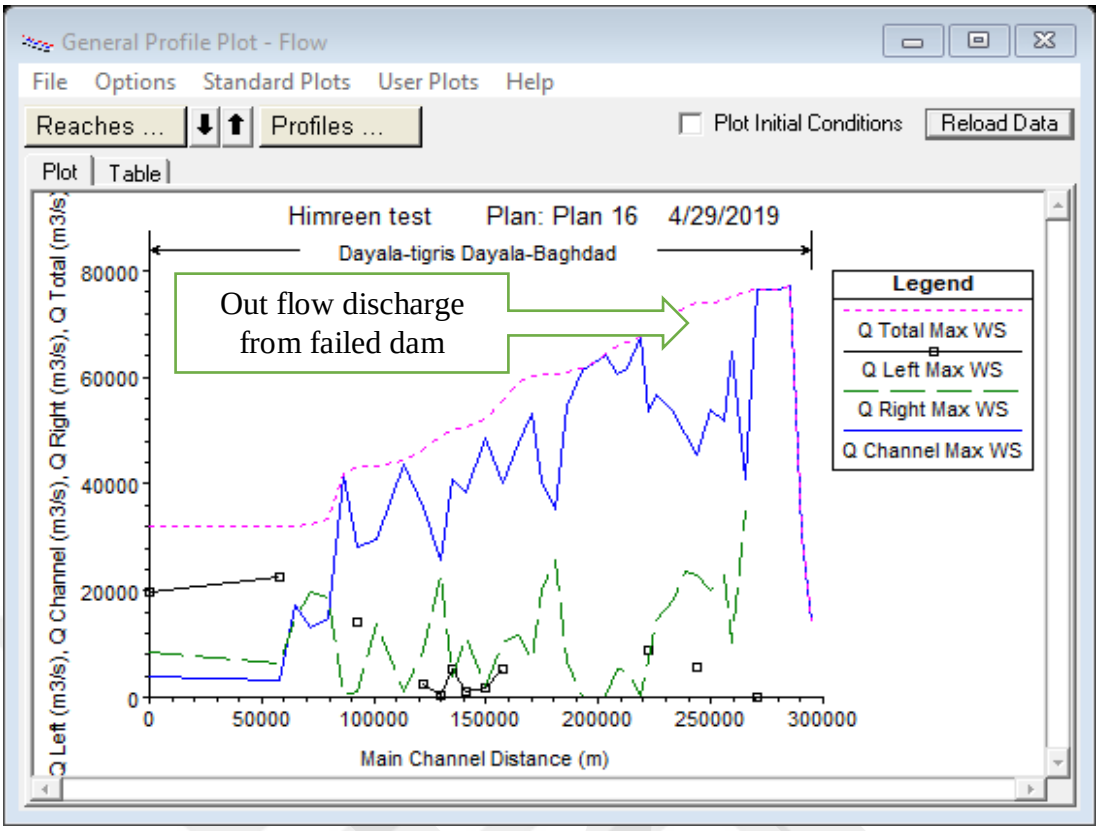

Figure 3.50 Variation of Flood Discharge Along the Longitudinal Profile of the Diayla River of Scenario 3

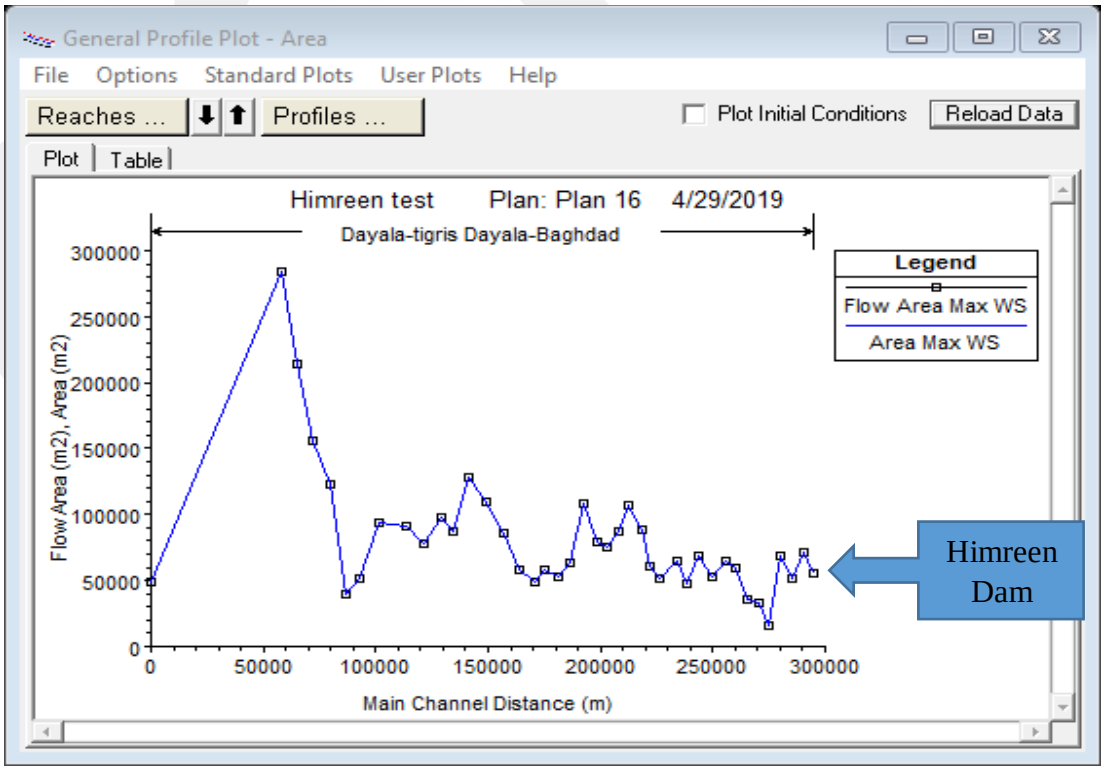

Figure 3.51 Flow Area for Diayla River of Scenario 3

Fig 3.52 shows the stages and flow hydrograph during the failure stage .Fig 3.53 shows the detailed output tables for a cross-section. Fig 3.54 shows unsteady flow analysis. Fig 3.55 shows input data on Himreen overtopping case. The starting time to dam failure is 24 hours which means the maximum time from overtopping to total failure while processing progress for the wave's continuity for 4 days, which means the maximum time needed to reach the water wave to Nomania and also to cover the whole 300 km of distance.

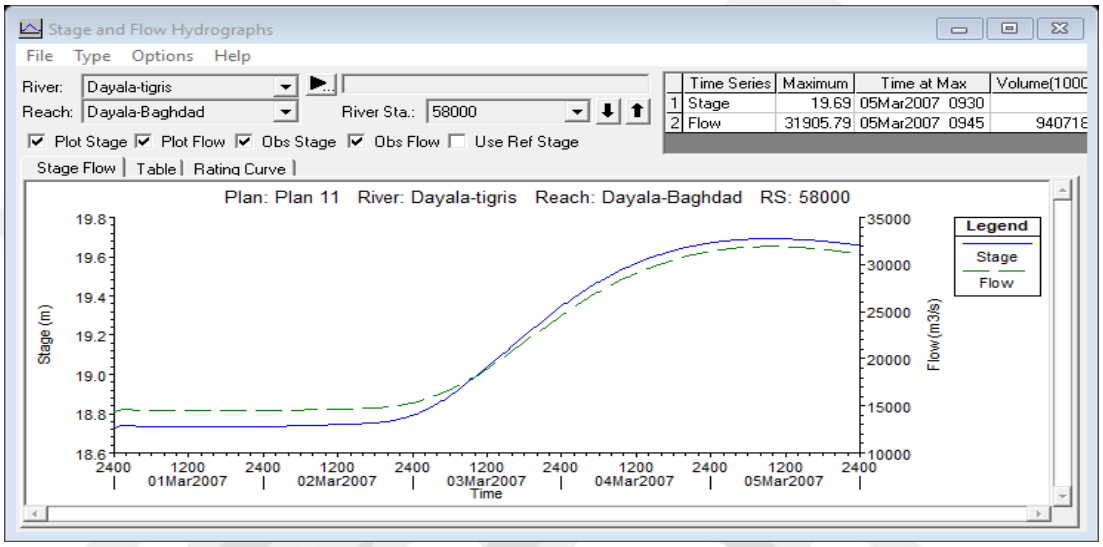

Figure 3.52 Stage and Flow Hydrograph of Station Number 58000 of Scenario 3

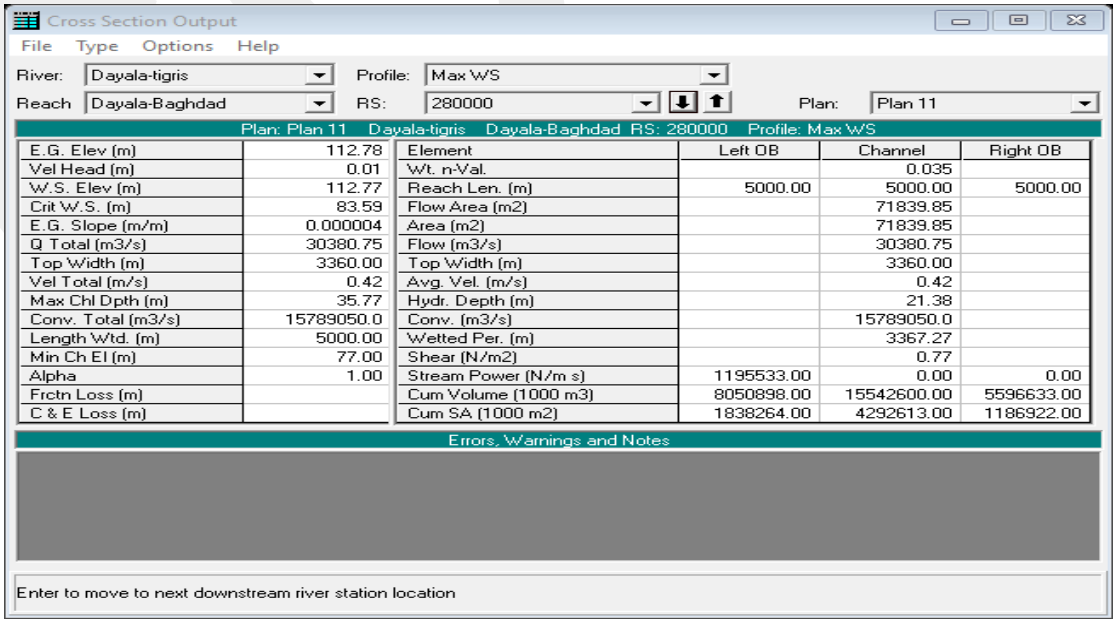

Figure 3.53 Detailed Output Tables of Scenario 3 Cross-Section Number 280000

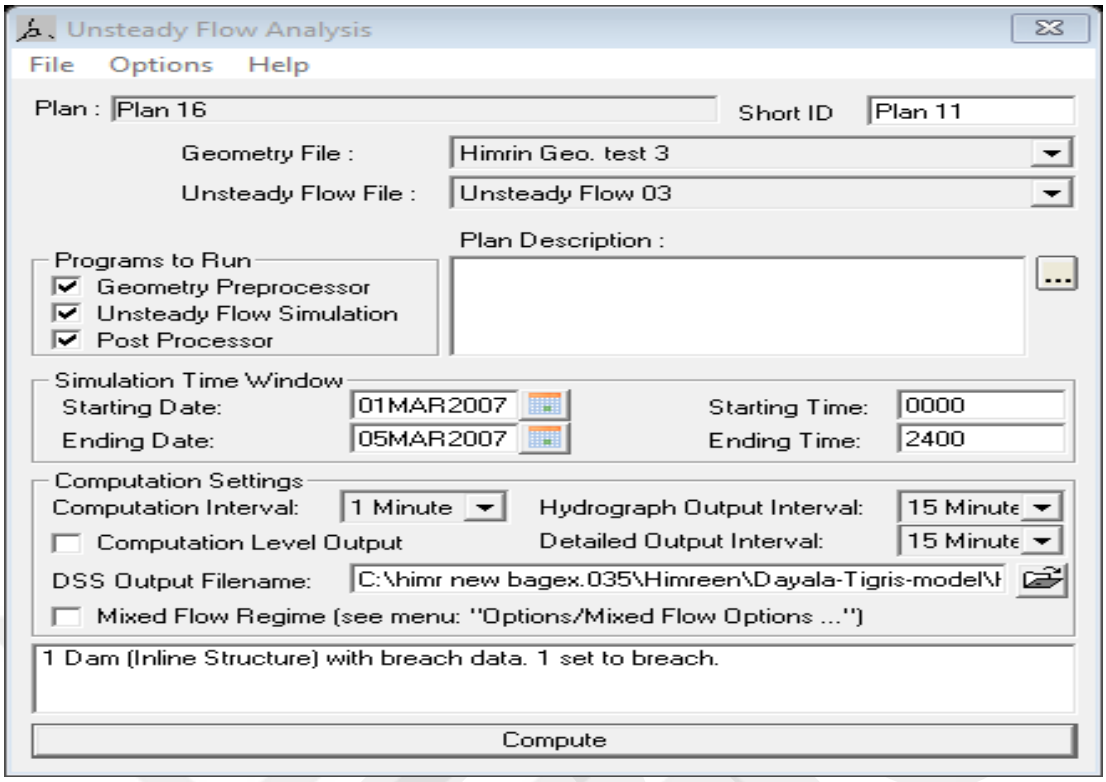

Figure 3.54 Unsteady Flow of Scenario 3

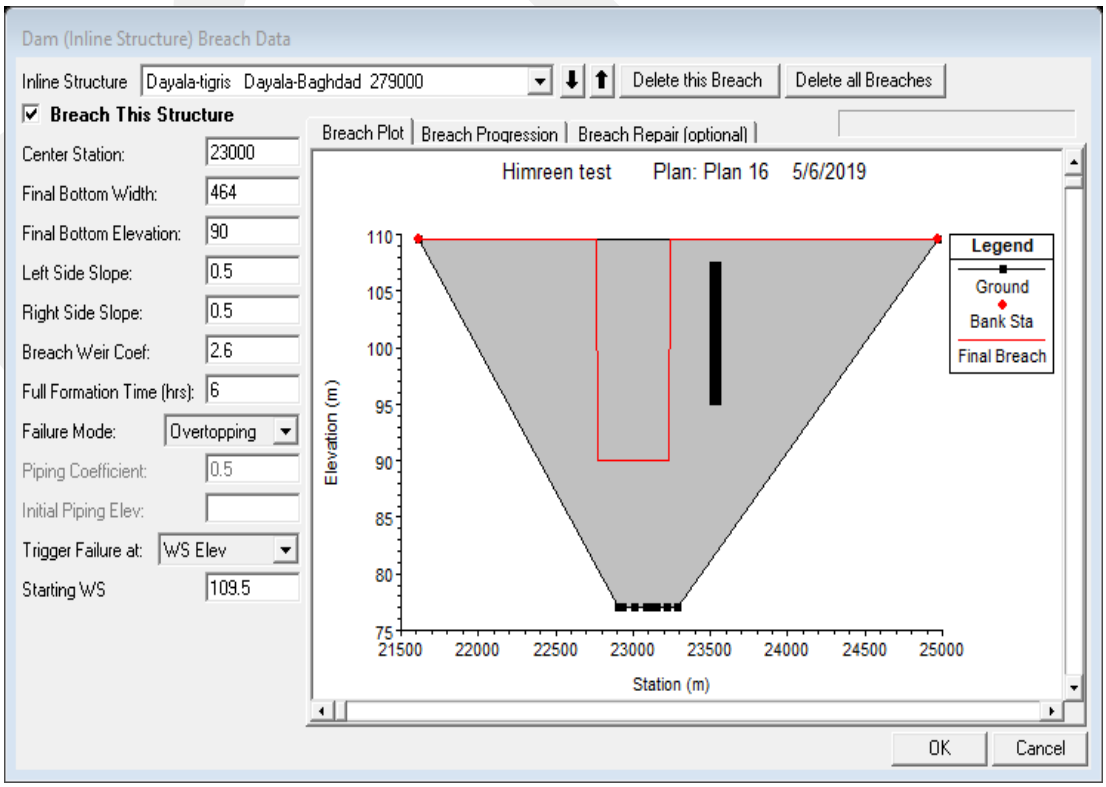

Figure 3.55 Data for Himreen Dam (Overtopping Case) of Scenario 3

CHAPTER 4
RESULTS AND DISCUSSIONS

4.1 Introduction:

Failure scenarios of the Himreen dam simulations have been presented in previous chapter. This chapter summaries the results of those simulations and discusses the influence of Manning's coefficient on the results.

4.2 Simulation Results of Scenario 1:

As indicated in the previous chapter, Manning's roughness value n=0.028 is used for all 41 cross sections roughness coefficient. Simulation results for this case are tabulated and summarised in Table 4.1. This table shows the behaviour of the flow out hydrograph resulting from the failure of the Himreen dam for scenario 1. Initially when the breach starts, the amount of discharge from this breach is small in quantity. When the breach expands the discharge increases as the time passes, and finally when whole body of the dam collapses the discharge takes its maximum values. This situation is shown in Table 4.1. In cross-section 1, initially 14113.85 m^3/sec discharge is released from the breach and when the breach expands and time passes a higher discharge value is observed at the downstream cross-sections. Therefore, at cross-section number 278500 the magnitude of discharge increases to max peak of 91114.01 m^3/sec. Due to time passed and expansion of cross-sections downstream the discharge in cross-sections decreases. This can be seen in Table 4.1 starting from cross-section number 277500, in which the discharge is 89964.83 m^3/sec until cross-section number 58000 in which the discharge is 33854.06 m^3/sec.

Table 4.1 Discharge, Channel Bottom Elevation and Water Surface Elevation

Cross-section number	River Station	Q Discharge (m^3/sec)	Channel Bottom Elevation (m)	W.S. Elev (m)
1	281000	14113.85	80.00	109.72
2	280000	30339.91	77.00	112.77

Table 4.1 Continued

3	278500	91114.01	73.00	95.54
4	277500	89964.83	70.00	93.35
5	275205.3	89901.80	65.00	81.69
6	270425.0	89831.66	60.00	71.81
7	265347.2	88669.56	54.00	62.72
8	259785.5	86760.38	48.90	60.51
9	255800.2	85895.38	49.00	59.52
10	249783.5	84686.52	48.07	57.40
11	243924.3	84611.33	46.29	55.43
12	238188.8	83905.30	40.17	52.54
13	233856.0	82046.76	34.74	50.66
14	226015.7	81483.37	34.01	48.01
15	221954.0	77081.34	34.60	46.33
16	218333.7	72430.05	30.79	45.49
17	212761.0	70548.93	32.04	45.00
18	208067.9	69493.98	31.16	44.61
19	202887.7	67126.95	30.91	43.82
20	198127.0	64873.98	32.00	43.02
21	192439.9	63902.23	29.46	42.44
22	186310.9	63407.90	27.75	41.55
23	180803.1	63062.80	29.53	40.12
24	174825.0	62793.23	26.00	38.53
25	170412.4	62730.20	28.59	36.93
26	164214.1	61914.41	24.75	34.37
27	157223.0	58037.84	21.24	32.74
28	149372.8	54098.66	20.76	32.14
29	141194.2	53089.05	20.06	31.86
30	134656.9	52326.36	20.05	31.51
31	129279.0	51561.30	22.70	31.17
32	121508.0	49439.48	21.65	30.50
33	113642.2	47582.13	20.60	29.80

Table 4.1 Continued

34	101221.4	46586.54	17.09	29.05
35	92584.28	46256.93	18.06	27.92
36	86530.63	44484.57	16.27	26.32
37	79634.42	35464.02	12.55	25.42
38	71849.33	34507.02	12.78	25.36
39	64801.00	34097.64	15.00	25.34
40	58116.75	33980.41	14.05	25.32
41	58000	33854.06	14.05	19.47

Table 4.2 shows the velocity of the water in the channel of the Diayla River, top width of the surface area of the flow, average flow velocity, energy grade line and Froude number for all cross-sections. As expected, it can be seen from this table that when a cross-section area (or flow area) decreases average velocity increases and Froude number increases.

Table 4.2 Flow Variables Resulting From Simulation Results of Scenario 1

No cross sec.	**River Station**	**E.G.L Elev (m)**	**Velocity (m/s)**	**Flow Area (m^2)**	**Top Width (m)**	**Froude Number**
1	281000	109.72	0.25	55960.89	3360.00	0.02
2	280000	112.78	0.42	71829.59	3360.00	0.03
3	278500	95.94	2.83	32204.44	4933.69	0.35
4	277500	93.67	2.52	35649.21	5374.41	0.31
5	275205.3	88.28	11.37	7904.81	525.98	0.94
6	270425.0	72.24	2.88	31162.21	17616.37	0.69
7	265347.2	63.06	2.61	33955.34	6417.88	0.36
8	259785.5	60.63	1.47	56223.52	14303.72	0.24
9	255800.2	59.62	1.36	61947.29	14625.52	0.21
10	249783.5	57.56	1.58	49077.79	15414.14	0.30
11	243924.3	55.51	1.16	67620.57	20073.29	0.21
12	238188.8	52.75	1.74	43400.37	15380.62	0.35

Table 4.2 Continued

13	233856.0	50.76	1.31	60484.55	15877.81	0.22
14	226015.7	48.16	1.75	47754.28	13755.45	0.29
15	221954.0	46.44	1.44	53337.81	18306.76	0.27
16	218333.7	45.53	0.93	78458.11	22985.80	0.16
17	212761.0	45.03	0.73	97473.91	21435.50	0.11
18	208067.9	44.65	0.90	78397.89	21398.74	0.15
19	202887.7	43.87	1.02	65977.74	22193.15	0.19
20	198127.0	43.06	0.94	69229.94	22608.25	0.17
21	192439.9	42.47	0.66	97057.82	25388.76	0.11
22	186310.9	41.62	1.13	55485.50	17578.55	0.20
23	180803.1	40.22	1.22	46521.89	14623.26	0.23
24	174825.0	38.61	1.18	50693.22	16090.53	0.22
25	170412.4	37.04	1.45	42730.96	16323.31	0.29
26	164214.1	34.45	1.26	49910.79	20990.11	0.25
27	157223.0	32.77	0.79	74895.34	26623.03	0.15
28	149372.8	32.15	0.54	97346.28	29161.03	0.10
29	141194.2	31.87	0.42	117631.70	28597.68	0.07
30	134656.9	31.54	0.69	77578.41	25311.98	0.12
31	129279.0	31.19	0.50	88409.63	27801.03	0.10
32	121508.0	30.52	0.71	68583.50	27978.96	0.14
33	113642.2	29.81	0.60	80610.88	27630.22	0.11
34	101221.4	29.06	0.53	82654.76	28872.05	0.10
35	92584.28	27.98	0.97	44585.48	15667.40	0.19
36	86530.63	26.41	1.29	34690.77	12078.44	0.24
37	79634.42	25.42	0.26	115911.80	25874.95	0.04
38	71849.33	25.37	0.18	147269.30	35307.43	0.03
39	64801.00	25.34	0.14	204213.50	42029.83	0.02
40	58116.75	25.33	0.14	273311.60	46420.40	0.02
41	58000	19.5	0.81	42624.82	2468.57	0.18

Table 4.3 shows the water depth, which is the difference between water surface elevation and channel bottom elevation. The maximum water depth is 35.77 m in cross-section number 280000. This cross-section is located just downstream of the dam and its area is equal to dam body cross-section. The cross-section area increases towards the downstream direction due to spreading of the flood and thus flow depths decrease. Due to topography, flow depths slightly increase at some locations as shown in Table 4.3.

Table 4.3 Water Depths Obtained from the Simulation Results of Scenario 1

Cross-sections Number	River Station	Channel bottom Elevation (m)	Water surface Elevation (m)	Water depth (m)
1	281000	80.00	109.72	29.72
2	280000	77.00	112.77	35.77
3	278500	73.00	95.54	22.54
4	277500	70.00	93.35	23.35
5	275205.3	65.00	81.69	16.69
6	270425.0	60.00	71.81	11.81
7	265347.2	54.00	62.72	8.72
8	259785.5	48.90	60.51	11.61
9	255800.2	49.00	59.52	10.52
10	249783.5	48.07	57.40	9.33
11	243924.3	46.29	55.43	9.14
12	238188.8	40.17	52.54	12.37
13	233856.0	34.74	50.66	15.92
14	226015.7	34.01	48.01	14
15	221954.0	34.60	46.33	11.73
16	218333.7	30.79	45.49	14.7
17	212761.0	32.04	45.00	12.96
18	208067.9	31.16	44.61	13.45
19	202887.7	30.91	43.82	12.91

Table 4.3 Continued

20	198127.0	32.00	43.02	11.02
21	192439.9	29.46	42.44	12.98
22	186310.9	27.75	41.55	13.8
23	180803.1	29.53	40.12	10.59
24	174825.0	26.00	38.53	12.53
25	170412.4	28.59	36.93	8.34
26	164214.1	24.75	34.37	9.62
27	157223.0	21.24	32.74	11.5
28	149372.8	20.76	32.14	11.38
29	141194.2	20.06	31.86	11.8
30	134656.9	20.05	31.51	11.46
31	129279.0	22.70	31.17	8.47
32	121508.0	21.65	30.50	8.85
33	113642.2	20.60	29.80	9.2
34	101221.4	17.09	29.05	11.96
35	92584.28	18.06	27.92	9.86
36	86530.63	16.27	26.32	10.05
37	79634.42	12.55	25.42	1287
38	71849.33	12.78	25.36	12.58
39	64801.00	15.00	25.34	10.34
40	58116.75	14.05	25.32	11.27
41	58000	14.05	19.47	5.41

It is important to depict the arrival time and magnitude of peak discharge to cities located downstream of the dam. Table 4.4 shows the distance, wave height, peak discharge and time of arrival of the flood wave to Barwana, Baquba, Khan Bani Saad, Baghdad, Al-Azezia, and Nomania. It can be noticed that the wave height in Baquba is 12.37 m and in Baghdad is 12.53 m. These cities are the most populated areas. Fig 4.1 also shows longitudinal profile water surface and channel bottom longitudinal profile for the Diayla River. Fig 4.2 shows the inundation map for scenario 1. As can be seen from this figure, these cities Al-Moqdadia, Al-Sada, Al-Hemedad, Al-

Nahrwan, Al-Bejea, Al-Ameen, Al-Swera, Al-Adala, Al-Shehemia and Al-Zubedia are all influenced adversely if the Himreen Dam fails. Summary of this analysis is given in Table 4.4.

Table 4.4 Summary Results of Overtopping Himreen Dam Failure for Scenario 1

Scenario 1 (n=0.028)				
Location	**Distance from Himreen dam (km)**	**Wave height (m)**	**Discharge (m^3/sec)**	**Time Reach (hr)**
Downstream Himreen Dam	1.5	22.54	91114.01	7.45
Greater Barawana	27.5	16.69	89901.80	8.00
Baquba	68	12.37	83950.3	14.40
Khan Bani Saad	92	12.91	67126.95	22.00
Baghdad	120	12.53	62793.23	28.30
Al-Azezia	230	12.58	34507.02	84.30
Al-Nomania	300	5.41	33854.06	87.45

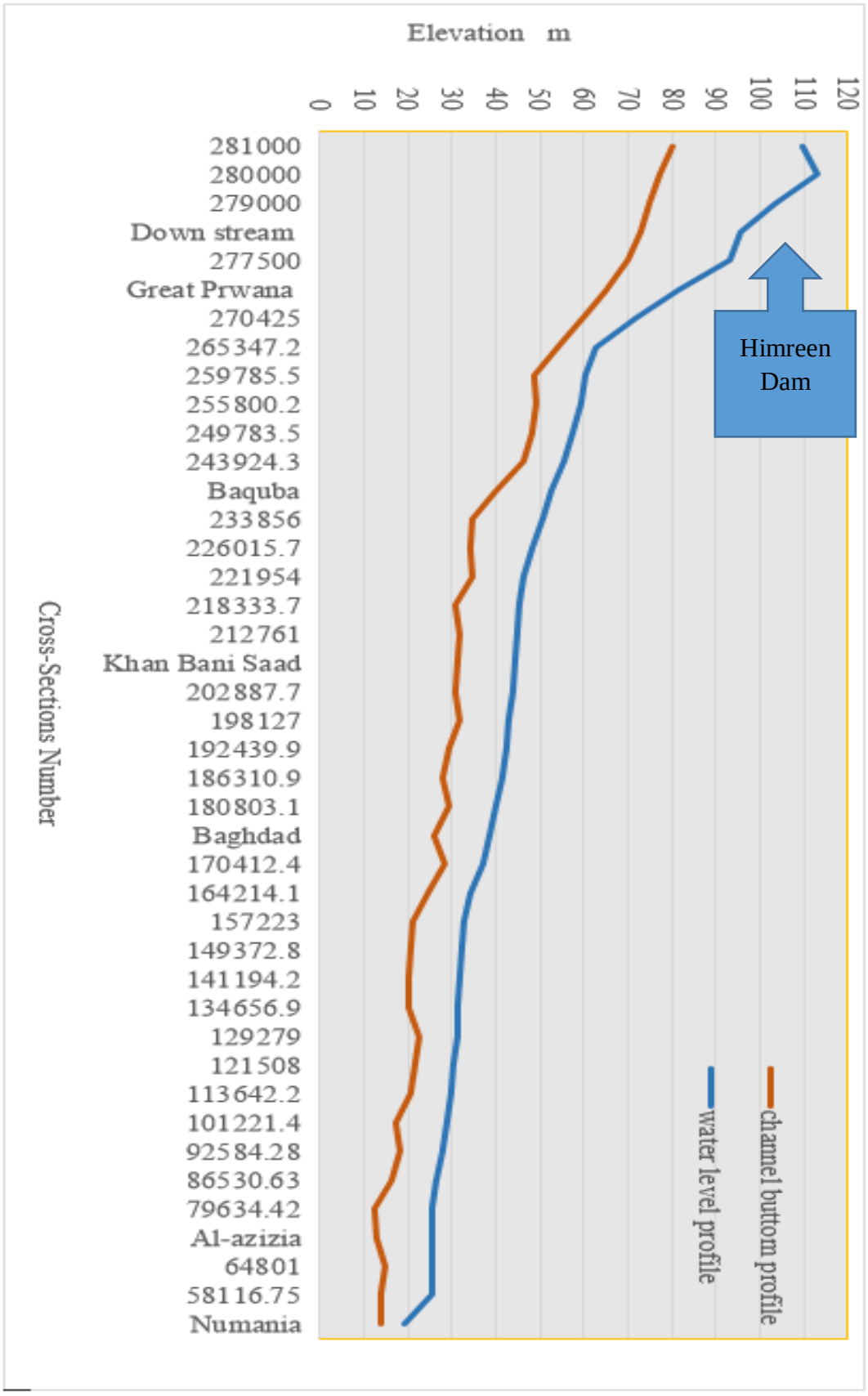

Figure 4.1 Water Surface Profile for Scenario 1

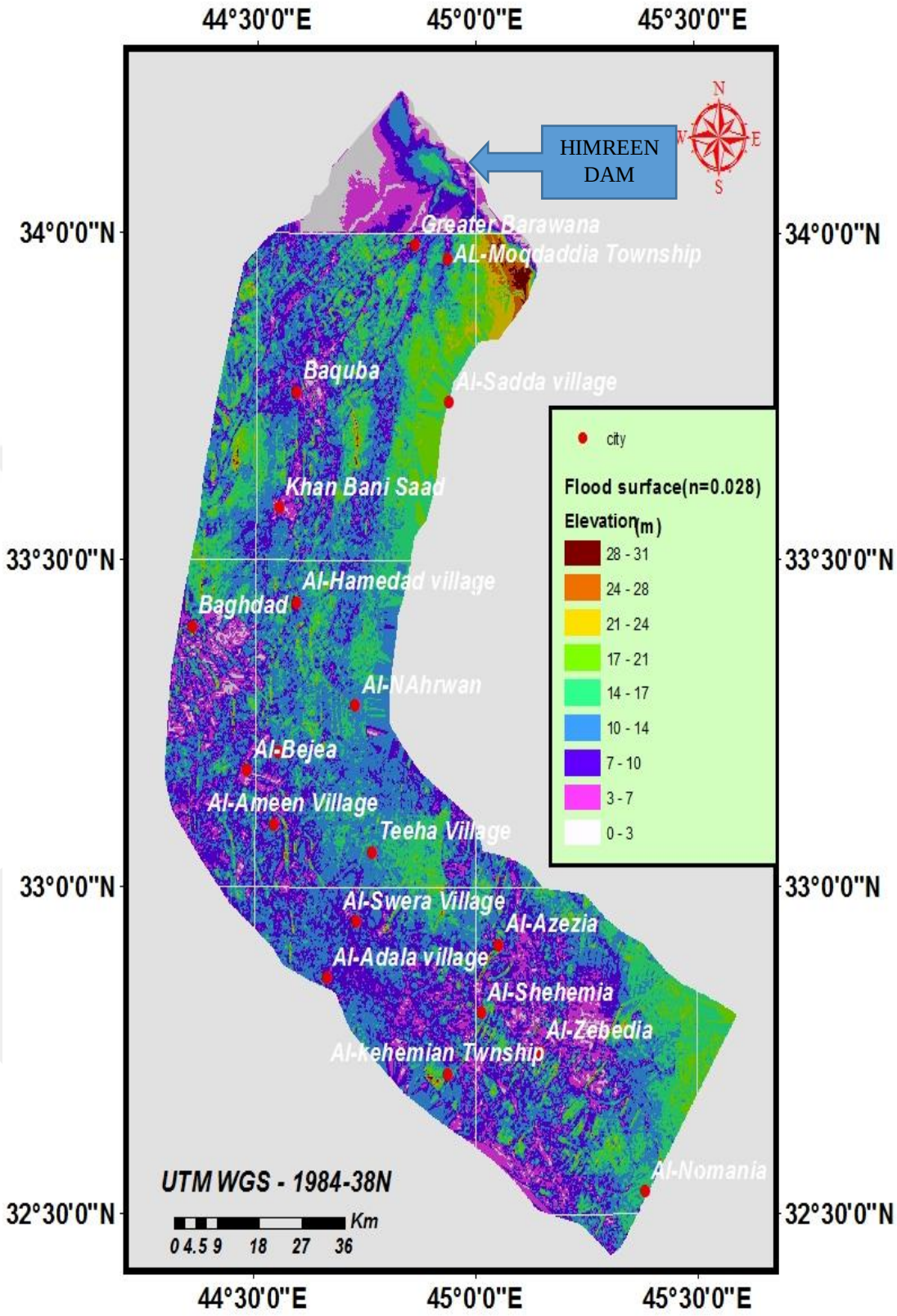

Figure 4.2 The Inundation Map of Scenario 1

4.3 Simulation Results of Scenario 2:

Manning's roughness value n=0.030 is used for all 41 cross sections in this scenario. Simulation results for this case are tabulated and summarised in Table 4.5. This table shows the behaviour of the out flow hydrograph resulting from the failure of the Himreen dam for scenario 2.

In cross section 1 initially 14107 m^3/sec discharge is released and when the breach expands and time passes a higher discharge value of 30350.70 is calculated in cross-section 2. Due to an increase of time and expansion of cross-sections, the discharge in cross-sections downstream decreases. As can be seen in Table 4.5 starting from cross-section number 277500, the discharge is 89232.13 m^3/sec to cross-section number 58000 the discharge is 33193.4 m^3/sec.

Table 4.5 Discharge, Channel Bottom, and Water Surface Elevation

Cross-section number	**River Station**	**Q Discharge (m^3/sec)**	**Channel Bottom Elevation (m)**	**W.S. Elevation (m)**
1	281000	14107.68	80.00	109.72
2	280000	30350.70	77.00	112.77
3	278500	90523.80	73.00	95.92
4	277500	89232.13	70.00	93.73
5	275205.3	89161.88	65.00	82.21
6	270425.0	89064.98	60.00	71.90
7	265347.2	87806.77	54.00	62.92
8	259785.5	86085.73	48.90	60.68
9	255800.2	85278.16	49.00	59.68
10	249783.5	83711.05	48.07	57.54
11	243924.3	83750.70	46.29	55.53
12	238188.8	82525.43	40.17	52.68
13	233856.0	80486.22	34.74	50.83
14	226015.7	79899.21	34.01	48.14

Table 4.5 Continued

15	221954.0	75300.64	34.60	46.46
16	218333.7	71583.15	30.79	45.62
17	212761.0	69466.13	32.04	45.12
18	208067.9	68233.77	31.16	44.72
19	202887.7	66015.77	30.91	43.94
20	198127.0	63637.84	32.00	43.13
21	192439.9	62557.38	29.46	42.55
22	186310.9	62118.38	27.75	41.66
23	180803.1	61724.58	29.53	40.24
24	174825.0	61466.73	26.00	38.64
25	170412.4	61379.54	28.59	37.03
26	164214.1	60456.78	24.75	34.47
27	157223.0	56949.85	21.24	32.85
28	149372.8	53160.07	20.76	32.25
29	141194.2	52086.66	20.06	31.96
30	134656.9	51282.97	20.05	31.61
31	129279.0	50557.13	22.70	31.27
32	121508.0	48394.17	21.65	30.59
33	113642.2	46418.79	20.60	29.90
34	101221.4	45407.03	17.09	29.16
35	92584.28	45182.59	18.06	28.06
36	86530.63	43615.45	16.27	26.44
37	79634.42	34880.07	12.55	25.49
38	71849.33	33808.95	12.78	25.43
39	64801.00	33437.01	15.00	25.40
40	58116.75	33315.59	14.05	25.39
41	58000	33193.40	14.05	19.54

Table 4.6 shows the velocity of the water in the channel of the Diayla River, top width surface area of flow, average velocity, energy grade line, and Froude number for all

cross-sections. As expected, it can also be seen from this table that when cross-section area (flow area) decreases, average velocity and Froude number increases.

Table 4.6 Flow Variables Resulting from Simulation Results of Scenario 2

Cross-section number	River Station	E.G.L Elev. (m)	Velocity (m/s)	Flow Area (m^2)	Top Width (m)	Froude Number
1	281000	109.72	0.25	55960.89	3360.00	0.02
2	280000	112.78	0.42	71831.66	3360.00	0.03
3	278500	96.28	2.65	34138.13	5171.72	0.33
4	277500	94.01	2.36	37746.82	5696.95	0.29
5	275205.3	88.27	10.90	8179.24	533.80	0.89
6	270425.0	72.28	2.72	32783.42	18136.46	0.64
7	265347.2	63.23	2.46	35247.43	6562.08	0.34
8	259785.5	60.80	1.40	58734.89	14497.61	0.23
9	255800.2	59.77	1.30	64312.94	14829.68	0.20
10	249783.5	57.69	1.49	51277.56	15774.14	0.28
11	243924.3	55.61	1.11	69703.63	20242.91	0.20
12	238188.8	52.86	1.63	45495.59	15716.85	0.32
13	233856.0	50.91	1.24	63067.20	16153.27	0.20
14	226015.7	48.27	1.65	49606.07	14318.39	0.28
15	221954.0	46.55	1.35	55676.01	18650.09	0.25
16	218333.7	45.65	0.88	81434.95	23245.83	0.15
17	212761.0	45.14	0.70	100103.5	21799.68	0.10
18	208067.9	44.76	0.86	80900.75	21481.16	0.14
19	202887.7	43.98	0.97	68566.55	22625.61	0.18
20	198127.0	43.17	0.89	71779.15	22983.87	0.16
21	192439.9	42.57	0.63	99806.61	25553.48	0.10
22	186310.9	41.72	1.07	57472.13	17835.65	0.19
23	180803.1	40.33	1.15	48263.08	14888.06	0.22
24	174825.0	38.71	1.11	52463.76	16452.15	0.20

Table 4.6 Continued

25	170412.4	37.12	1.37	44358.48	16903.16	0.27
26	164214.1	34.53	1.18	51903.84	21333.09	0.24
27	157223.0	32.88	0.76	77873.80	27074.59	0.14
28	149372.8	32.26	0.52	100535.9	29460.77	0.09
29	141194.2	31.97	0.41	120589.3	28821.05	0.07
30	134656.9	31.63	0.66	80074.09	25691.00	0.12
31	129279.0	31.28	0.48	90951.63	28170.75	0.09
32	121508.0	30.62	0.67	71235.08	28317.43	0.13
33	113642.2	29.92	0.56	83525.80	27982.38	0.10
34	101221.4	29.17	0.50	85970.53	29645.03	0.10
35	92584.28	28.11	0.90	46779.83	16267.50	0.17
36	86530.63	26.51	1.21	36150.76	12729.33	0.23
37	79634.42	25.49	0.25	117821.9	26132.73	0.04
38	71849.33	25.43	0.17	149753.5	35561.80	0.03
39	64801.00	25.41	0.14	207086.3	42123.81	0.02
40	58116.75	25.39	0.13	276426.6	46489.69	0.02
41	58000	19.57	0.77	44291.75	25270.84	0.17

Table 4.7 shows water depths, which is the difference between water surface elevation and channel bottom elevation. The maximum water depth is 35.77 m in cross-section number 280000. This cross-section is the dam body cross section.

Table 4.7 Water Depths Obtained from the Simulation Results of Scenario 2

Cross Sections number	**River Station**	**Channel Bottom Elevation (m)**	**Water Surface Elevation (m)**	**Water Depth**
1	281000	80.00	109.72	29.72
2	280000	77.00	112.77	35.77
3	278500	73.00	95.92	22.92

Table 4.7 Continued

4	277500	70.00	93.73	23.73
5	275205.3	65.00	82.21	17.21
6	270425.0	60.00	71.90	11.9
7	265347.2	54.00	62.92	8.92
8	259785.5	48.90	60.68	11.78
9	255800.2	49.00	59.68	10.68
10	249783.5	48.07	57.54	9.47
11	243924.3	46.29	55.53	9.27
12	238188.8	40.17	52.68	12.51
13	233856.0	34.74	50.83	16.09
14	226015.7	34.01	48.14	14.13
15	221954.0	34.60	46.46	11.86
16	218333.7	30.79	45.62	14.83
17	212761.0	32.04	45.12	13.08
18	208067.9	31.16	44.72	13.56
19	202887.7	30.91	43.94	13.03
20	198127.0	32.00	43.13	11.13
21	192439.9	29.46	42.55	13.09
22	186310.9	27.75	41.66	13.91
23	180803.1	29.53	40.24	10.71
24	174825.0	26.00	38.64	12.64
25	170412.4	28.59	37.03	8.44
26	164214.1	24.75	34.47	9.72
27	157223.0	21.24	32.85	11.61
28	149372.8	20.76	32.25	11.49
29	141194.2	20.06	31.96	11.9
30	134656.9	20.05	31.61	11.56
31	129279.0	22.70	31.27	8.57
32	121508.0	21.65	30.59	8.94
33	113642.2	20.60	29.90	9.3
34	101221.4	17.09	29.16	12.07

Table 4.7 Continued

35	92584.28	18.06	28.06	10
36	86530.63	16.27	26.44	10.17
37	79634.42	12.55	25.49	12.94
38	71849.33	12.78	25.43	12.65
39	64801.00	15.00	25.40	10.4
40	58116.75	14.05	25.39	11.34
41	58000	14.05	19.54	5.49

Table 4.8 summaries important information about the arrival time and magnitude of peak discharge to cities located downstream of the dam, Barwana, Baquba, Khan Bani Saad Baghdad, Al-Azezia, and Nomania. It can be noticed that the wave height in Baquba is 12.51 m and in Baghdad it is 12.64 m. These cities are the most populated areas. Fig 4.3 also shows longitudinal profile of water surface and channel bottom for the Diayla River, in addition the location of the important cities. Fig 4.4 shows the inundation map for scenario 2. As can be seen from this figure that these cities are Al-Moqdadia, Al-Sada, Al-Hemedad, Al-Nahrwan, Al-Bejea, Al-Ameen, Al-Swera, Al-Adala, Al-Shehemia and Al-Zubedia, are all influenced adversely if the Himreen Dam fails.

Table 4.8 Summary results of Overtopping Himreen Dam failure for Scenario 2

Scenario 2 (n=0.03)				
Location	**Distance from Himreen dam (km)**	**Wave height (m)**	**Discharge (m^3/sec)**	**Time Reach (hr)**
Downstream Himreen Dam	1.5	22.92	90523.8	8.00
Greater Barwana	27.5	17.21	89161.88	8.15
Baquba	68	12.51	82525.43	4.30
Khan Bani Saad	92	13.03	66015.77	22.45
Baghdad	120	12.64	61466.73	29.30
Al-Azezia	230	12.65	33808.95	93.15
Al-Nomania	300	5.49	33193.4	95.45

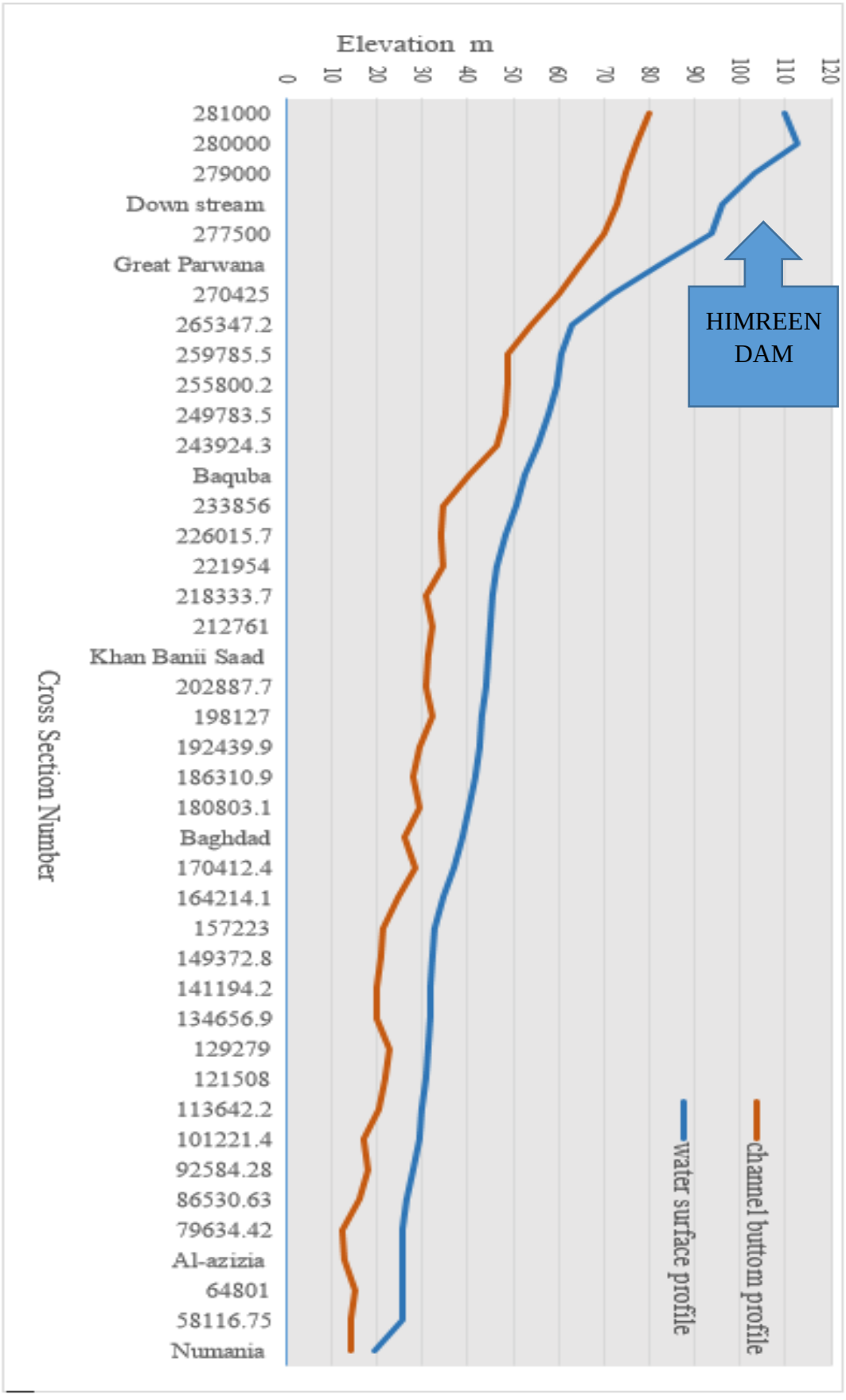

Figure 4.3 Water Surface Profile for Senario 2

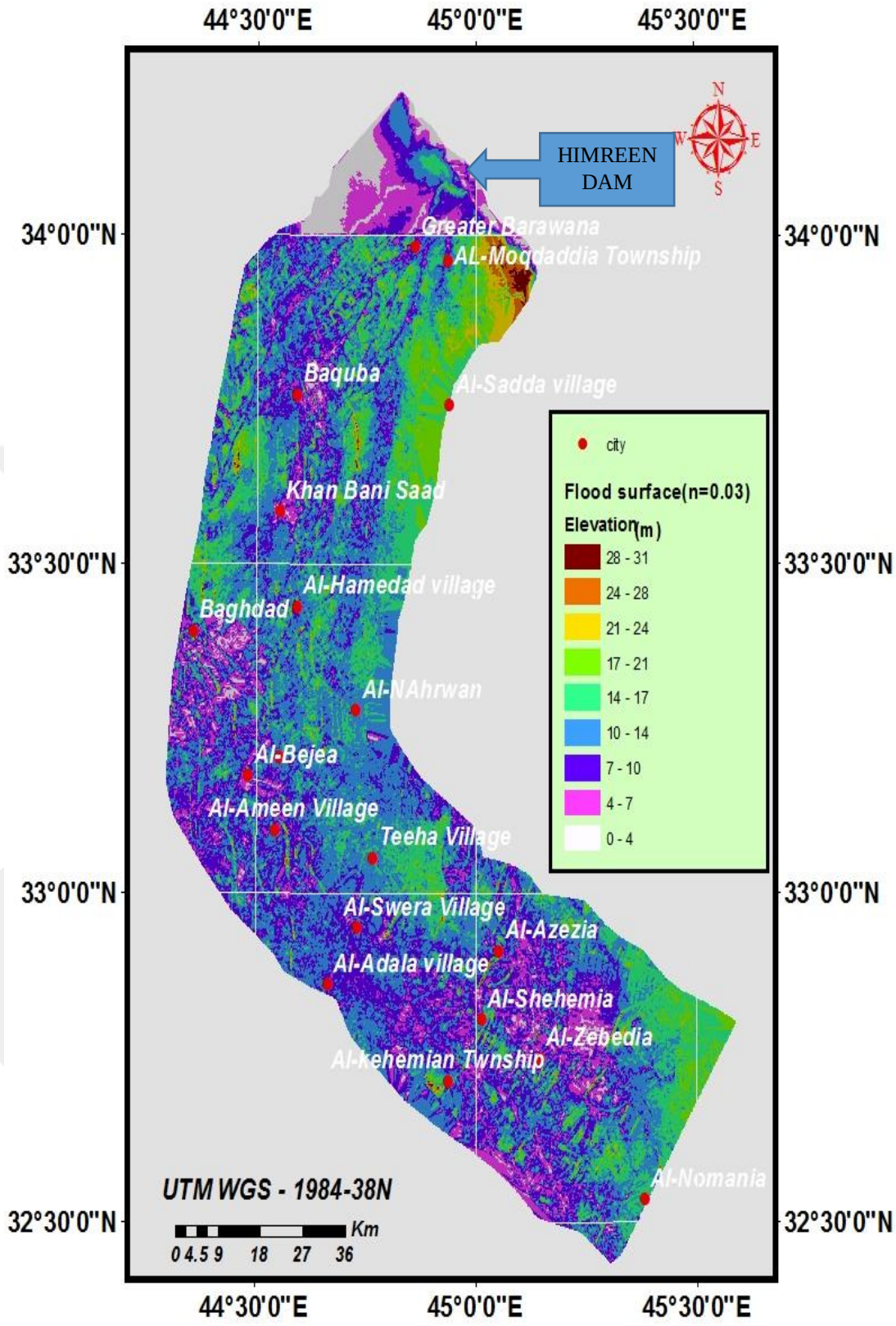

Figure 4.4 The Inundation Area Map of Scenario 2

4.4 Simulation Results of Scenario 3:

Manning's roughness value n=0.035 is used for all 41 cross sections in this scenario. Simulation results for this case are tabulated and summarised in Table 4.9. This table shows the behaviour of the out flow hydrograph resulting from the failure of the Himreen dam for scenario 3. In cross-section 1, initially 14091.28 m^3/sec discharge is released and when the breach expands and time passes higher a discharge value of 77201.80 m^3/sec is calculated in cross-section.

Therefore, at cross-section number 278500 the magnitude of discharge increases to a max peak of 77201.8 m^3/sec. Due to time passed and expansion of cross-sections downstream, the discharge in cross-sections decreases. This can be seen in Table 4.9 starting from cross-section number 277500, in which the discharge is 76534.27 m^3/sec to cross-section number 58000 in which the discharge is 31905.89 m^3/sec.

Table 4.9 Discharge, Channel Bottom, and Water Surface Elevation

Cross section number	River Station	Q Discharge (m^3/sec)	Channel Bottom Elevation (m)	Water Surface Elevation (m)
1	281000	14091.28	80.00	109.72
2	280000	30380.75	77.00	112.77
3	278500	77201.80	73.00	98.73
4	277500	76534.27	70.00	98.08
5	275205.3	76581.13	65.00	87.42
6	270425.0	76493.91	60.00	71.91
7	265347.2	76076.95	54.00	63.00
8	259785.5	75002.60	48.90	60.74
9	255800.2	74493.30	49.00	59.74
10	249783.5	73983.23	48.07	57.60
11	243924.3	73969.86	46.29	55.51
12	238188.8	72988.77	40.17	52.78
13	233856.0	71860.09	34.74	50.95
14	226015.7	71311.34	34.01	48.26
15	221954.0	69077.13	34.60	46.72

Table 4.9 Continued

16	218333.7	67806.22	30.79	45.92
17	212761.0	66546.01	32.04	45.42
18	208067.9	65828.71	31.16	45.02
19	202887.7	64385.23	30.91	44.26
20	198127.0	62626.93	32.00	43.46
21	192439.9	61574.87	29.46	42.87
22	186310.9	61101.27	27.75	41.99
23	180803.1	60721.74	29.53	40.58
24	174825.0	60475.07	26.00	38.95
25	170412.4	60345.18	28.59	37.30
26	164214.1	59230.89	24.75	34.74
27	157223.0	55704.48	21.24	33.15
28	149372.8	52110.59	20.76	32.53
29	141194.2	50874.95	20.06	32.23
30	134656.9	49928.04	20.05	31.87
31	129279.0	49055.23	22.70	31.51
32	121508.0	46600.89	21.65	30.84
33	113642.2	44525.32	20.60	30.16
34	101221.4	43494.73	17.09	29.43
35	92584.28	43307.90	18.06	28.37
36	86530.63	42046.30	16.27	26.70
37	79634.42	33639.05	12.55	25.66
38	71849.33	32571.76	12.78	25.60
39	64801.00	32167.20	15.00	25.56
40	58116.75	32022.67	14.05	25.55
41	58000	31905.89	14.05	19.69

Table 4.10 shows the velocity of the water in the channel of the Diayla River, top width, surface area of flow, average velocity, energy grade line and Froude number for all cross-sections. As expected, it also can be seen from this table that when cross-section area (flow area) decreases, average velocity and Froude number increases

whereas when cross-section area (flow area) increases, average velocity and Froude number decrease.

Table 4.10 Flow Variables Resulting from Simulation Results of Scenario 3

Cross-section number	River Station	E.G.L Elev. (m)	Velocity (m/sec)	Flow Area (m^2)	Top Width (m)	Froude No.
1	281000	109.72	0.25	55961.89	3360.00	0.02
2	280000	112.78	0.42	71839.85	3360.00	0.03
3	278500	98.84	1.51	51263.70	6825.50	0.18
4	277500	98.14	1.12	68076.35	8404.98	0.13
5	275205.3	88.67	4.96	15454.93	3321.90	0.73
6	270425.0	72.19	2.33	32916.39	18213.37	0.55
7	265347.2	63.23	2.10	35770.18	6579.90	0.29
8	259785.5	60.83	1.20	59611.51	14553.46	0.19
9	255800.2	59.81	1.12	65200.90	14897.31	0.17
10	249783.5	57.71	1.30	52284.87	16013.25	0.24
11	243924.3	55.57	0.99	69278.24	20210.97	0.18
12	238188.8	52.91	1.40	47156.11	15955.32	0.27
13	233856.0	51.01	1.07	65137.76	16346.65	0.17
14	226015.7	48.36	1.41	51386.78	14828.16	0.24
15	221954.0	46.79	1.14	60655.41	19409.18	0.20
16	218333.7	45.95	0.77	88675.90	23988.11	0.13
17	212761.0	45.44	0.63	106851.1	22556.73	0.09
18	208067.9	45.05	0.77	87389.84	21743.18	0.12
19	202887.7	44.29	0.85	75958.08	23643.10	0.15
20	198127.0	43.49	0.79	79491.34	24055.36	0.14
21	192439.9	42.89	0.57	108012.0	26025.85	0.09
22	186310.9	42.04	0.95	63420.91	18318.78	0.16
23	180803.1	40.65	1.03	53458.25	15520.49	0.19
24	174825.0	39.01	0.99	57638.88	17445.70	0.18
25	170412.4	37.38	1.21	49196.69	17913.59	0.23
26	164214.1	34.80	1.03	57990.66	22589.26	0.20

Table 4.10 Continued

27	157223.0	33.17	0.67	86028.40	28001.03	0.12
28	149372.8	32.55	0.47	109095.3	30361.01	0.08
29	141194.2	32.24	0.37	128465.8	29671.95	0.06
30	134656.9	31.89	0.59	86758.35	26584.64	0.10
31	129279.0	31.52	0.43	97839.88	29189.14	0.08
32	121508.0	30.85	0.58	78276.17	29277.19	0.11
33	113642.2	30.18	0.49	91018.54	29011.84	0.09
34	101221.4	29.44	0.44	94168.38	31056.08	0.08
35	92584.28	28.41	0.77	51945.12	17476.07	0.15
36	86530.63	26.76	1.07	39689.79	14294.20	0.20
37	79634.42	25.67	0.23	122399.0	26752.17	0.04
38	71849.33	25.60	0.16	155650.0	36219.73	0.03
39	64801.0	25.56	0.13	213831.4	42329.33	0.02
40	581167.5	25.55	0.13	283793.9	42329.77	0.01
41	58000	19.71	0.67	48313.70	26057.76	0.02

Table 4.11 shows water depths, which is the difference between water surface elevation and channel bottom elevation. The maximum water depth is 35.77 m in cross-section number 280000. This cross-section is the dam body cross section.

Table 4.11 Water Depths Obtained from the Simulation Results of Scenario 3

Cross Section Number	**River Station**	**Channel Bottom Elevation (m)**	**Water surface Elevation (m)**	**Water depth (m)**
1	281000	80.00	109.72	29.72
2	280000	77.00	112.77	35.77
3	278500	73.00	98.73	25.73
4	277500	70.00	98.08	28.08
5	275205.3	65.00	87.42	22.42
6	270425.0	60.00	71.91	11.91

Table 4.11 Continued

7	265347.2	54.00	63.00	9
8	259785.5	48.90	60.74	11.84
9	255800.2	49.00	59.74	10.74
10	249783.5	48.07	57.60	9.53
11	243924.3	46.29	55.51	9.22
12	238188.8	40.17	52.78	12.61
13	233856.0	34.74	50.95	16.21
14	226015.7	34.01	48.26	14.25
15	221954.0	34.60	46.72	12.12
16	218333.7	30.79	45.92	15.13
17	212761.0	32.04	45.42	13.38
18	208067.9	31.16	45.02	13.86
19	202887.7	30.91	44.26	13.35
20	198127.0	32.00	43.46	11.46
21	192439.9	29.46	42.87	19.41
22	186310.9	27.75	41.99	14.24
23	180803.1	29.53	40.58	11.05
24	174825.0	26.00	38.95	12.95
25	170412.4	28.59	37.30	8.71
26	164214.1	24.75	34.74	9.99
27	157223.0	21.24	33.15	11.91
28	149372.8	20.76	32.53	11.77
29	141194.2	20.06	32.23	3.17
30	134656.9	20.05	31.87	11.82
31	129279.0	22.70	31.51	8.81
32	121508.0	21.65	30.84	9.19
33	113642.2	20.60	30.16	9.56
34	101221.4	17.09	29.43	12.34
35	92584.28	18.06	28.37	10.31
36	86530.63	16.27	26.70	10.43

Table 4.11 Continued

37	79634.42	12.55	25.66	13.11
38	71849.33	12.78	25.60	12.82
39	64801.00	15.00	25.56	10.56
40	58116.75	14.05	25.55	11.5
41	58000	14.05	19.69	5.64

Table 4.12 summarises important information about arrival time and magnitude of peak discharge to cities located downstream of the dam: Barwana, Baquba, Khan Bani Saad Baghdad, Al-Azezia, and Nomania. It can be noticed that the wave height in Baquba is 12.61 m and in Baghdad it is 12.95 m; these cities are the most populated areas. Fig 4.5 shows longitudinal profile of water surface and channel bottom for the Diayla River. Fig 4.6 shows the inundation map for scenario 3. As can be seen from this figure, these cities; Al-Moqdadia, Al-Sada, Al-Hemedad, Al-Nahrwan, Al-Bejea, Al-Ameen, Al-Swera, Al-Adala, Al-Shehemia and Al-Zubedia, are all influenced adversely if the Himreen dam fails.

Table 4.12 Summary Results of Overtopping Himreen Dam Failure for Scenario 3

Scenario 3 (n=0.035)				
Location	**Distance from Himreen dam (km)**	**Wave height (m)**	**Discharge (m^3/sec)**	**Time reach (hr)**
Downstream Himreen Dam	1.5	25.73	77201.8	11.00
Greater Barawana	27.5	22.42	76581.13	11.15
Baquba	68	12.61	72988.77	17.15
Khan Bani Saad	92	13.35	64385.23	28.00
Baghdad	120	12.95	60475.07	34.45
Al-Azezia	230	12.82	32571.76	102.15
Al-Nomania	300	5.64	31905.89	105.45

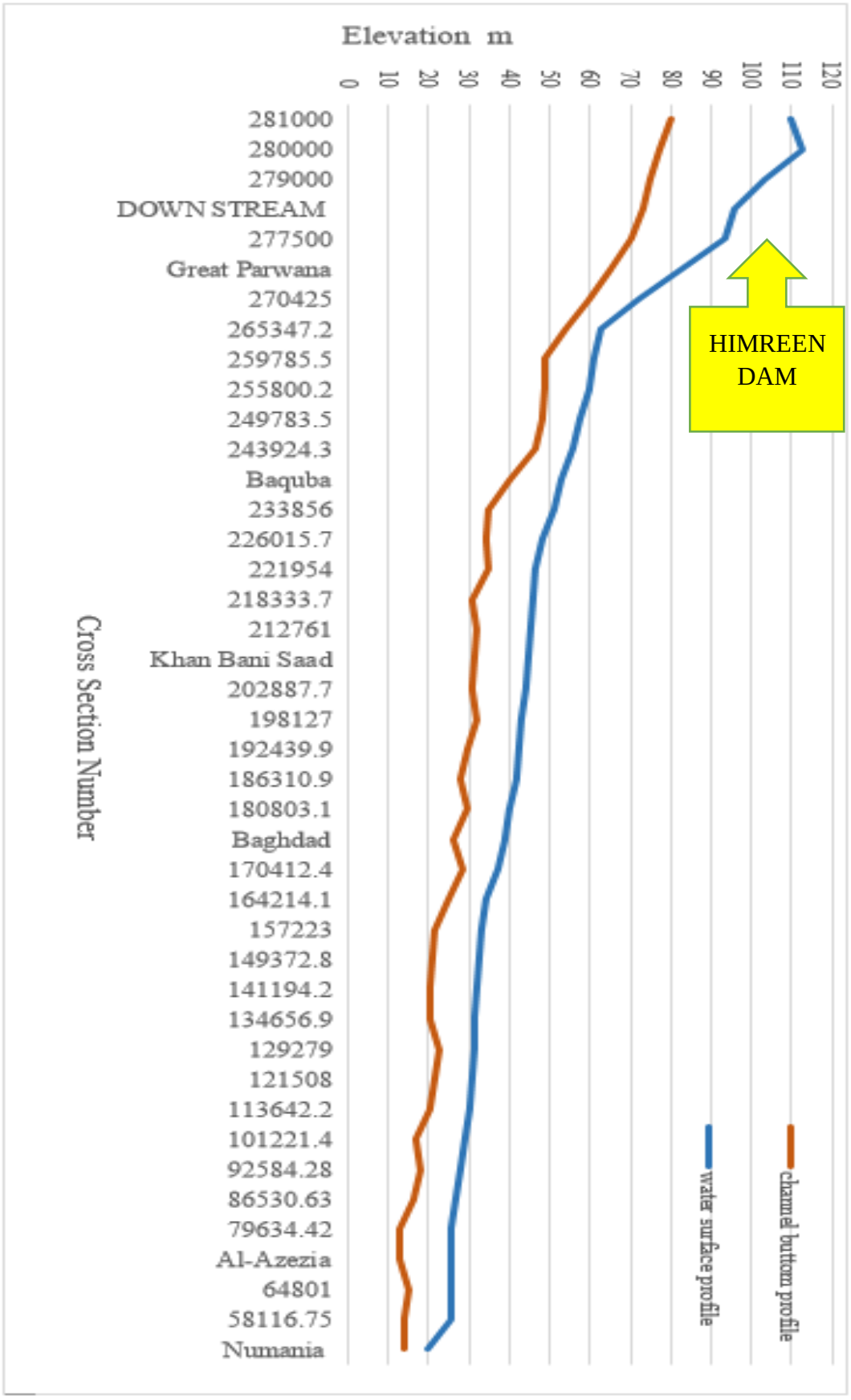

Figure 4.5 Water Surface Profile for Scenario 3

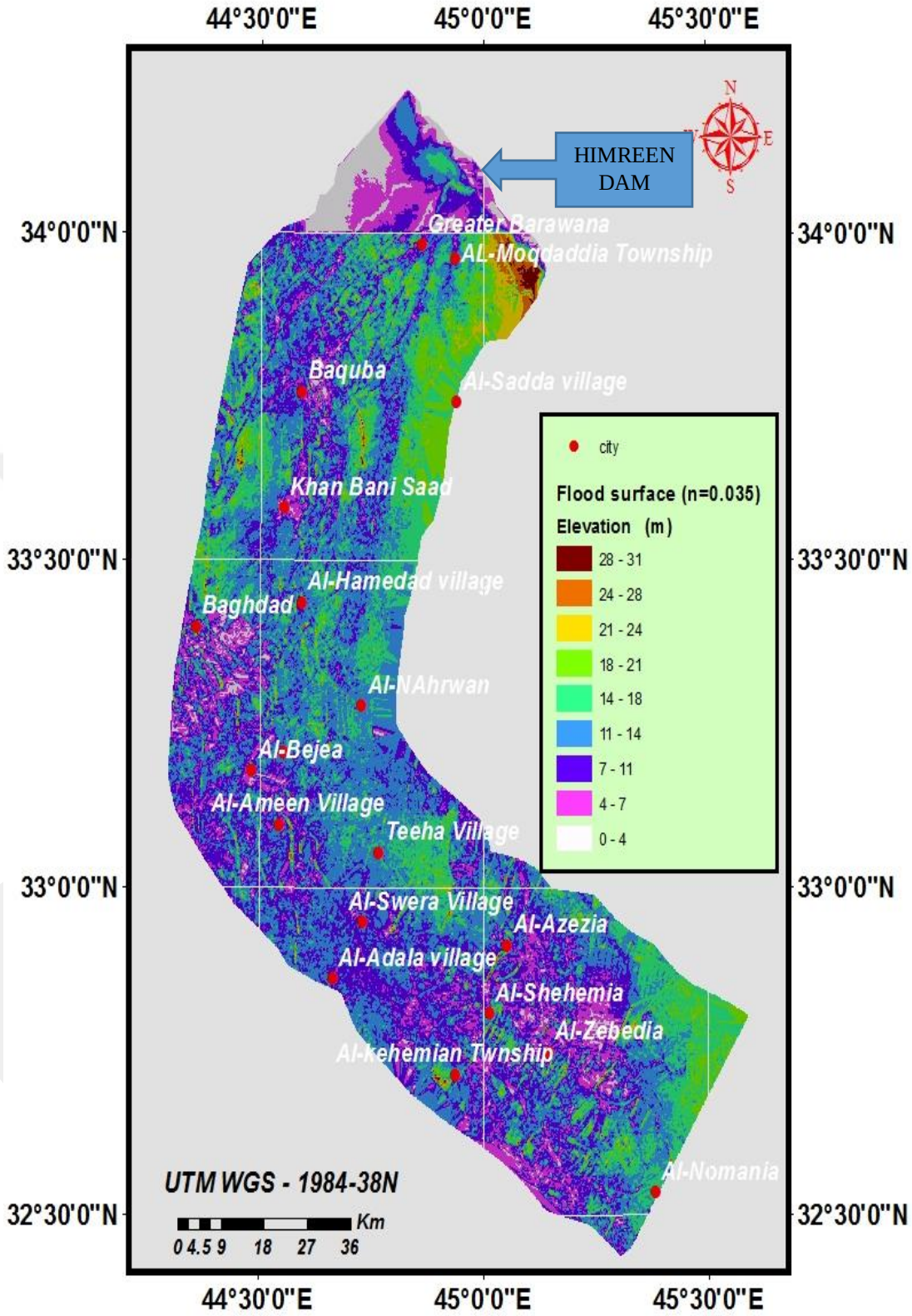

Figure 4.6 The Inundation Map of Scenario 3

4.5. Comparison of Water Depths in Three Scenarios:

In order to show the effect of Manning's roughness coefficient on the flow depths in the cross-sections, Table 4.13 has been tabulated. As can be seen from this table, water depths calculated in three scenarios in the cross-sections did not change considerably. The reason for this is because of the main channel 1-D flow is dominate and Manning's roughness is an important parameter for flow depth.

Table 4.13 Variation of Water Depths in Three Scenarios

Number	Cross-section	Scenario 1 n=0.028	Scenario 2 n=0.030	Scenario 3 n=0.035
1	281000	29.72	29.72	29.72
2	280000	35.77	35.77	35.77
3	278500	22.54	22.92	25.73
4	277500	23.35	23.73	28.08
5	275205.3	16.69	17.21	22.42
6	270425.0	11.81	11.9	11.91
7	265347.2	8.72	8.92	9
8	259785.5	11.61	11.78	11.84
9	255800.2	10.52	10.68	10.74
10	249783.5	9.33	9.47	9.53
11	243924.3	9.14	9.27	9.22
12	238188.8	12.37	12.51	12.61
13	233856.0	15.92	16.09	16.21
14	226015.7	14	14.13	14.25
15	221954.0	11.73	11.86	12.12
16	218333.7	14.7	14.83	15.13
17	212761.0	12.96	13.08	13.38
18	208067.9	13.45	13.56	13.86
19	202887.7	12.91	13.03	13.35
20	198127.0	11.02	11.13	11.46

Table 4.13 Continued

21	192439.9	12.98	13.09	19.41
22	186310.9	13.8	13.91	14.24
23	180803.1	10.59	10.71	11.05
24	174825.0	12.53	12.64	12.95
25	170412.4	8.34	8.44	8.71
26	164214.1	9.62	9.72	9.99
27	157223.0	11.5	11.61	11.91
28	149372.8	11.38	11.49	11.77
29	141194.2	11.8	11.9	3.17
30	134656.9	11.46	11.56	11.82
31	129279.0	8.47	8.57	8.81
32	121508.0	8.85	8.94	9.19
33	113642.2	9.2	9.3	9.56
34	101221.4	11.96	12.07	12.34
35	92584.28	9.86	10	10.31
36	86530.63	10.05	10.17	10.43
37	79634.42	12.87	12.94	13.11
38	71849.33	12.58	12.65	12.82
39	64801.00	10.34	10.4	10.56
40	58116.75	11.27	11.34	11.5
41	58000	5.41	5.49	5.64

Fig 4.7 shows the water depth for the three scenarios of n values 0.028, 030, and 0.035. Fig 4.8 shows the discharge for the three scenarios and Fig 4.9 shows the time arrival for wave height and distance for the three scenarios. It can be seen from Fig 4.7 that these rage of variation of roughness values, water depths for n=0.035 are higher only at three location at Barwana, Baquba and at cross-section number 1924399 which is just upstream of Baghdad, whereas as at cross-section number 141194 water depth is lower than the other two scenarios.

Even through Fig 4.7 shows higher water depths in scenario 3, Fig 4.8 shows that the discharge in scenario 3 for all cross-sections is lower than in scenario 1 and 2.

The reason for this is because higher Manning's roughness causes higher water depth by creating higher resistance to the flow and thus lower velocities. This can be seen from Table 4.2, 4.6 and 4.10. Cross-section velocities shown in Table 4.2 and 4.6 are higher than those cross-section velocities shown in Table 4.10, thus discharge values for scenario 1 and 2 are higher than discharge in scenario 3.

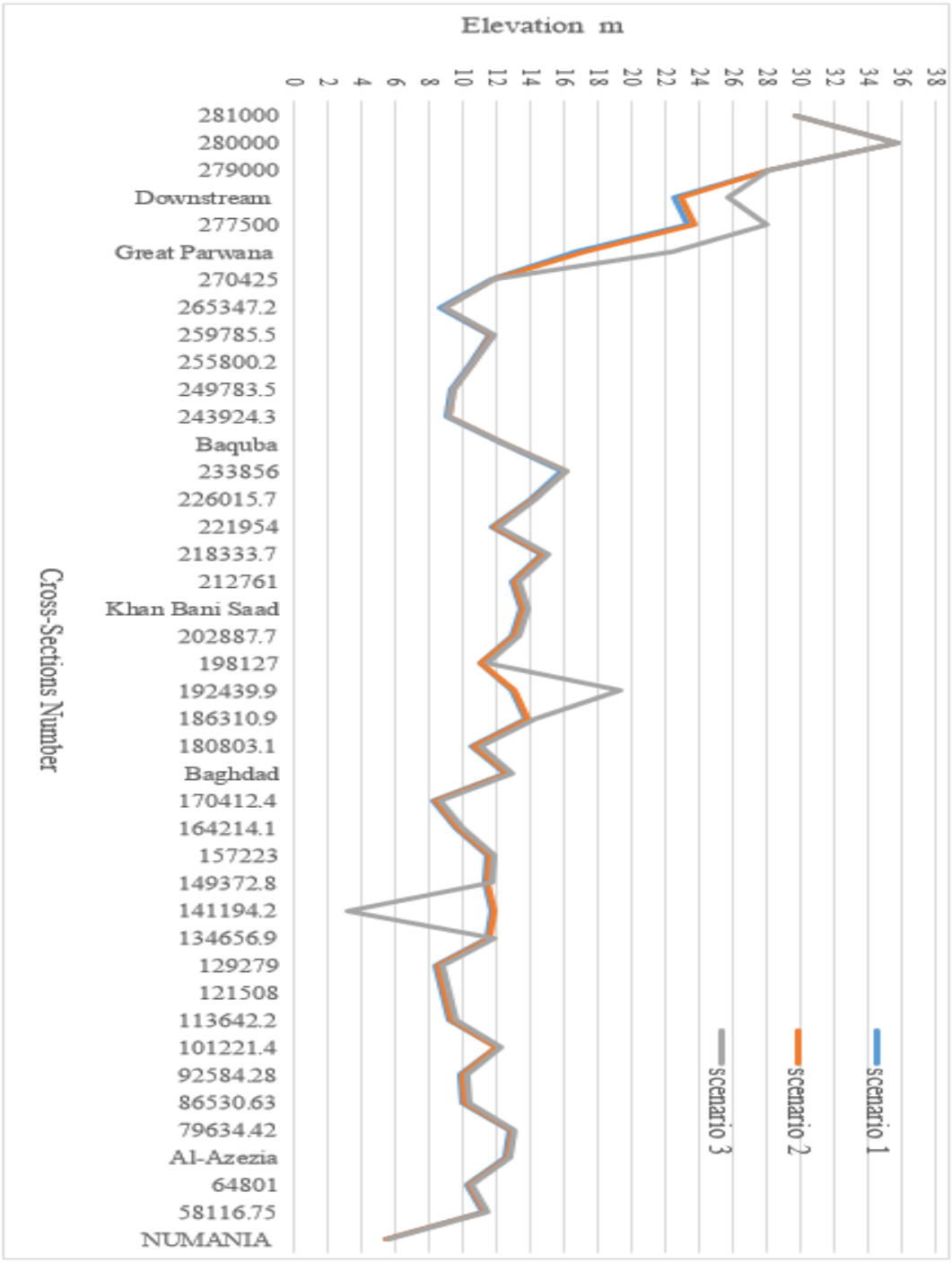

Figure 4.7 Water Depth for Three Scenarios

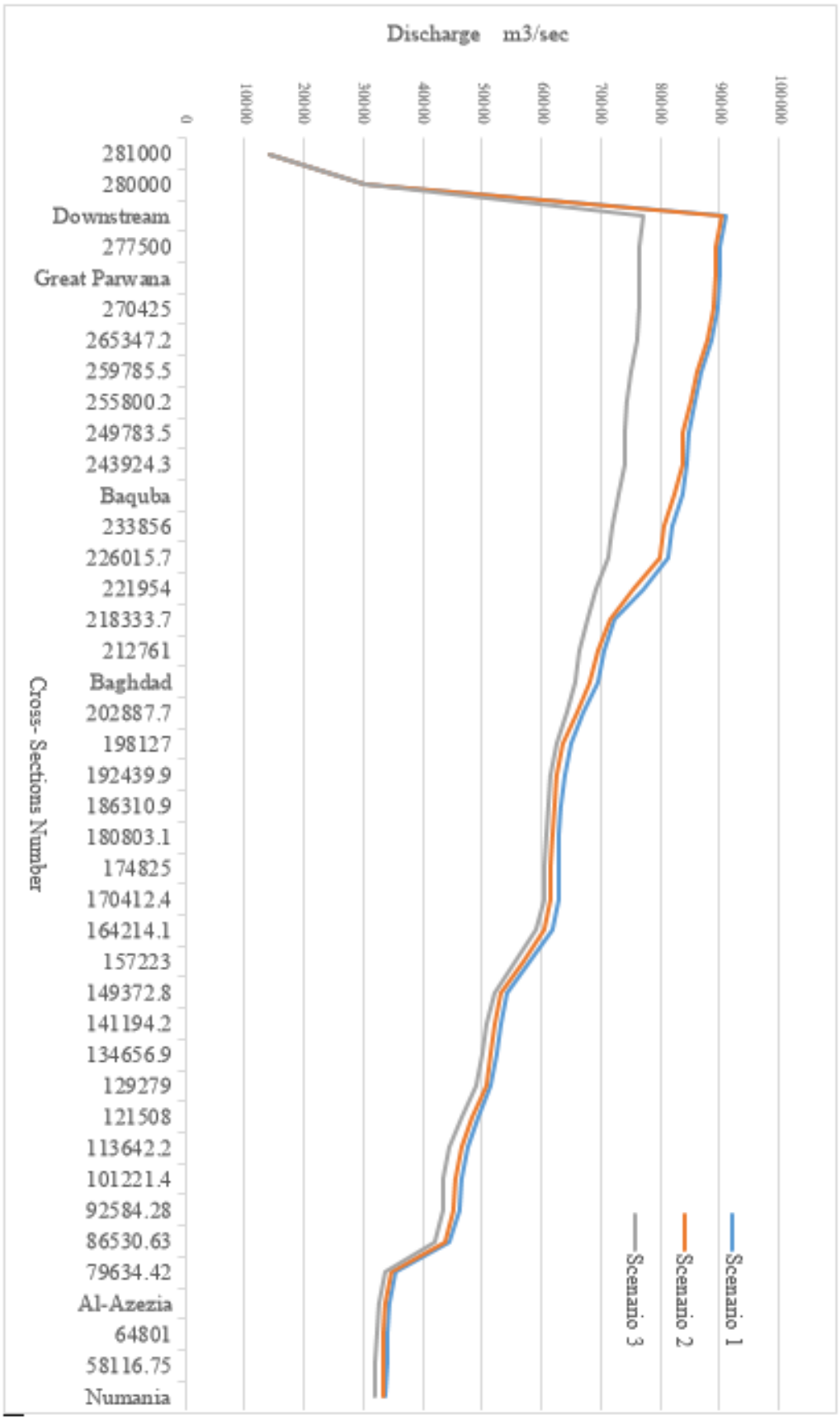

Figure 4.8 The Discharge for Three Scenarios

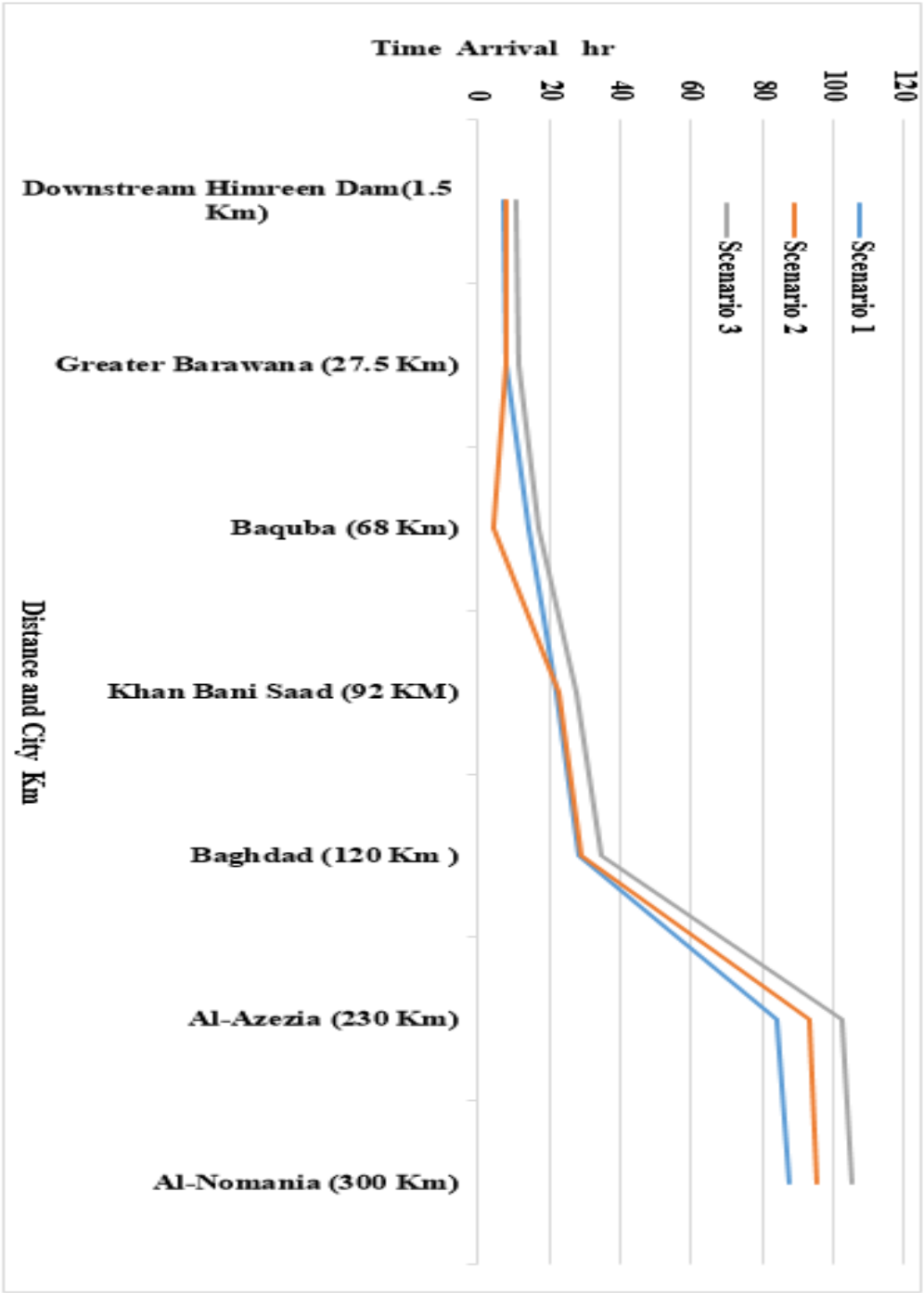

Figure 4.9 Flood Arrival Time With Respect to Cities

Fig 4.9 shows arrival time to cities located at downstream of the Himreen dam for three scenarios.

As can be seen from this figure, values of flood arrival time for scenario 3 are higher than those values in scenario 1 and 2. The difference in flood arrival times for scenarios 1, 2 and 3 is small until Baquba; however, this difference increases at locations downstream of Baquba.

Although inundation areas did not change considerably from their simulation of three scenarios, the discharge and time of arrival of peak discharge in scenario 1 are higher than those values in scenario 2 and scenario 3. The flood wave height in scenario 3 is higher than those results in other scenarios. Thus, it can be used as the most critical scenario of this study.

4.6 Discussion of Simulation Results:

In order to start simulation scenarios, the model was calibrated based on comparison of calculated flood levels with those values of previous flooding level in the area. In order to show the effects of roughness coefficient on the magnitude of the flood, water depth and arrival times a sensivity analysis was performed by using three different Manning's Roughness. The results obtained from simulations from three scenarios of flooding events, resulting from the failure of the Himreen Dam, show that size inundations areas did not change considerably.

The discharge in scenario 1, in cross-section 280000 discharge is 14113.85 m^3/sec and in cross-section 281000 discharge is 30339.91 m^3/sec respectively. In case of complete failure of the dam, the discharge increases to the maximum value of 91114.01 m^3/sec in cross-section number 278500, because of the great amount of released water from the reservoir. The discharge in other cross-sections decreases, starting from cross-section number 277500, which is 89964.83 m^3/sec to cross-section number 58000 with a discharge of 33854 m^3/s, and the same trends, occurred in the other scenarios 2 and 3. Three scenario analyses based on changing Manning's roughness were done. For scenario1, n=0.028, scenario 2 n=0.030, and in scenario 3, n=0.035 were used and these values are based on observation of flooding event occurring in the Diayla River [28].

Manning's roughness was kept constant for all the cross-sections during each scenarios. From the results of simulation for all three scenarios, the elevation flood wave height in scenario 3 is the most critical due to high resistance caused by high roughness in this scenario. The value of elevation of flood wave in Nomania is 19.69 m (above sea level) and the depth of water in Nomania is 5.64 m. The water depth in Baghdad it is 12.95 m, in Khan Bani Saad it is 13.35 Al-Azezia 12.82m, and in Barwana it is 22.42 m.

The results show that the magnitude of discharge in scenario 1 is higher than the other scenarios discharges. The value of discharge in Barwana is 89900 m3/s flood arrival time is 8 hr, and the magnitude of discharge in Nomania decreases to 33854.06 m^3/s and the arrival time of the flood wave to Nomania is 87.45 hr. The wave height, flow area, and velocity are different from one cross-section to another depending on the cross-section itself if compared with the cross-sections before and after. The study is based on field cross-sections data; so that the results are reasonable and can be considered as a first approach to prepare flood risk management plans for the area. The elevation for overtopping is 109.5 m, which is the top elevation for the dam while 107.5 m is the maximum flood elevation.

CHAPTER 5

CONCLUSIONS AND RECOMMINDATIONS

The human population is increasing at an uncontrolled rate and city centre are located near shores of seas or ocean and nearby rivers. Generally, local authorities allow people to settle in flood plains of rivers subjected to frequent flooding events. Many cities are also developed by rivers controlled by dams upstream. Due to unexpected hydrological events or deterioration of dams, these cities are subjected to severe and high danger of flooding resulting from the failure of the dam. It is shown in this study that hypothetical failure of the Himreen Dam on the Diayla River in northeastern Iraq could cause extensive damage to Great Barwana, Baquba and Baghdad. Especially, great Barwana town is located 27.5 km downstream of the dam and Baquba is 68 km downstream of the dam.

In order to determine inundation areas resulting from possible failure of the Himreen dam, HEC-RAS model is used. Numerical model was calibrated to determine the value of average Manning's roughness coefficient n=0.028 of the Diayla River bed. This value of Manning's roughness coefficient was determined based on a comparison of flood levels calculated by a modelling study and previously observed flood levels during flooding events that occurred in the area. Sensivity analysis was performed using three different n values 0.028, 0.030 and 0.035 of the Diayla riverbed in order to determine the effect of roughness on the magnitude, depth velocity and arrival time of the flood.

Analysis of the results obtained from HEC-RAS model showed that the most critical scenario is scenario 3, because the flood wave depth in this scenario has the highest values and they could cause more damage. Analysis of the results from this scenario in the towns and cities located downstream of the Himreen Dam are shown as follows.

- Peak discharge in Barawana will be **76581.13** m^3/sec, the wave height will be **22.42** m and time of arrival to flood peak will be **11.15** hr.
- Peak discharge in Baquba will be **72988.80** m^3/sec, the flood wave height will be **12.61** m and time arrival to flood peak will be **17.15** hr.

- Peak discharge in Khn Bani Saad will be **64385.23** m^3/sec, the flood wave height will be **13.35** m and time of arrival to flood peak will be **28** hr.
- Peak discharge in Baghdad will be **60475.07** m^3/sec, the flood wave height will be **12.95** m and time of arrival to flood peak will be **34.34** hr.
- Peak discharge in Al-Azezia will be **32571.80** m^3/sec, the flood wave height will be **12.82** m and time of arrival to flood peak will be **102.15** hr.
- Peak discharge in Nomania will be **31905.90** m^3/sec, the flood wave height will be **5.64** m and time of arrival to flood peak will be **105.45** hr.

As seen from the inundation maps influenced areas from the failures of the Himreen Dam cover 300 km from the Himreen Dam to Nomania. As expected, the most damage to properties and loss of human life will be in Baquba whose population is 400000 people.

Probable damage should be determined according to these values, which are obtained from dam break analysis. When dam break analysis is evaluated by considering only the loss of human life for the cities nearest to the dam, determination of population in settlement centre and preparation of evacuation plans for the population at risk should be the first step in establishing an emergency action plan.

Performing flood hazard and flood risk analysis of the region may be helpful for insurance companies in establishing more concrete risk balance sheets and more realistic emergency action plans. In addition, similar (more detailed) analysis should be done for the region considered in this study using digital elevation maps together with more sufficient cross-sections.

REFERENCES

[1] M. A. Rashid, "Transient Simulation and Hypothetical Model for AL-ADHAIM Dam–Break," Doctor Thesis, University of Technology, Baghdad, Iraq, 1999.

[2] G.Arthur, "Teton Dam Failure," pp.61-71 in. "The Elevation of Dam Safety Engineering Foundation Conference Proceeding," Asilomar, Nov.28 – Dec. 3 1979). American Society of Civil Engineers, New York, 523p, 1977.

[3] A.H. Daher, "Hypothetical Failure of Sencherib Dam," Master's Thesis, University of Baghdad, 2001

[4] ICOLD International Committee on Large Dams "Dams and Floods Guidelines and Case History," Paris, Bulletin 125, 2007.

[5] G. Arila, and T.Nair. "Dam Break Analysis using Boss Dam Break," International Conference on Water Resources," Coastal and Ocean Engineering ICWRCOE. Elsevier Aquatic Procedia: Four (2015)853-860, 2015.

[6] L.Berg, ICOLD, "Dams and Floods," Spin, Committee on Dam and Flood, 2003.

[7] ICOLD, "International Erosion of Exiting Dams," Paris, bulletin 164, 2017.

[8] X. Zhao, D. Liang, and M. Martinelli, "Numerical Simulations of Dam Break Floods with M-PA," International Conference on the material point method, MPM. Elsevier, Procedia Engineering. (175(2017)133-140, 2017.

[9] L. Zhao, X. B. Y. Liu and T. C. L. Jia Mao, "A Novel Well-Balance Scheme for Modeling of Dam Break Flow in Drying Wettings Areas," Elsevier, Campaterand Fluids (136,324-330), 2016.

[10] P.Hawker, "Review of the Role of Dams and Floods Management,Thematic Review Assessment of Flood Control and Management Options," Washington State, Department of geology, 2000.

[11] O. Seyeda, S Abbas and R. A. Akhtari, "Dam Break Flow solution using artificial neural network," Elsevier, Ocean Engineering 142,125-132, 2017.

[12] U.S department of the Interior, "Dams and Public Safety," Bureau of Reclamations, USA Awater Resources, Technical Publication, 1990.

[13] K. Ostad, A. Askari and M. Shayancjad, "Usage of Rockfill Dams in the HEC-RAS Software for the Purpose of Controlling Floods," American Journal of Fluid Dynamics, 5(1):23-29, 2015.

[14] E. M. Mariam, "Study Flood Wave Caused by Dam Break, Using HEC-RAS Program," Master's thesis, Damascus University, 2015.

[15] US Army Corp of Engineering January, "Hydraulic Engineer Center application guide," USA, 2010.

[16] A. J. Wardena, "Water Resource Commission China Research Training Advisor," International Centre for Water Hazard and Risk Management Supervisor, Diming long MEE -07175, Hydrology Bureau, 2001.

[17] P.K Mohaptra and M. Bhallamudi, "Advanced in Water Resources," Elsevier vol 19, No 3 pp 181-187,0309-1708(95)00036-4, 1996.

[18] T. C. T. Anchaali and C. C. Rasri, "Numerical Modeling of dam failure due to flow overtopping," Hydrological Science Journal, 2001.

[19] Z. Bozkus and A. Kasap, "Comparison of Physical and Numerical Dam Break Simulation," Turkey Journal of Engineering and Environmental science, 22(1998), 429-443, Aug. 1997.

[20] J. Jorgeson, X. Y.Ying and W.Law, "Two Dimensional Modeling of Dam Breach Flooding," US-China workshop on advanced computational modelling in hydro science engineering, Oxford Mississippi USA, 2001.

[21] ICOLD "Dam Safety Management Operational Phase of the Dam Life Cycle," Bulletin 154, Paris, 2017.

[22] S.P Kaushish, and M Gopalkaarishnan "Dams Safety Evaluation, proceedings of 3rd," International Conference, Panaji, India, 2002.

[23] National Performance of Dams Program, " Dam Failure in U.S," Dept of Civil Engineering of Enviromantal Engineering, Stanford University , USA , September 2018.

[24] ICOLD, "Reservoir Landslides Investigations and management guidelines and case histories," Bulletin 124, 2002.

[25] F. Lemperere, "Dams and Floods," Elsevier, Engineering 3144-149, Hydroscope, Paris 92190, 2017.

[26] D. Chadlapoudrs, "Examples, Statistics and Failure Moods of Tailings Dams and Consequence of Failure," SNC.LAVALIN, 2015.

[27] ICOLD, "Recommendations for Operation Maintance and Rehabilitation," Bulletin 168, Paris, 2017.

[28] "Data from Ministry of Iraqi Water Resources", (unpublished data).

[29] "http://agromet.gov.iq/index.php?name=News&file=article&sid=207," Ministry Of Agriculture.

[30] "USGS, Science for changing world stream Gag Descriptions and streamflow statistics for sites in the Tigris River and Euphrates River Basins, Iraq, " prepared in cooperation with MOWR (Ministry of Iraqi Water Resources), under a spices of the U.S. department of defense task force for business and stability operations," 2010.

[31] The institution of Civil Engineers "Floods and Reservoirs Safety," London, T. Telford, third edition, 1999.

[32] V.T.Chow, "Open Channel Hydraulics," University of Illions, New York USA, Professor of Hydraulic Engineering, MCGRAW-HILL COMPANY, 1999.

APPENDIX

RECLAMATION OF THE HIMREEN DAM

NO	CONTENT
A.1	Max inflow and out flow
A.2	Inflow – out flow 1991
A.3	Inflow – out flow 1992
A.4	Inflow – out flow 1993-1994
A.5	Inflow – out flow 1996
A.6	Inflow – out flow 1997
A.7	Inflow – out flow 2000-2001
A.8	Inflow – out flow 2002-2003
A.9	Inflow – out flow 2004-2005
A.10	Inflow – out flow 2006-2007
A.11	Inflow – out flow 2008-2009
A.12	Inflow – out flow 2010-2011-2012
A.13	Inflow – out flow 2013-2014-2015
A.14	Inflow – out flow 2016-2017-2018

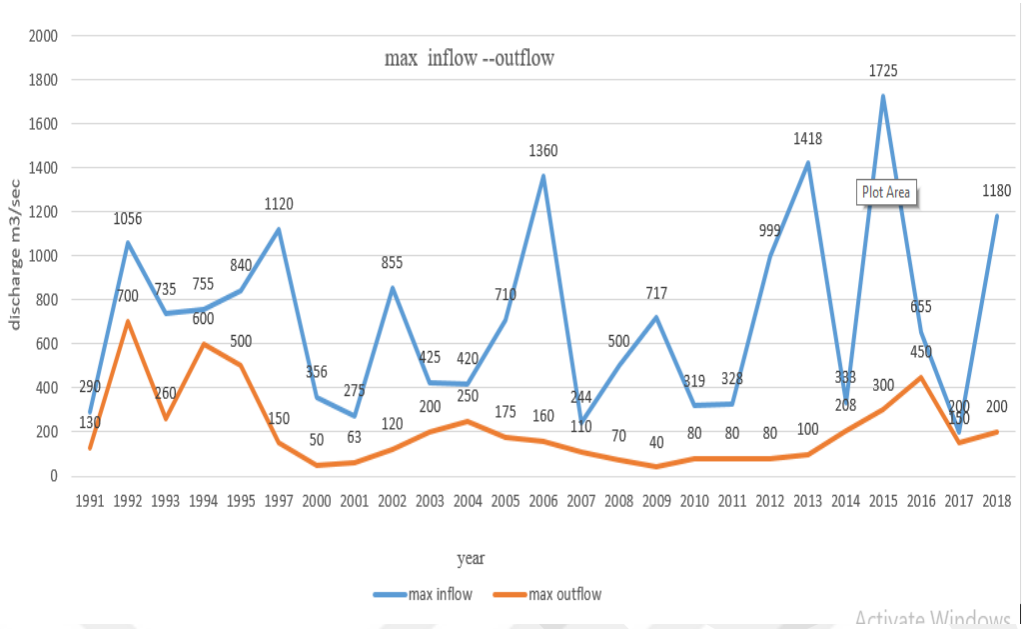

Figure A.1 The maximum Inflow and Outflow

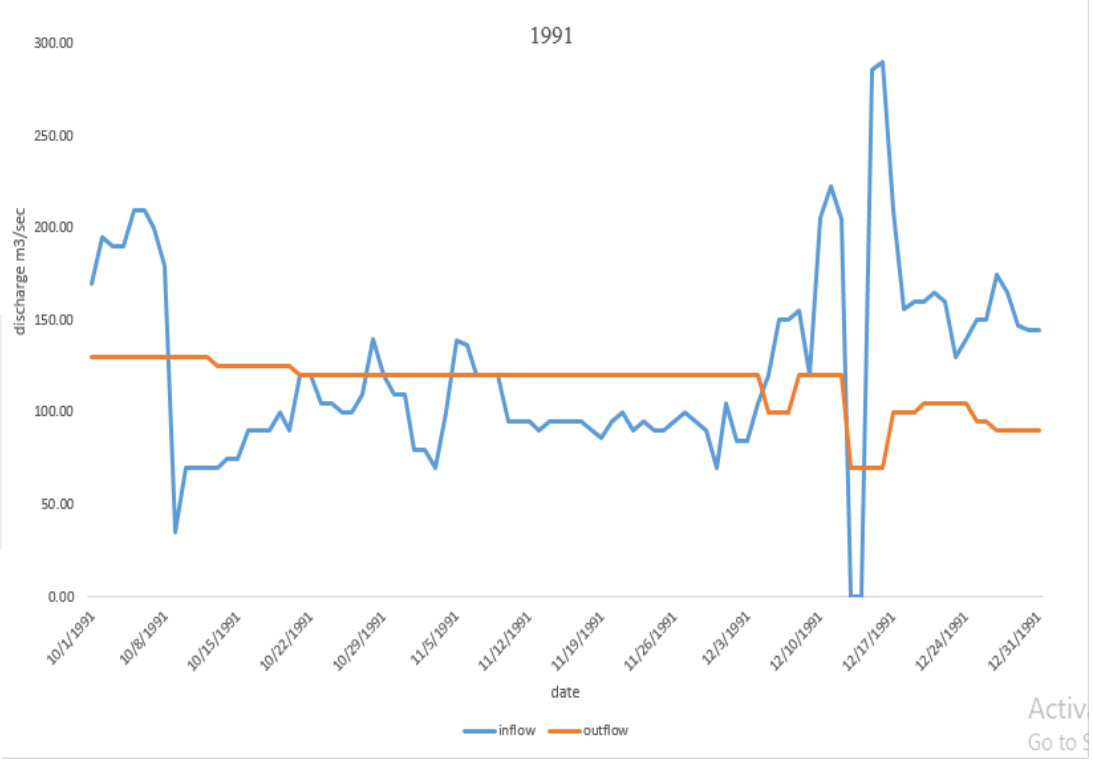

Figure A.2 The Inflow and Outflow for Himreen Dam in Year 1991

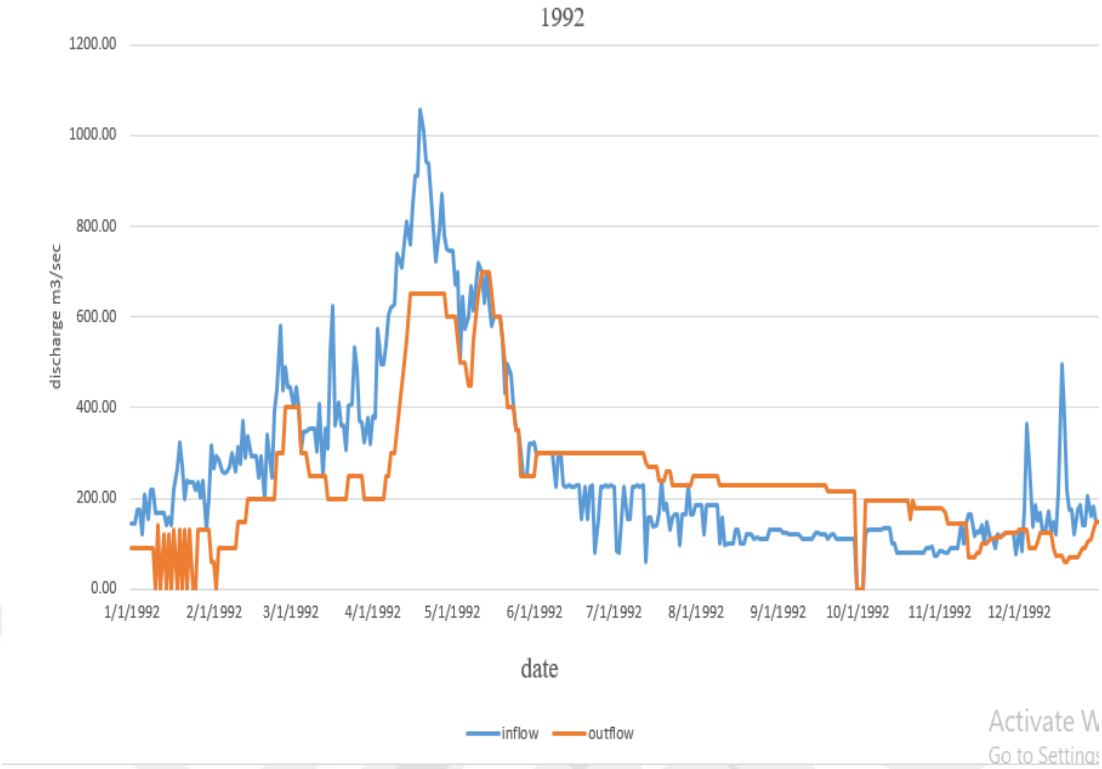

Figure A.3 The Inflow and Outflow for Himreen Dam in Year 1992

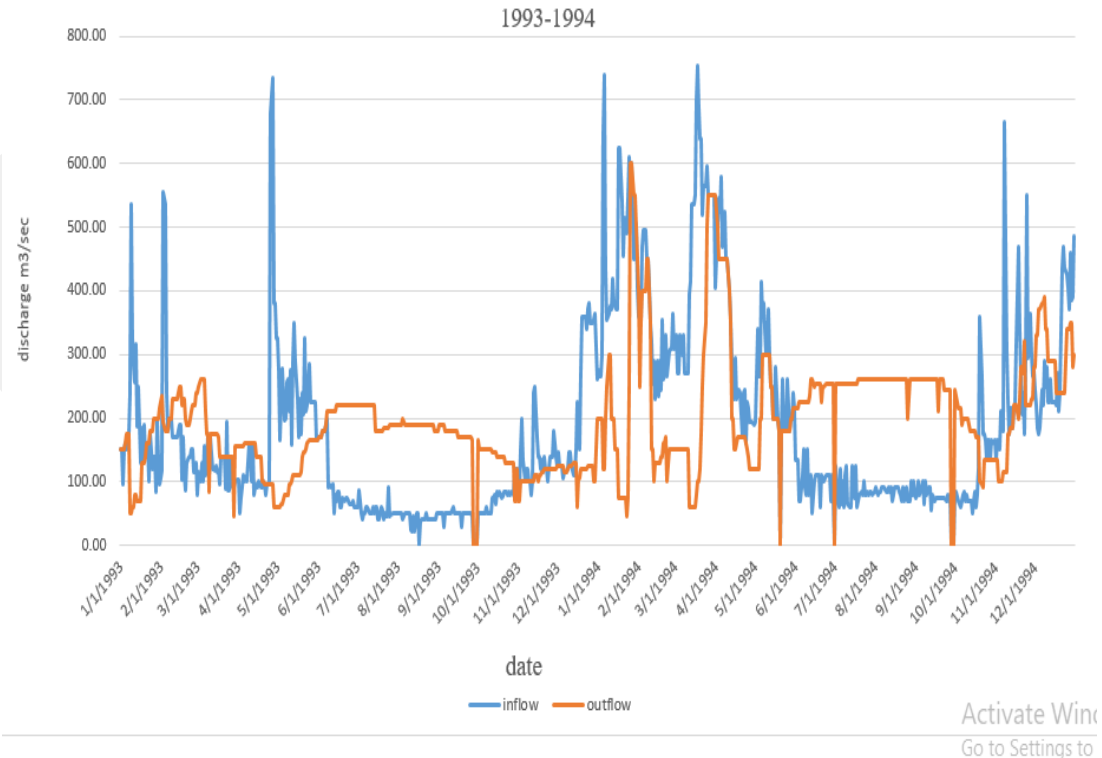

Figure A.4 The Inflow and Outflow for Himreen Dam in Year 1993

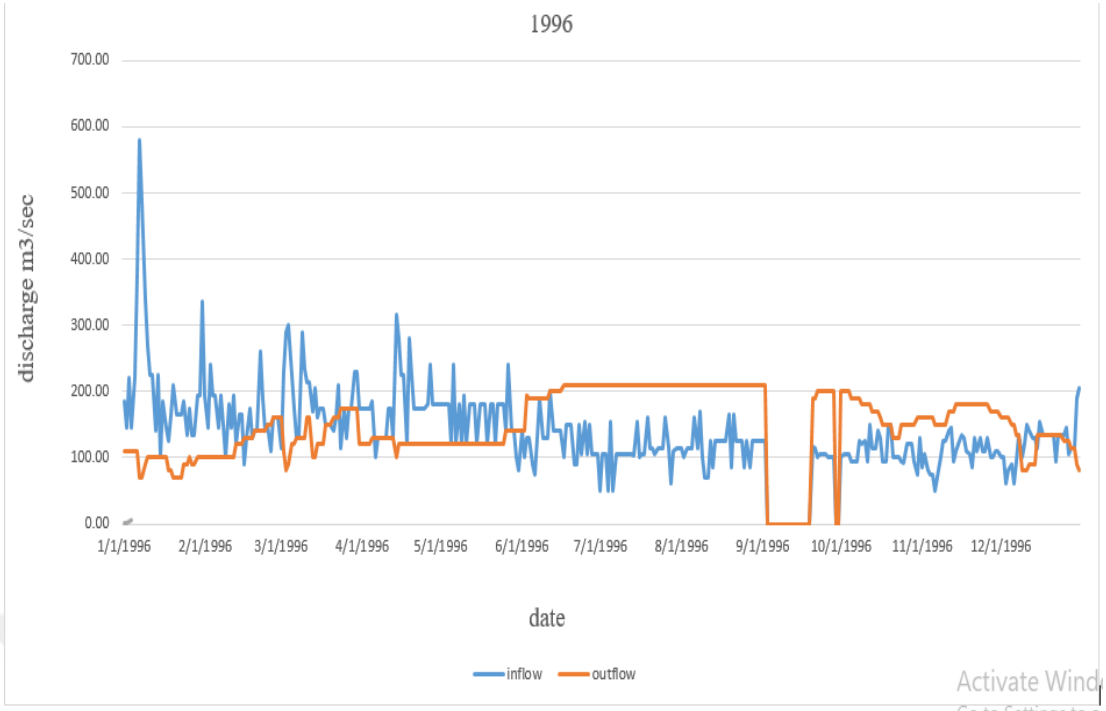

Figure A.5 The Inflow and Outflow for Himreen Dam in Year 1996

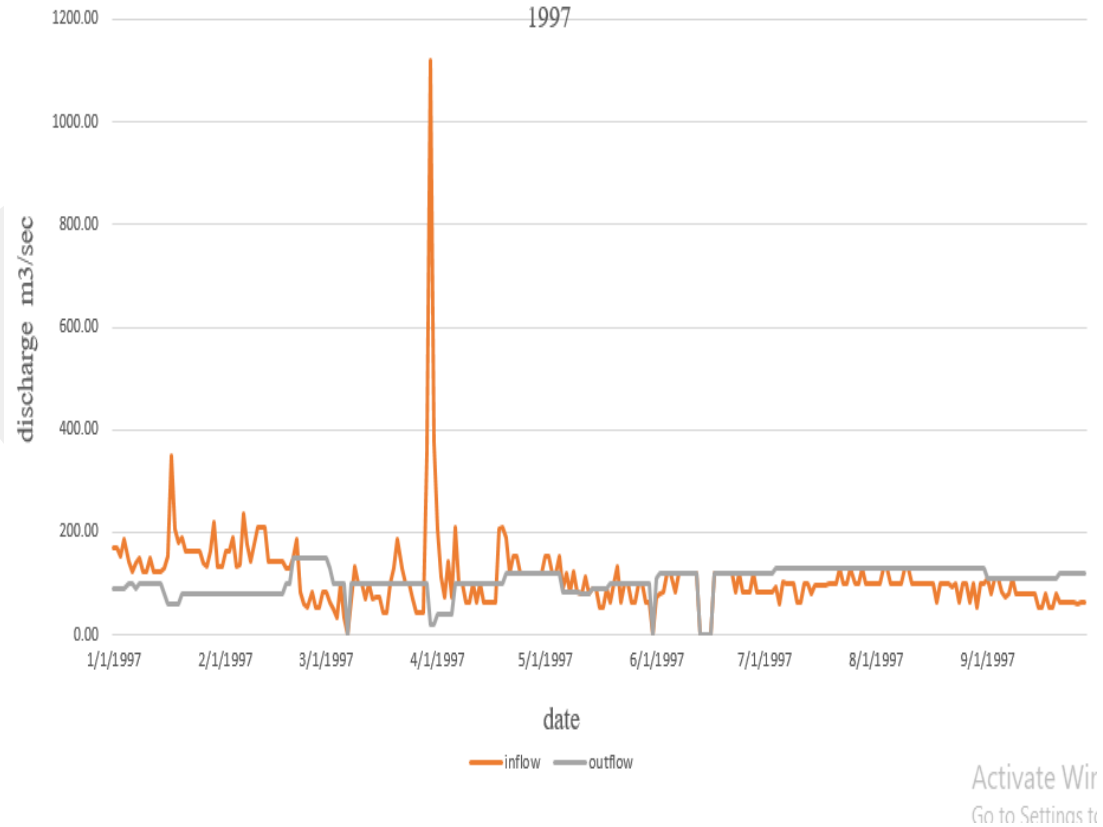

Figure A.6 The Inflow and Outflow for Himreen Dam in Year 1997

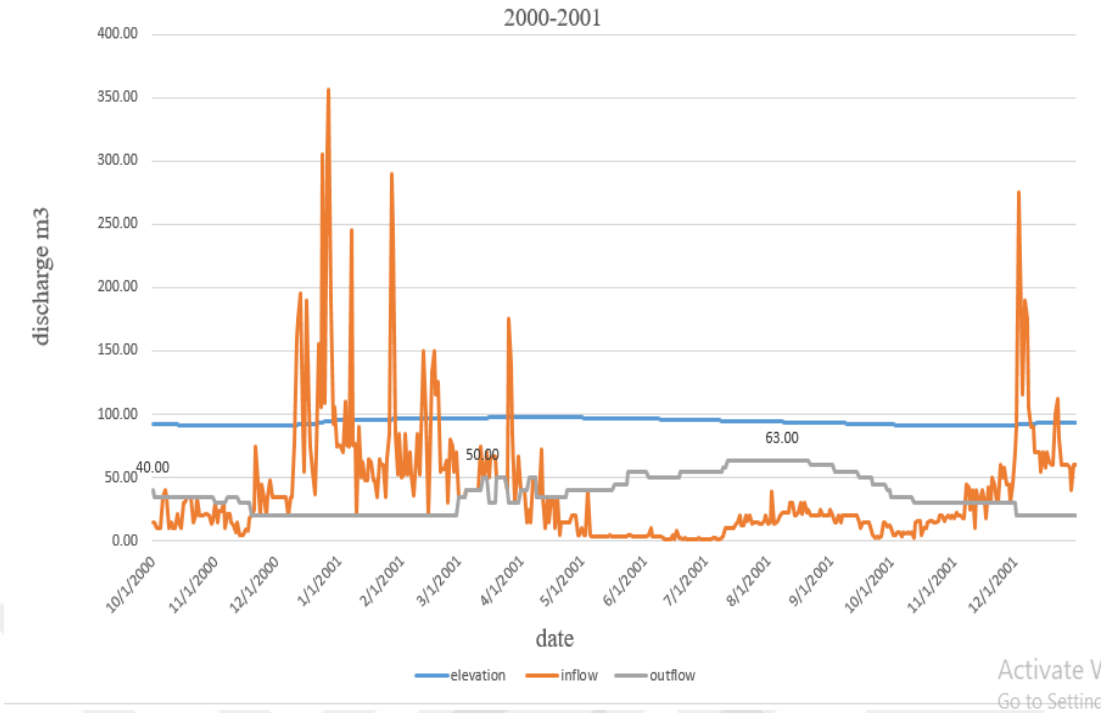

Figure A.7 The Inflow and Outflow for Himreen Dam in Year 2000-2001

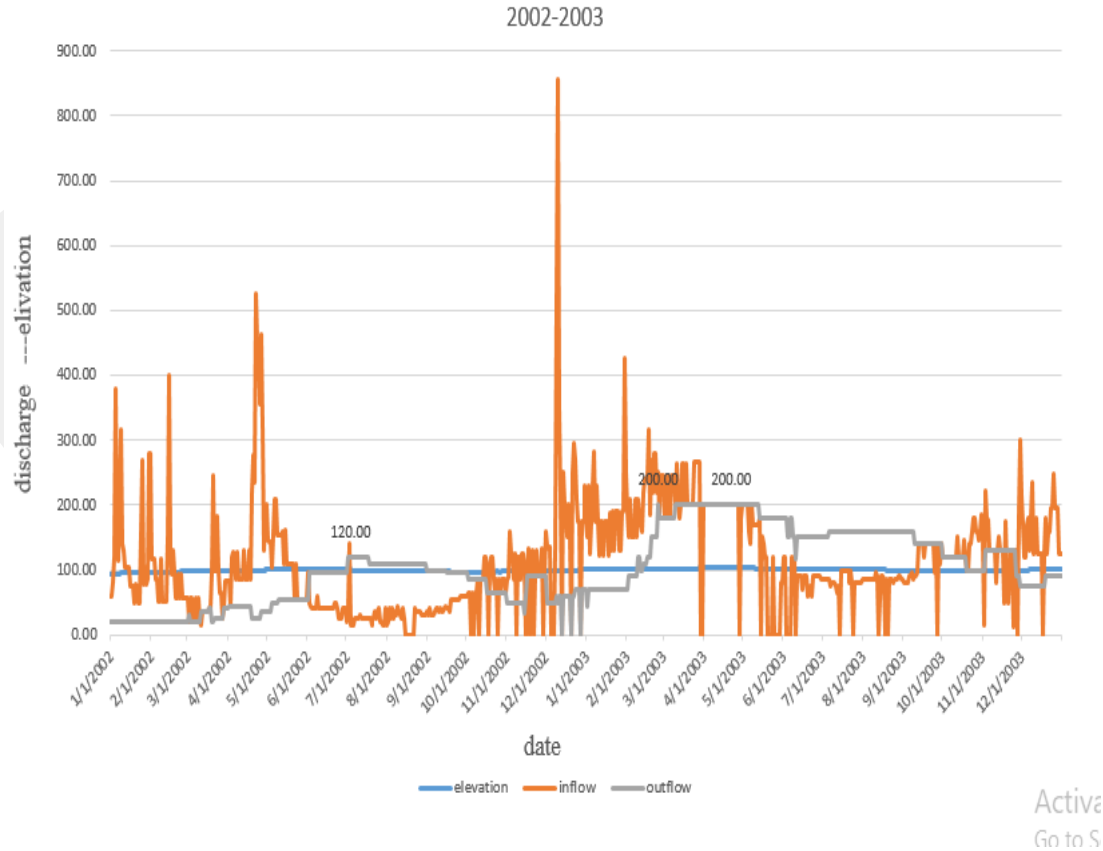

Figure A.8 The Inflow and Outflow for Himreen Dam in Year 2002-2003

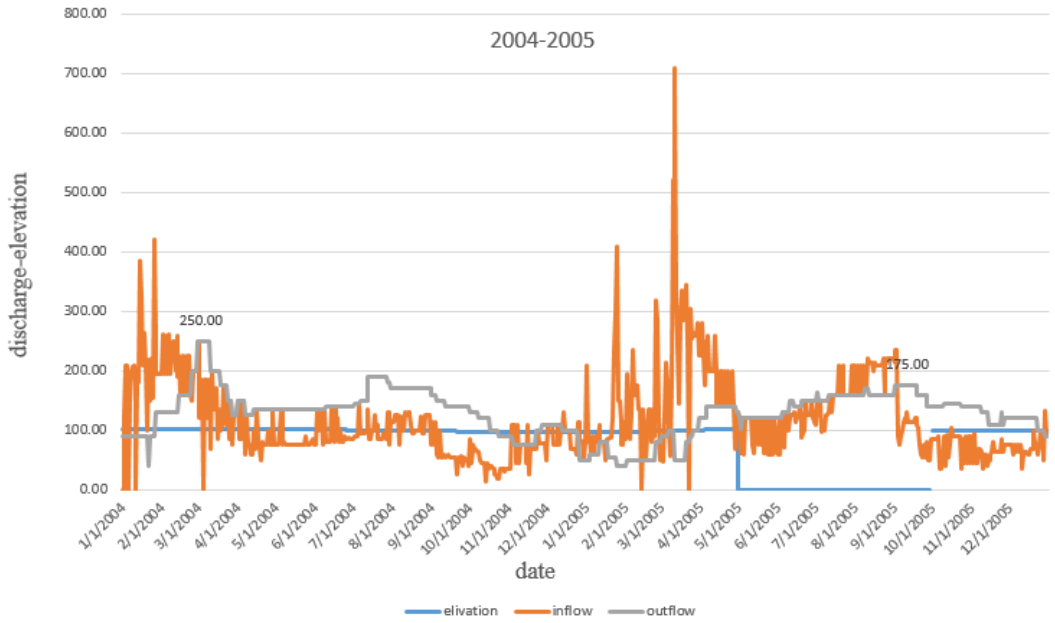

Figure A.9 The Inflow and Outflow for Himreen Dam in Year 2004-2005

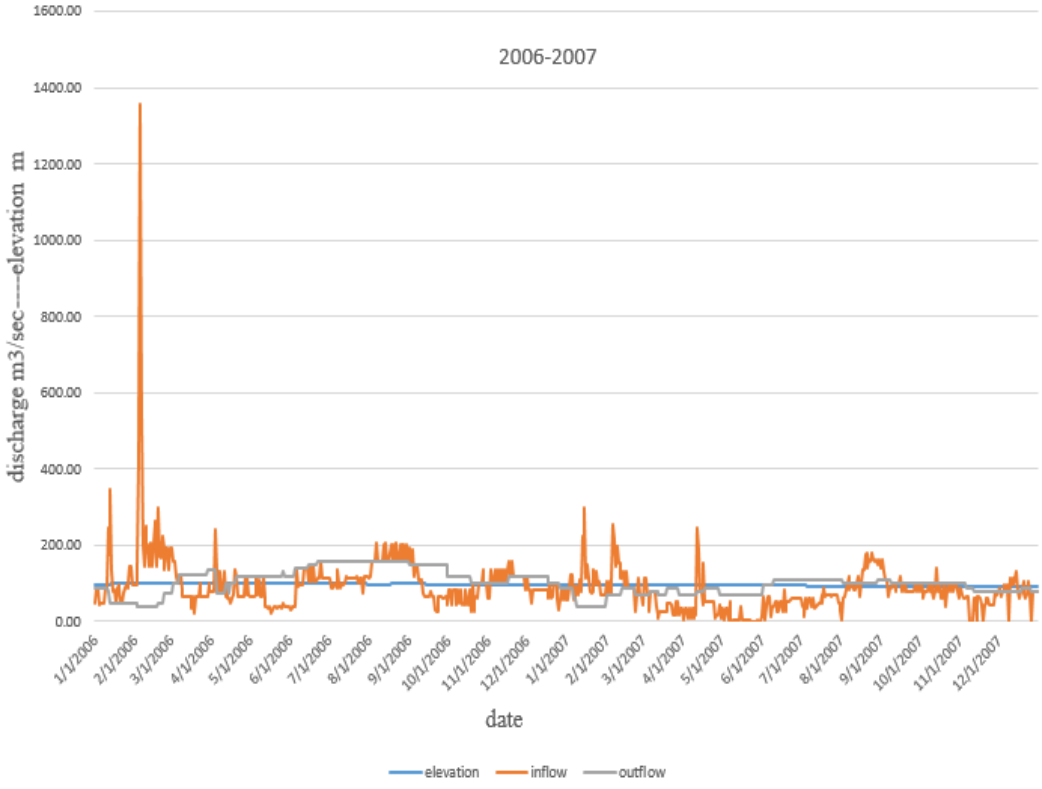

Figure A.10The Inflow and Outflow for Himreen Dam in Year 2006-2007

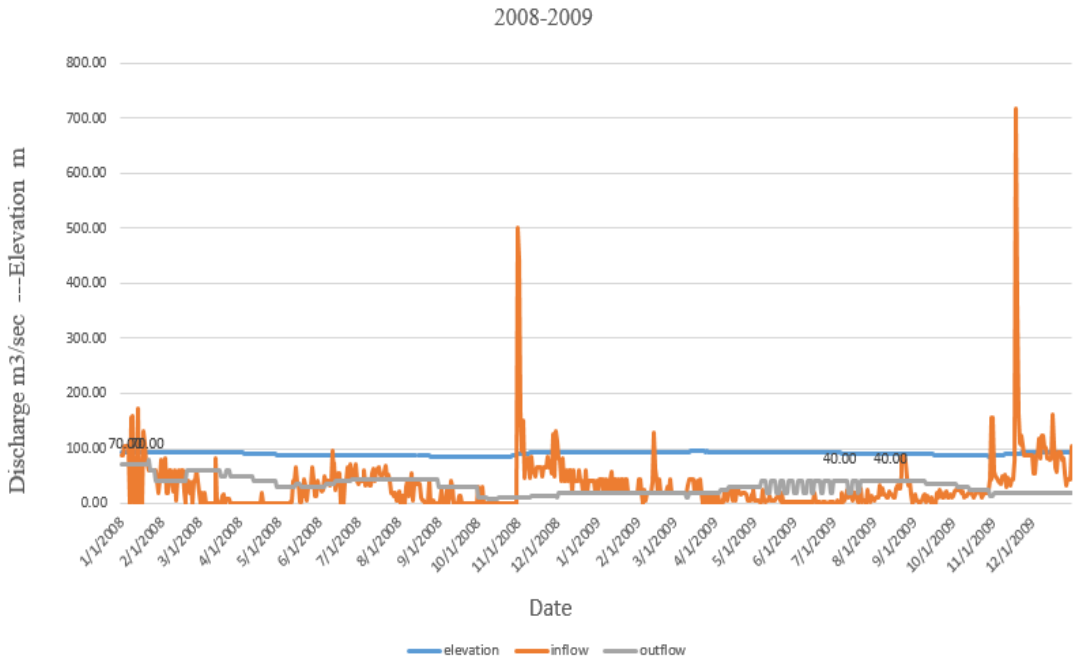

Figure A.13 The Inflow and Outflow for Himreen Dam in Year 2008-2009

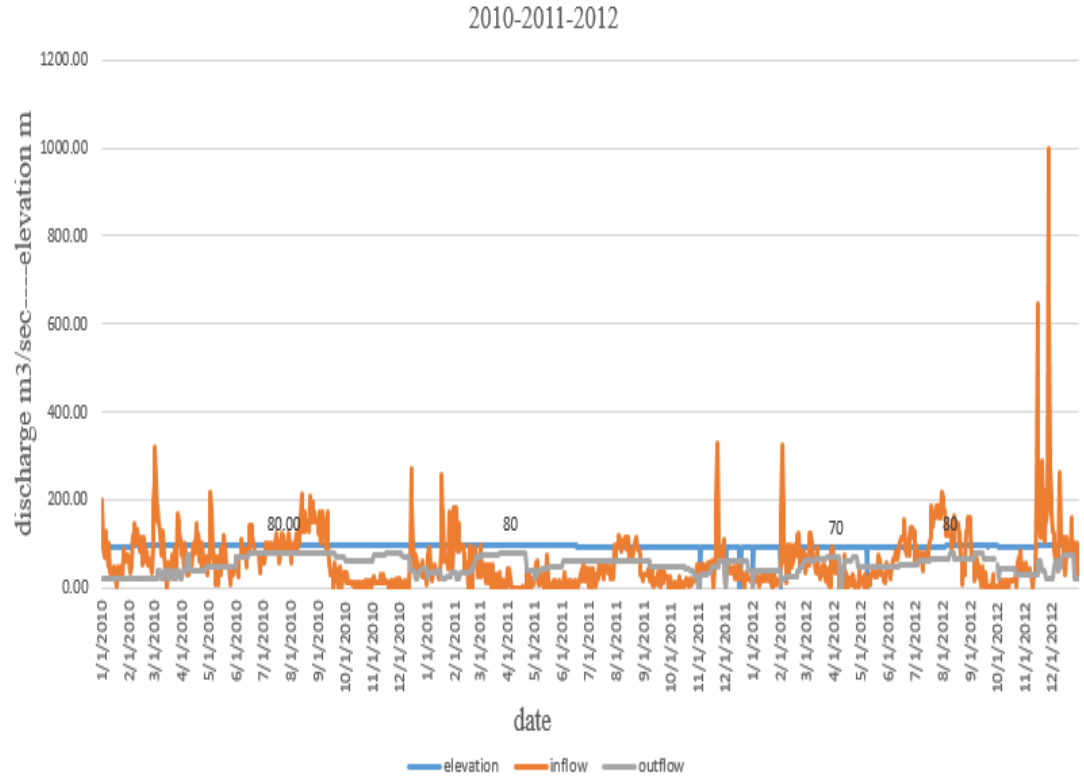

Figure A.12 The Inflow and Outflow for Himreen Dam in Year 2010-2011-2012

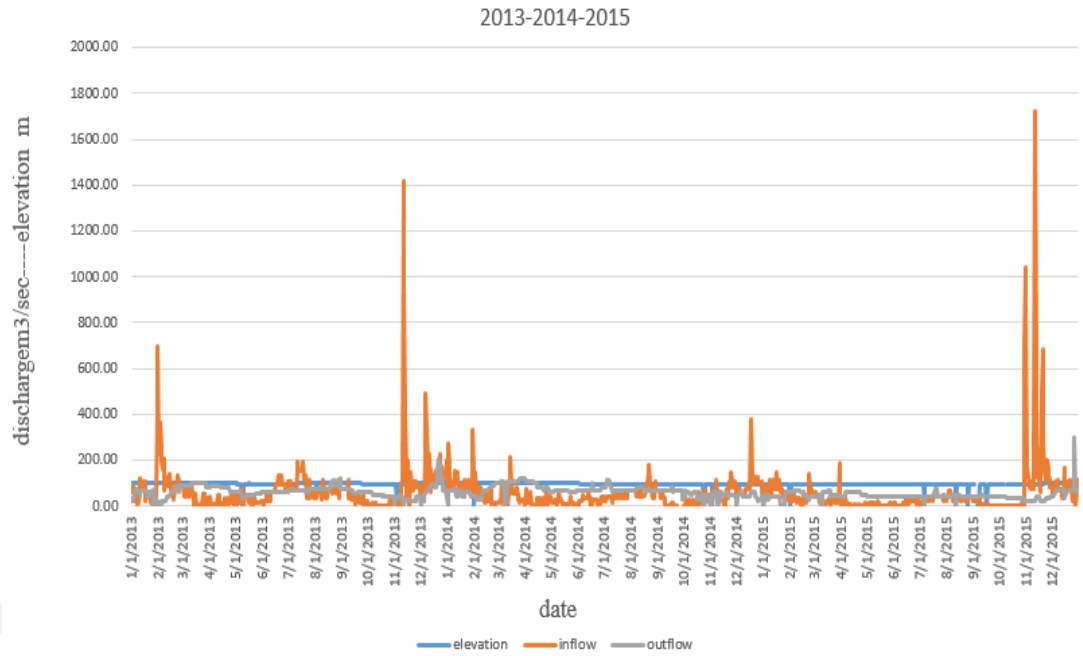

Figure A.13 The Inflow and Outflow for Himreen Dam in Year 2013-2014-2015

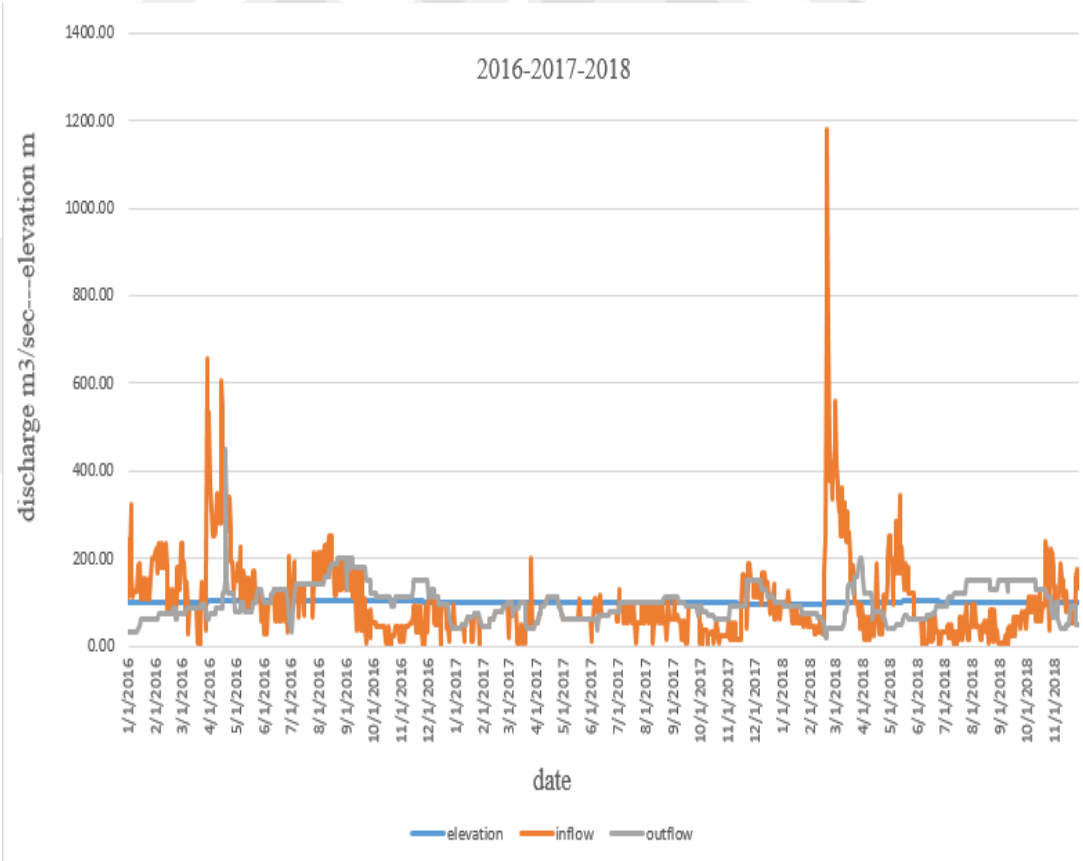

Figure A.14 The Inflow and Outflow for Himreen Dam in Year 2016-2017-2018